Università degli Studi di Ferrara

DOTTORATO DI RICERCA IN

"BIOCHIMICA, BIOLOGIA MOLECOLARE E BIOTECNOLOGIE"

CICLO XXVI

COORDINATORE Prof. Francesco Bernardi

Molecular mechanisms impairing biosynthesis and function of hemostatic proteins

Settore Scientifico Disciplinare BIO/11

Dottorando

Dott. Matteo Campioni

Tutore

Prof. Francesco Bernardi

Co-tutore

Prof. Mirko Pinotti

Anni 2011/2013

Contents

Summary

Abstract

The gene mutations leading to hemorrhagic disorders provide peculiar models to elucidate molecular mechanisms underlying protein biosynthesis, and the relationship between the structure and function.

The research activity has been focused on the molecular defects leading to severe deficiency of Factor IX (FIX), a serine protease with a key role in the intrinsic pathway of blood coagulation, and of von Willebrand factor (VWF), a large multimeric protein essential for the primary hemostasis.

In particular, I investigated mechanisms due to three different molecular defects such as nonsense and missense mutations in F9 gene, associated with type I hemophilia B, and an in-frame deletion in the VWF gene, displaying a dominant-negative effect.

Results from investigations in patients' plasma and the expression of nonsense FIX variants in eukaryotic cells led to the demonstration of trace levels of full-length FIX molecules even in the presence of nonsense mutations through a mechanism of ribosome read-through. The efficiency was dependent of the specific nonsense mutation and on it sequence context. Moreover, I investigated the susceptibility of a panel of nonsense FIX mutations to the induction of readthrough by aminoglycosides. The data suggested a direct relationship between the spontaneous and the drug-induced readthrough. Overall data indicated that not all nonsense mutations can be considered truly "null-mutations", a finding that have pathophysiological implications.

The severe p.Tyr450Cys mutation in the carboxyl-terminal region of coagulation FIX was chosen as model to study the interplay between impaired protein biosynthesis and/or function caused by missense mutations in relation to specific protein regions, which has been poorly investigated. Results from the expression of a panel of recombinant variants demonstrated the key role of the tyrosine phenyl group for both FIX secretion and coagulant activity. Comparison among highly homologous coagulation serine proteases indicate that additive or compensatory pleiotropic effects on secretion and function by carboxyl-terminus mutations produce life-threatening or mild phenotypes in the presence of similarly reduced protein amounts.

Finally I contributed to the characterization of the dominant inheritance in VWD, due to two essential process in VWF dimerization and multimerization VWD can express dominant-negative features. Previous study characterized and demonstrate d the modulation of this dominant effect. In our study we reproduced in vivo the effect of dominance and through a creation of an artificial mutation, we demonstrated in vitro an in vivo the key role of interaction between wild type and mutant protein monomers during dimerization and or multimerization, We believe that our finding have general implication for the dominant forms of VWD, the most frequent inherited bleeding disorders in humans.

Abbreviations

The standard abbreviations used in this thesis follow IUPAC rules. All the abbreviations are defined also in the text when they are introduced for the first time.

bp: base pais
cDNA: Complementary DNA
DNA: DeoxyriboNucleic acid
dNTPs: Deoxynucleoside triphosphate (A, C, G and T)
ELISA: Enzyme-Linked Immuno Sorbent Assay
FIX: Factor IX
FVII: Factor VII
FX: Factor X
Kb: Kilobase
kDa: Kilodalton
NMD: Non sense Mediated Decay
nt: Nucleotides
PBS: Phosphate bufer saline
PTC: Premature Termination Codon
PTC: Premature termination codon
RNA: RiboNucleic Acid
SDS: N-lauroylsarcosine sodium salt
TF: Tissue Factor
VWF: Von Willebrand Factor
WB: Western Blotting Assay
WT: Wild-type
X: Stop Codon

Introduction

Hemostasis

It is known since long time that hemostasis is a dynamic process whereby blood is maintained fluid under normal life conditions, but is allowed to rapidly clot in case of trauma to prevent excessive blood loss and death. This mechanism is carefully regulated and ~~it~~ involves various cellular and molecular components.

Blood coagulation is part of this important organism defense mechanism. In resting state the endothelial cell inhibit the platelet adherence and thus the activation of the blood coagulation, and are responsible of synthesis of prostacyclin, heparin-like substances and hold protein complexes (thrombin-thrombomodulin), leading to generation of anticoagulant proteins (activated protein C), which prevent clot formation in heath normal blood vessels (Furie and Furie 1992).

After vessel injury, damaged endothelial cells expose negatively charged phospholipids and platelets can adhere to macromolecules in subendothelial tissues and then aggregate to form the primary hemostatic plug that temporary blocks blood loss.

The interaction between platelets and the damaged endothelium requires von Willebrand Factor (VWF), a large multimeric plasma protein which acts as a bridge by binding exposed collagen in the sub-endothelium and a specific receptor on platelet surface Glicoprotein Ib. The phospholipids composition of the platelet membrane changes, resulting in the exposure of negatively charged phopshatidylserine on the outer leaflet of platelet membrane (Bevers, Comfurius et al. 1982, Bevers, Comfurius et al. 1983). The activation of platelets by thrombin, ADP, thromboxane A2 or epinephrine triggers characteristic morphological and biochemical alterations in the platelet(Furie and Furie 1992).

Activated platelets secrete α-granules, containing fibrinogen, Factor V (FV), Factor VIII (FVIII), vWF and other proteins involved in haemostasis, and δ-granules, containing calcium ions and ADP, and aggregate at the site of injury, forming a sort of plug that provisionally blocks blood loss. The expression on the platelet surface of a receptor (glycoprotein IIb-IIIa) for plasma proteins (fibrinogen) mediates platelet aggregation (Dahlback 2005).

These events are followed by inflammation and repair reactions. Thrombin plays a key role in these processes by chemotactically drawing leukocytes to the site of injury and by stimulating tissue remodelling and mitogenesis. P-selectin expressed on the platelet membrane in the haemostatic plug acts as a receptor for monocytes and neutrophils which, in addition to providing ideal membrane surfaces for blood coagulation, sustain the inflammatory response. During wound healing, the fibrin clot is degraded by the serine protease plasmin, a process known as fibrinolysis (Collen 1999, Riddel, Aouizerat et al. 2007).

Blood coagulation

In a classical view coagulation is represented as a “cascade” or “waterfall” model, divided into two pathways: an “intrinsic pathway”, so named because all the components are present in blood, and an “extrinsic pathway”, in which the subendothelial cell membrane protein tissue factor (TF) is required in addition to circulating components. The initiation of both pathways resulted in activation of Factor X (FX) and the eventual generation of a fibrin clot through a common pathway (Luchtman-Jones and Broze 1995). Although these concepts represented a significant advance in the understanding of coagulation and served for many years as a useful model, more recent clinical and experimental observations (Kleinschnitz, Stoll et al. 2006) explain how the cascade hypothesis does not fully and completely reflect the events of hemostasis in vivo.

A cell-based model of coagulation explain, in a more physiological way, how coagulation cascade evolves in consequence of a vascular injury, underlying the roles of cellular elements. Several cells play different roles in the coagulation process, due to their procoagulant and anticoagulant properties.

A cell-based model of coagulation explain, in a more physiological way, how coagulation cascade evolves in consequence of a vascular injury, underlying the roles of cellular elements. The cascade model included the recognition of negative charged phospholipids, principally phosphatidylserine, as a requirement for the assembly and the full function of coagulation complexes, but the role of cells, especially platelets, was thought to be primarily to provide anionic phospholipids and not to be actively involved in the process.

Several cells play different roles in the coagulation process, due to their procoagulant and anticoagulant properties. Blood platelets and TF-bearing microparticles (MPs) play a major role in supporting procoagulant reactions, supplying negatively charged phospholipids essential for the correct assembly of molecular complexes. Microparticles are vesicles that carry a cytoskeleton surrounded by a membrane consisting of a phospholipid bilayer which shows a high density of negative charged phospholipids, particularly phosphatidylserine, on its outer membrane layer (Lechner and Weltermann 2008). Among the various hypothesis functions of MPs and one of the most studied is their possible role in hemostasis and thrombosis, and the capacity by monocytes of shedding microparticles selectively enriched in TF has been observed (Del Conde, Shrimpton et al. 2005). Vascular endothelial cells play a key role in maintaining the anticoagulant properties of the vasculature; thus the process of coagulation is prevented, at least in part, by keeping the two cell types (platelets and endothelial cells) apart until an injury makes activation of the coagulation system indispensable.

Coagulation pathway proceeds as a sequence of events localized on the site of vessel injury, essentially the whole process can be condensed in four different phases: initiation, amplification, propagation and last but not least termination.

Initiation phase

The process of blood coagulation starts by the exposure of TF-expressing cells to flowing blood. TF is expressed constitutively on cells such as smooth muscle cells and fibroblasts but not on resting endothelium. TF is also expressed in several other districts that constitute an hemostatic envelope normally not in contact with blood (Dahlback 2005). Disruption of the endothelium walls or activation of endothelial cells or monocytes results in the exposure of TF on blood flow. Stronger evidence suggests that TF also circulates in blood exposed on the surface of MPs; this TF derive from various cell types: white blood cells, endothelial cells, and platelets, and might play important roles in development of pathological thrombosis (Osterud and Bjorklid 2006).

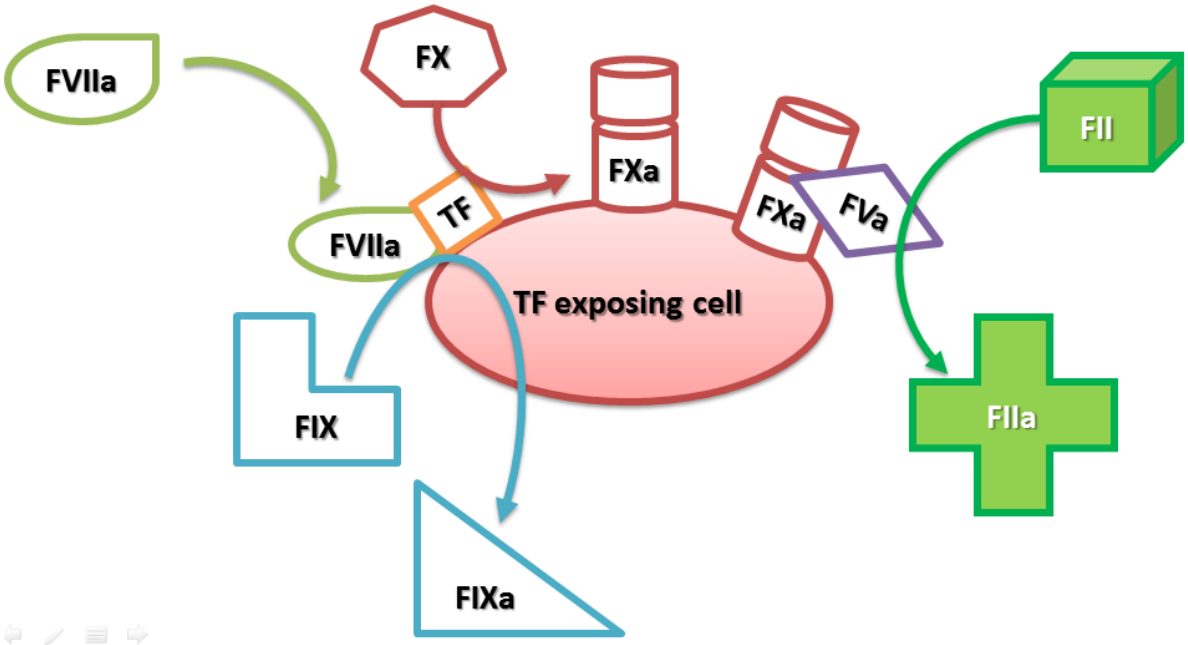

Figure 1: FVIIa bound to TF activates FX and FIX. FXa formed binds to FVa on that cell and converts prothrombin to thrombin.

Upon an injury, FVIIa, present at trace levels in plasma, binds tightly to TF and forms the TF/FVIIa complex that activates small amounts of FX and Factor IX (FIX). Activated FX (FXa) associates with its cofactor, activated Factor V (FVa), and forms the prothrombinase complex on the surface of the TF-bearing cells (Monroe and Hoffman 2006), leading to the conversion of small amounts of circulating Prothrombin (II) to Thrombin (IIa). The active form of FV derives from one of several sources. The adhesion process to components as collagen partially activates platelets and promotes secretion of partially activated FV from their α-granules. Zymogen FV can also be converted to FVa by thrombin, FXa (Monkovic and Tracy 1990).

The localization to the cell surface make FXa relatively protected from inactivation mediated by protease inhibitors. However, FXa molecules that dissociate from TF-bearing cells are

rapidly inhibited in the fluid phase by Tissue Factor Pathway Inhibitor (TFPI) and Antithrombin (AT). Thus, the presence of inhibitors localizes FXa activity to the surface on which it was converted to the active enzyme form. Contrarily, FIXa can move from TF-bearing cells to the platelet surface since it is not inhibited by TFPI and more slowly inhibited by AT than FXa.

The coagulation proteins leave the vasculature, percolate through the tissues, and are found in the lymph roughly in proportion to their molecular size (Miller, Howarth et al. 2000); thus FVII is probably bound to extravascular TF even in the absence of an, and the extravascular FX and FIX can be activated as they pass through the tissues. This idea is consistent with the finding that low levels of the activation peptides from coagulation factors are present in the blood of normal individuals injury (Monroe and Hoffman 2006).

This process does not lead to clot formation under normal circumstances, because the really large components of the coagulation process, platelets and Factor VIII (FVIII)/ VWF complex, are kept sequestered in the vascular space. Coagulation only proceeds when damage to the vasculature allows platelets and Factor VIII/ VWF exposure into the extravascular tissues.

Amplification phase

The small amount of thrombin generated on the TF-bearing cell in the initiation phase, has several important functions; one of that is activation of platelets resulting in an increase in phosphatidylserine exposure on the membrane outer leaflet, thus serving as a surface for assembly and activity of the coagulation complexes. Although platelets have already adhered at the site of injury and become partially activated, the addition of thrombin can induce a higher level of procoagulant activity than adhesive interactions alone (Alberio and Dale 1999). As a result platelets release partially activated forms of FV onto their surfaces. Another function of thrombin formed during the initiation phase is the activation of the cofactors FV and FVIII on the activated platelet surface. In this process, the FVIII/ VWF complex is dissociated, permitting VWF to mediate additional platelet adhesion and aggregation at the site of injury

Thrombin also activates Factor XI (FXI), activated by the prekallekrein – kininogen – Factor XII cascade in the classic “intrinsic parhway”, which acts as a “booster” of thrombin generation on the platelet surface (Alberio and Dale 1999). This finding also strengthen the hypothesis that the intrinsic mechanism gives no contribute to in vivo coagulation process. By the end of the amplification phase, successive stage is a production of great amount of thrombin, called propagation phase.

Propagation phase

Now activated-Factor IX (FIXa) surface of activated platelets generated during the initiation phase can now bind to its cofactor, activated-Factor VIII (FVIIIa), on the platelet surface, assembling in the so called “tenase-complex”, additional FIXa is supplied by platelet-bound activated-FactorXI (XIa). Because FXa cannot move effectively from the TF-bearing cell to the activated platelet, FXa must be provided directly on the platelet surface by FIXa/FVIIIa

complex. Then FXa rapidly associates with FVa bound to the platelet during the amplification phase, producing a powerful increase in thrombin generation to provide rapidly to clot (Dahlback 2005, Monroe and Hoffman 2006). Due to the burst of production during propagation phase more than 95% of the total thrombin generated in a single event of clotting (Mann, Brummel et al. 2003).

The burst of thrombin generated on the platelet surface produces a stable clot structure, indeed, thrombin does additional actions responsible for clot stabilization: activation the fibrin stabilizing factor Factor XIII (FXIII) (Lorand 2001); cleavage of a receptor that contributes to the full activation of platelets the protease-activated receptor-4 (PAR-4)31]; and (Ofosu 2003) activation of thrombin activable fibrinolysis inhibitor (Bajzar, Manuel et al. 1995). Thrombin activable fibrinolysis inhibitor (TAFI) is a carboxypeptidase that removes terminal lysine residues from fibrin, thereby removing potential binding sites for fibrinolytic enzymes and enhancing clot resistance to fibrinolysis (Nesheim 1998) the failure in TAFI activation can contribute significantly to the bleeding tendency in hemophilia (Mosnier, Lisman et al. 2001).

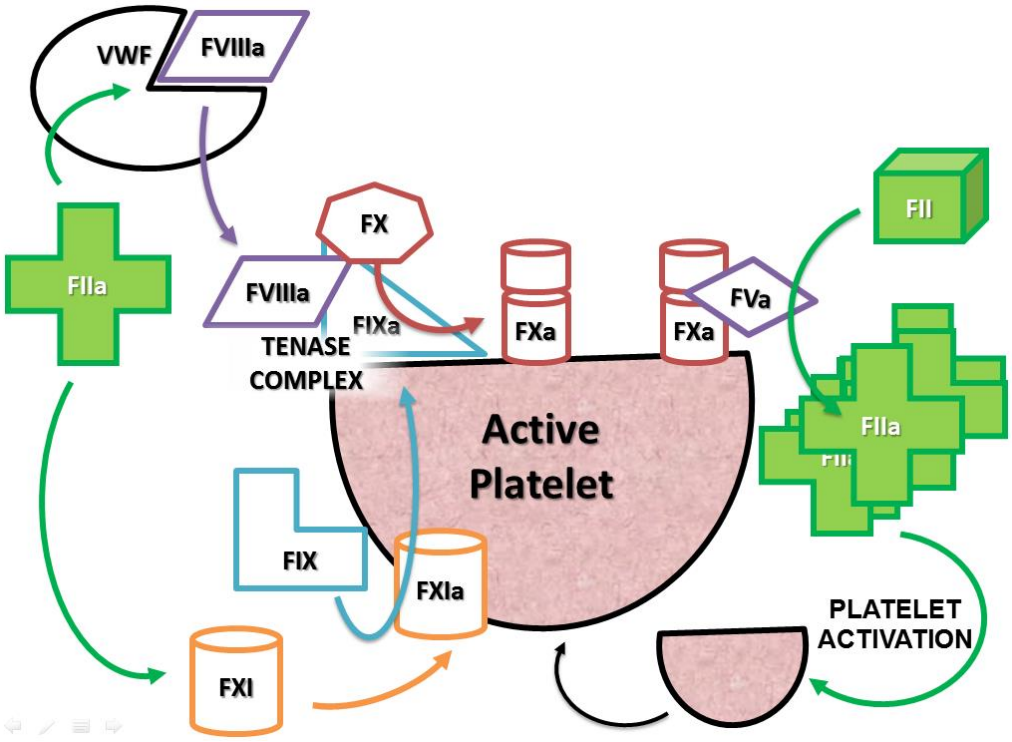

Figure 2: Cascade reaction and signal amplification during propagation phase.

Termination phase

Once a fibrin platelet clot is formed over a damaged area, the clotting process must be limited to avoid thrombotic occlusion in other normal areas of the vasculature (Hoffman 2003).

The TF/FVIIa activity is inhibited by the Kunitz-type inhibitor TFPI, secreted by endothelium. TFPI binds to FXa forming a quaternary complex with TF/FVIIa that quickly limits coagulation (Broze, Girard et al. 1990).

The serine protease inhibitor Antithrombin (AT) inhibit the enzymes of the coagulation system, its physiological role is to protect the circulation from free enzymes and limit the coagulation process to sites of vascular damage; AT is known as the major thrombin-inactivating protein (Beresford and Owen 1990). Circulating AT is a relatively inefficient, but its activity is stimulated by heparin and presumably by heparin-like molecules such as sulphated glycosaminoglycans that normally are synthesized and expressed by endothelial cells (Weitz 2003). This increased efficiency of AT by heparin is the molecular basis for the use of heparin as a therapeutic anticoagulant and coating for medical devices.

While TF-bearing cells and platelets have procoagulant functions, vascular endothelial cells have anti-coagulant features.

The protein C (PC) anticoagulant system inhibits the procoagulant functions of FVIIIa and FVa, the cofactors involved the tenase (FIXa/FVIIIa) and prothrombinase (FXa/FVa) complexes, respectively (Dahlback 2005). The key component in this system is PC, a vitamin K-dependent zymogen (pro-enzyme) and it is activated by thrombin bound to the membrane protein thrombomodulin (TM), that acting as a receptor for thrombin on the surface of intact endothelial cells. Upon binding to TM, the specificity of thrombin is changed, becoming more effective at activating PC than clotting fibrinogen or activating platelets (Ye, Esmon et al. 1991) changing its activity from a pro-coagulant to an anti-coagulant effect depending of its localization.

Activated PC (APC) cleaves just few peptide bonds in each of the phospholipid membrane-bound cofactors FVa and FVIIIa, resulting in the inactivation of the cofactors, moreover APC can also cleave the intact form of FV (Dahlback 2004). APC-mediated cleavage of factor V results in generation of anticoagulant FV that works in synergy with protein S as APC cofactor in the degradation of FVIIIa; indeed, FV can act as a procoagulant and as anticoagulant cofactor too, in fact procoagulant factor Va being formed by limited proteolysis by thrombin or factor Xa, anticoagulant FV activity is reached after proteolysis by APC (Dahlback 2000).

APC activity is enhanced by protein S (PS) another vitamin K-dependent inhibitory cofactor; normally in humans, protein S can be found for the ≈30% as of circulating free protein in plasma and the remaining ≈70% is bound to the complement regulatory protein C4b-binding protein, however only the free form of PS can works as a cofactor to APC.

In addition to TM and heperan-like glycosaminoglycans on surface of endothelial cells is present a cell-surface ADPase (CD39) that metabolizes ADP that is normally released from activated platelets, CD39 catalysis block aggregation of platelets in proximity to healthy endothelium to avoid uncontrolled aggregation and thrombus formation.

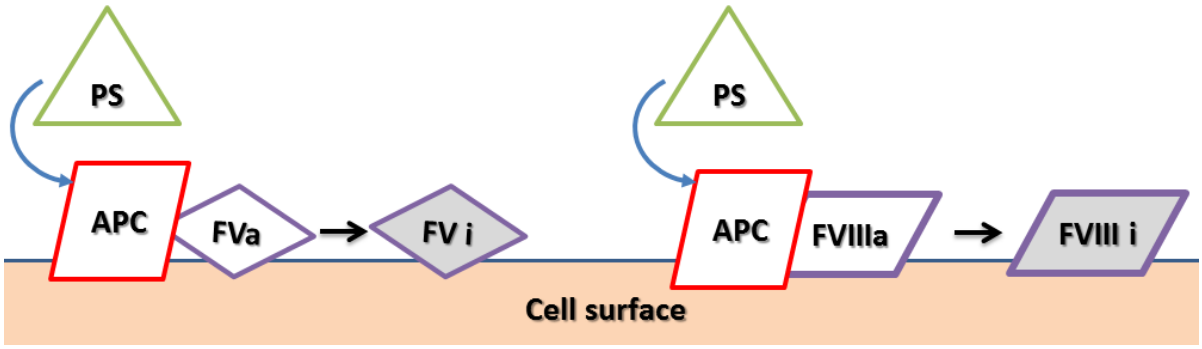

Figure 3: The protein C pathway on the left inactivation of FVa by APC and PS, on the rigth Inactivation of FVIIIa by APC and PS

Macromolecular complexes in blood coagulation

Activation and activity of clotting factors does not occur in the solution phase, but in macromolecular complexes on the membrane surfaces; each complex include a vitamin K-dependent serine protease, a non-enzymatic protein cofactor and a zymogen substrate, as well as Ca^{2+} ions (Mann, Nesheim et al. 1990).

Complex	Enzyme	Cofactor	Substrate
Initiation complex	FVIIa	TF	FIX, FX
Prothrombinase	FXa	FVa	PT
Intrinsic tenase	FIXa	FVIIIa	FX
Protein C-ase	Thrombin	TM	PC

Table 1: Macromolecular complexes in blood coagulation.

The protein-phospholipids and protein-protein interactions within the macromolecular complexes enhance reaction rates by several orders of magnitude, by affecting both the affinity constant (K_M) for the substrate and the turnover (k_{cat}) of the enzyme. Moreover, localization of different enzyme complexes on the same nearby membrane surfaces allows to canalize successive reaction, like industrial assembly line, this circumstance also protects activated factors from inactivation by circulating inhibitors (Neurath 1984).

Localizated on membrane and associated as macromolecular complexes, coagulation reactions are finely regulated. In fact complex assembly requires a number of simultaneous events: the conversion of a zymogen to the active serine protease, the activation of a procofactor to the active cofactor and the availability of negatively charged phospholipid membranes. All these different condition guarantees the confinement of the coagulation process to the site of injury escaping to the risk of uncontrolled thrombisis (Mann, Nesheim et al. 1990).

The catalytic domains of the coagulation serine proteases are highly homologous(Neurath 1984) but despite the similarities, the coagulation proteases act on their substrates with precision and distinctive specificity (Neurath 1984). It is assumed that the substrate specificity arises from specific interactions between the enzyme active site and distinctive

sequences surrounding the scissile bond. In the case of FVIIa-TF, this assumption is supported by similarities between the residues preceding the scissile bonds in FIX and FX.

A series of studies have suggested a role for extended interactions between FX and surfaces in both FVIIa and TF during FX activation and evidences support a direct interaction between the N-terminal Gla domain in the FX light chain and regions of the FVIIa-TF complex near the membrane surface (Ruf, Kalnik et al. 1991). Since the activation peptide at the N-terminus of the heavy chain of FX is released upon cleavage, it is possible that the interactions between the substrate and the FVIIa-TF complex involve structural determinants common to FX and FXa, suggesting the usage of a common region of TF in a dual role, as cofactor for FXa-mediated FVII activation and as cofactor for FVIIa-mediated FX activation moreover same TF domain would also contact FIX during its FVIIa-mediated activation (Kirchhofer, Lipari et al. 2000).

FIX

F9 gene

Coagulation factor IX gene (F9, MIM#300746, Genebank accession number K02402.1) is located on the long arm the X chromosome, more towards the centromere at Xq28, in region q27.1-q27.2.

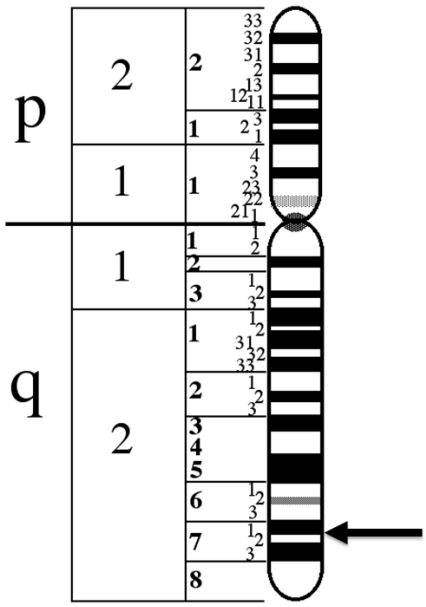

Figure 4: Localization of FIX gene on human X chromosome

The gene were cloned and sequenced by Kurachi e Davie in 1985; is approximately 34 kb in length and contains only eight exons named from a to h, the largest of which is only 1935 bp. The 95% of the transcript is composed by introns and the coding sequence is only 2803 bases in length and comprises a short 5' UTR (29 bp), an open reading frame plus stop codon (1383 bp) and a 3' UTR (1390 bp).

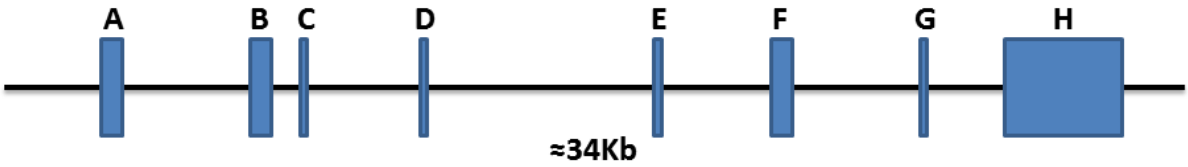

Figure 5: Schematic representation of human FIX gene.

FIX synthesis and maturation

The open reading frame encodes a pre-pro-protein of 461 amino acid. The first two exons (A, B) encode for pre-pro-peptide sequence (28 amino acid) that directs FIX to the endoplasmic reticulum for subsequent post-translational modification and secretion. The pro-peptide (18 amino acid) provides a binding domain for vitamin K dependent carboxylase, which carboxylates certain glutamic acid residues in the adjacent Gla domain (Anson, Choo et al. 1984). Part of exon B and exon C encode for the Gla domain which contains 12 residues of glutamic acid, that undergo ɣ-carboxylation. Exon D and E for 2 consecutive epidermal growth factor-like domains (EGF1 and EGF2) (Colman, Hirsh et al. 2001). Exon F encodes for the activation domain containing the cleavage sites for the FVIIa/TF complex leading to zymogen conversion into FIXa (Bowen 2002). The last two exons G and H encode for heavy chain where is located the serine protease domain, where take place the catalytic domain which is responsible for proteolysis and activation of FX to FXa.

FIX structure and activation

Factor IX also called Christmas factor or anti-haemophilic factor B, is a single chain protein synthetized in hepatocytes, secreted and freely circulating in blood flow as inactive zymogen. The biological relevance of this protein is glaring, in fact it has long been know that absence or low level activity of FIX causes haemophilia B (Biggs, Douglas et al. 1952).

Mature protein is 414 amino acid long with a molecular weight of 57 kDa, starting from N-end of the protein, first domain is extended for 46 amino acids and constitute Gla domain with 12 residues of ɣ-carboxylated glutamic acid this post translational modification guarantee correct protein folding and functionality of calcium binding domain (Li, Darden et al. 1997). Residues from 47 to 127 compose two EGF-Like domains, in second EGF-like domain we find a cysteine essential to keep joined FIX after activation, indeed from amino acid 128 and 195 is localized activation peptide that is removed after activation. Last 220 aminoacid compose the catalytic domain, where inside an hollow serine 365, histidine 221 and aspartic acid 269 compose the catalytic triad. Moreover is important to remind other important modification: asparagine 157 and 159, serine 61 and threonine 169 and 172 were glycosylated, partial hydroxylation of aspartic acid 64, sulphatation of tyrosine 155 and phosphorylation of serine 158, last but not least before secretion also pre-pro-peptide sequence were removed (Taran 1997, Colman, Hirsh et al. 2001).

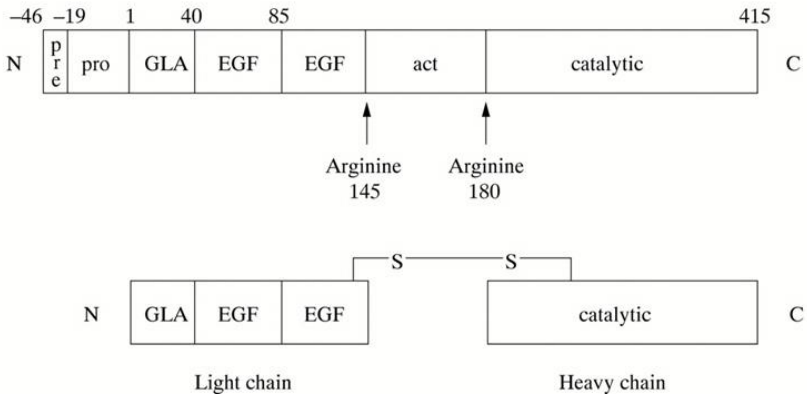

Figure 6: On top: FIX protein domains, on bottom: activated Factor IX comprising a N-terminal light chain and a C-terminal heavy chain held together by a disulphide bond between cysteine residue 132 and 279. Legend Gla: Gla domain; EGF: epidermal growth factor-like domain; Act: activation peptide released after proteolitic cleavage; catalytic: the serine protease domain.

Activation of factor IX involves cleavage of two peptide bonds, one on the C-terminal side of arginine 145 (α-cleavage) the other on the C-terminal side of arginine 180 (β-cleavage). These cleavages are caused by activated factor XI generated through the intrinsic pathway or via tissue factor/activated factor VII complex of the extrinsic pathway (Di Scipio, Kurachi et al. 1978). The activation cleavages generate an N-terminal light chain and a C-terminal heavy chain, held together by a disulphide bond between cysteine residues 132 and 279 (Bowen 2002).

Role of coagulation factor IX in the coagulation cascade.

Coagulation factors VIII and IX, whose deficiency are known to cause haemophilia A and B respectively, circulate as inactive precursors that are activated at the time of haemostatic challenge, via the intrinsic or extrinsic pathways (Zdziarska, Undas et al. 2009). As decribed before FVIII is a cofactor with no enzymatic activity per se; FIX is a serine protease with an absolute requirement for FVIII as cofactor. Upon activation, and in presence of calcium ions and phospholipid surfaces, FVIII and FIX form an active complex, which activates factor X. Subsequent stages of the cascade then proceed, culminating in the deposition of fibrin, the structural polymer of the blood clot (Bowen 2002).

Molecular basis of Hemophilia B

Hemophilia B (or Christmas disease) is a X-linked coagulopathy (Biggs, Douglas et al. 1952) caused by mutations in the *F9* gene. Generally, only male are symptomatic (incidence of 1:35000 live male births) due to the presence of two alleles in female subjects. Based on FIX levels (antigen and/or protein activity), patients experience severe hemorrhagic symptoms, not rarely life−threatening (central nervous system and gastrointestinal bleeds), or causing substantial handicap (hemarthrosis, muscle hematoma). Based on FIX levels on plasma, the phonotype of patients is classified as mild, moderate or severe:

- Mild , when the FIX level is included between 6 or 25% (0,05-0,40 IU/mL)

- Moderate, if FIX level is in 1-5% range (or 0,01-0,05 IU/mL)
- Severe , when the FIX level is below 1% or <0,01 IU/mL

Generally mild and moderate patients do not suffer of spontaneous hemorrhage, even if they can experience life threatening hemorrhage during surgery (even dentary surgery) if not properly treated. The mutations causing haemophilia B have been localized and characterized in several hundreds of patients. Based on the enormous number of mutations that have been elucidated it is clear now that the molecular bases of haemophilia are extremely diverse. Among all mutations, missense mutations are the most common (68%), followed by non-sense mutations (14%). Mutations altering splicing sequences have been found in 9% of all patients, with frame-shift mutation, promoter located and in frame deletion mutations ranging in 5%, 3% and 1% respectively. Point mutations (single nucleotide substitutions) are the most common gene defect and are present in approximately 90% of patients. Deletions are the second most common gene defects are present in approximately 5-10% of patients. Insertions and other rearrangements are quite rare within the haemophilia B population (Bowen 2002). The point mutations that occur in haemophilia B comprise missense mutation (these change a codon so that a different aminoacid is encoded), nonsense point mutation (these change an aminoacid codon into a translation stop codon), and mRNA splice site point mutations (these corrupt a true mRNA splice site, or create a novel one) (Koeberl, Bottema et al. 1990, Ketterling, Drost et al. 1999).

In particular mutations that destroy or create mRNA splice sites are associated with variable severity of haemophilia: this depends on whether some correct transcripts can be processed (mild to moderate disease) or whether there is a complete loss of correct mRNA processing (severe disease). Exon skipping is a possible consequence of a mutation affecting splicing: the outcome depends on whether the skip is in frame or results in a frame shift (Tavassoli, Eigel et al. 1998, Tavassoli, Eigel et al. 1998).

In haemophilia approximately 30% of mutations involves a CpG site; the remaining 70% of distinct point mutations do not occur a CpG sites and may arise, for example, as a result of nucleotide misincorporation during DNA replication (Bowen 2002).

In general nonsense mutations are associated with severe forms of haemophilia; exon skipping is a further possibility arising from a nonsense mutation and it is also extremely detrimental: an in frame skip will result in a protein lacking the aminoacids encoded by skipped exon, an out of frame skip will result in a frame shift (Dietz, Valle et al. 1993, Ketterling, Drost et al. 1999).

Deletions of *F9* gene include whole gene deletions, partial gene deletions at 5' or 3' end or within the gene, and microdeletions of one to several base pairs. A deletion, in general, has a high probability of destroying genetic function, removing domains of a protein, or introducing a frame shift, all of which are extremely detrimental. Therefore is not surprisingly that deletion are associated with severe forms of the disease (Cooper 1991, Giannelli and Green 1996).

Conventional treatment strategies hemophilia B

The current treatment is based on the intravenous administration of FIX (replacement therapy), either plasma derived or recombinant (Carcao and Aledort 2004, Pipe, High et al. 2008). However, there are still limitations that encourage research towards alternative therapeutic approaches. Moreover, the administration of a protein that the body is not able to synthetize by itself results, in a long term therapy, in the development of neutralizing FIX antibodies. The costs of substitutive treatments (≈50000 euro/year/person with severe disease) are prohibitive for the majority of the world hemophilia populations, so the demand for alternative therapies is growing up.

Enormous efforts have been pushed on substitutive gene therapy, and very recently it has been demonstrated that intravenous infusion of a AAV vector encoding FIX in HB patients resulted in FIX expression ranging from 1% to 6% for periods of 2 years, with amelioration of bleeding phenotypes (Nathwani, Tuddenham et al. 2011). DNA editing by using zinc finger nucleases has been also exploited in HB mouse models (Wang, Louboutin et al. 2011).

Von Willebrand Factor

Von Willebrand Factor in hemostasis

Von Willebrand Factor (VWF) is multimeric glycoprotein that play a major role in hemostasis; in normal condition it circulates inactive in plasma in a globular state, but in case of vascular injury, the shear stress and subendothelial matrix convert VWF in its active state, allowing platelet adhesion and aggregation; its function as a bridge is essential for the platelet plug formation because platelets are unable to bind directly matrix components; Moreover VWF is the plasmatic carrier of FVIII 8-10; preventing FVIII premature clearance from circulation (Arnout, Hoylaerts et al. 2006).

VWF plasmatic level is around 10 μg/ml, with 12 h of half-life but its levels are very variable into the population; plasmatic levels are genetically determined for the 66% and of this percentage, ≈30% of can be explained by ABO blood group, in fact people carrying blood group O usually have form 25% to 35% VWF antigen below the average of other groups (Gill, Endres-Brooks et al. 1987).

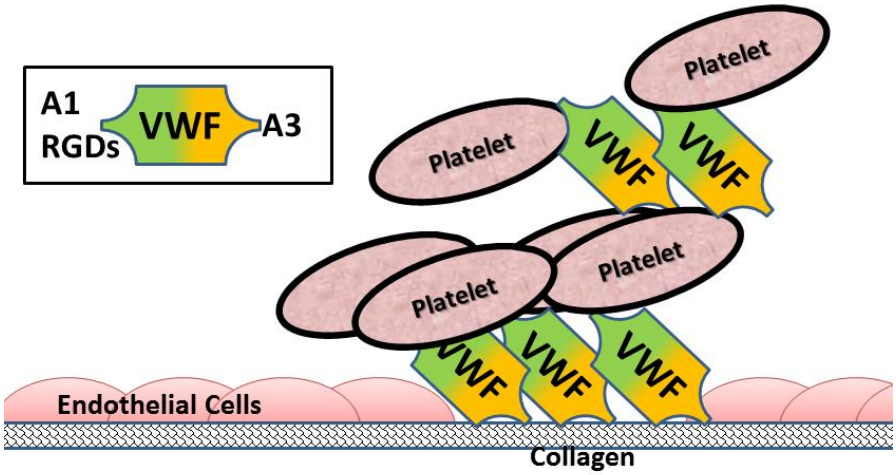

Figure 7: schematic representation of VWF interaction during endothelium damage.

Von Willebrand Factor structure and biosynthesis

VWF gene (178 kb) is located on the short arm of chromosome 12 (12p13.3), also present in human genome a pseudogenic fragments, which contain exons 23-28 (Marchetti, Patracchini et al. 1991). The funtional transcript is normally expressed only in endothelial cells and megakaryocytes, it is 9kb long and it contains 52 exons (Jaffe, Hoyer et al. 1974).

The protein is a single chain of 2813 amino acids and include a 22 residues of signal peptide, 741 residues of pro-peptide and finally the mature subunit of 2050 residues (FIGURE).

All the protein is composed by an highly repetitive structure with four mains domains, these domains have different function in maturation or activity of the mature protein (Springer 2011).

Pre-pro-VWF is translocated to the endoplasmic reticulum (ER) where it is extensively glycosylated but most important is the dimerization of "Cysteine Knot" (CK) domain (Katsumi, Kojima et al. 1998).

Dimerization occurs by disulfide bond formation between two C-terminal CK domain of two molecules of VWF; after dimerization proVWF dimers transported into the Golgi where the protein is N and O-linked glycosylated (Samor, Michalski et al. 1989). When VWF move to trans Golgi, Furin cut the D1-D2 domains of pro-peptide cleavage occurs and the process called multimerization will start (Sadler 2009); two D'D3 amino-terminal regions of align and multiple cysteine bond were formed (Springer 2011). VWF Multimers, which can rise above 20000 kDa and usually they were constitutively secreted (95%) of stored in Weibel-Palade body (WPB) in endothelial cells and α-granules in platelets (Michaux and Cutler 2004).

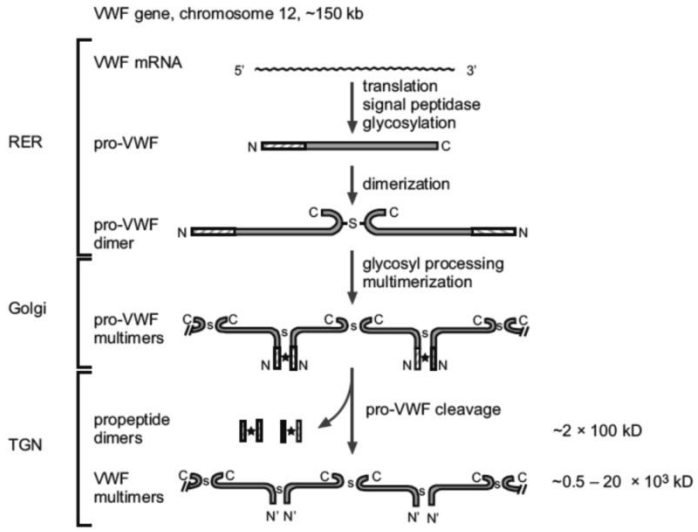

*Figure 8: Biosynthesis steps of von Willebrand factor. *:on-covalent interaction; s:disulphide bonds. (Verweij 1988)*

WPBs appear as tubules surrounded by a membrane and their formation is the direct consequence of multimerization. Release of WPB usually happens at sites of vascular damage where thrombogenic molecules are needed or after stimuli (Reininger 2008). Once secreted in blood flow, VWF size is well regulated by the enzymatic activity of a metallo-protease named ADAMTS-13 (Fujikawa, Suzuki et al. 2001).

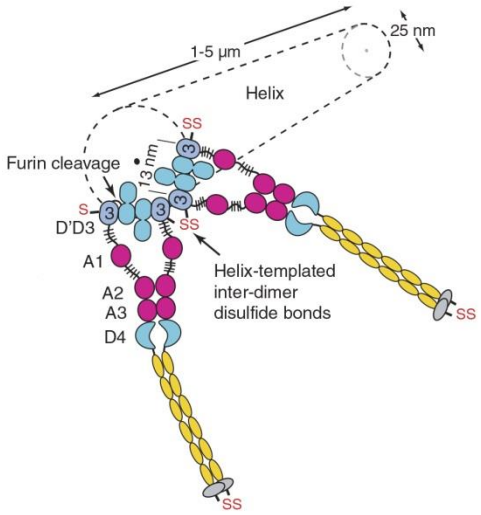

Figure 9: Weibel-Palade bodies formation and assembly, adapted from (Springer 2011)

VWF domains

After prepeptide first two domains D1-D2 contains pro-peptide which dispalys has signal and maturation features (Sadler 2009), then in D' and D3 domain we can find FVIII and heparin binding site, moreover it may contain the site of interaction for P-selectin which appears to anchor released ultra-large multimers to the surface of activated endothelial cells and contribute to present ADAMTS-13 cleavage site (Pimanda and Hogg 2002).

Following domains are A1-2 domains that contains the binding site for: platelet receptor GPIbα, heparin, botrocetin and probably also a binding site for collagen (Ruggeri 2007); moreover in A2 domain is present ADAMTS-13 cleavage site and in A3 domain are present the binding sites for type I and III collagens. C1 domain is known to host the RGD sequence for Integrin αIIβ3 binding. (Schneppenheim and Budde 2011). In the carboxyl terminal domain of the protein is present CK domain that as mentioned before it contains the essential cysteine for dimers formation (Schneppenheim, Budde et al. 2001, Tjernberg, Vos et al. 2004).

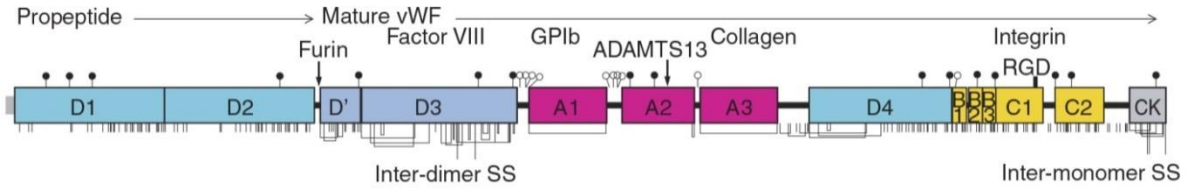

Figure 10: pre-pro-VWF domain organization (Springer 2011)

Von Willebrand Diseases

Von Willebrand Diseases (VWD) are a cluster of genetic inhered disorder characterized by deficient or defective VWF; VWD are considerate one of the most common inherited coagulation disorder in humans, in fact estimation shown that about the 1.3% of the population have reduced levels of VWF but only 1/1000 displays symptom of the disease (Keeney and Cumming 2001).

VWD were descrived for the first time in 1926 (Willebrand 1999 (1926)) but only in 1950 we isoled the "plasma factor" actually called VWF and actually 701 unique variant of this gene were reported (on line database http://www.vwf.group.shef.ac.uk)

Due to VWF peculiar characteristic and functions VWD displays a wide heterogeneity of symptoms that can be associated to qualitative and or quantitative defects. (Schneppenheim, Budde et al. 2001, Lillicrap 2007)

Von Willebrand disease was classified in three major categories:

- Type 1: it is the most frequent groups with around the 80% of total cases of VWD, it is characterized with quantitative deficiencies, patients shown reduced VWF levels from 40 to 1% of normal plasma levels, also factor VIII may be reduced;
- Type 2 collect all qualitative deficiencies of VWF, this class due to heterogeneity of defects is divided in 4 subgroups 2A, 2B, 2M and 2N;
- Type 3 is the most rare with the approximate prevalence of one on one million, it is characterized by the total absence of VWF and also FVIII levels are strongly impaired.
- Platelet-type or pseudo VWD is similar to Type 2B, but in this type the affected element is the platelets receptor GpIb.

Type 1 VWD show mild to moderate quantitative deficiency of VWF affecting multimers of all sizes, but VWF functionality is normal. Inheritance of this type is typically dominant with highly variable penetrance. Due to its variability diagnosis is difficult and the borderline between low VWF and type 1 still controversial.

Type 2 is a group that gather all qualitative defects; subclasses 2A, 2B, 2M displays common features, showing dominant inheritance, low VWF antigen, impaired collagen binding and increased bleeding time. Type 2N usually displays recessive trait and distinctive characteristics.

Type 2 A show the peculiar signature of VWF:RCo – VWF:Ag ratio <0,6; moreover this subclass show abnormal multimers pattern, normal or decreased FVIII antigen and it appear to be more susceptible to ADAMS-13 cleavage. This class is also divided in subtypes IIC, IID and IIE/F depending of the different mechanism of HMWMs impairment.

Type 2 B is characterized by gain-of-function of platelet binding, resulting in HMWM abnormal multimers pattern and platelets reduction.

Type 2 M is a sort of other face of the coin of type 2 B, it is characterized by defective binding to GpIb but with normal multimers pattern.

Type 2 N is different from all other types, it is characterized by decreased FVIII levels in the circulation due to inability of VWF to bind FVIII results in increased clearance of unbound FVIII; clinical symptoms are more similar of those of Haemophilia A.

Type 3 VWD is a recessive form of this disease and usually this type of VWD is caused by two null mutations; due of low or none circulating VWF also FVIII is impaired with plasmatic levels below 10% of PNP.

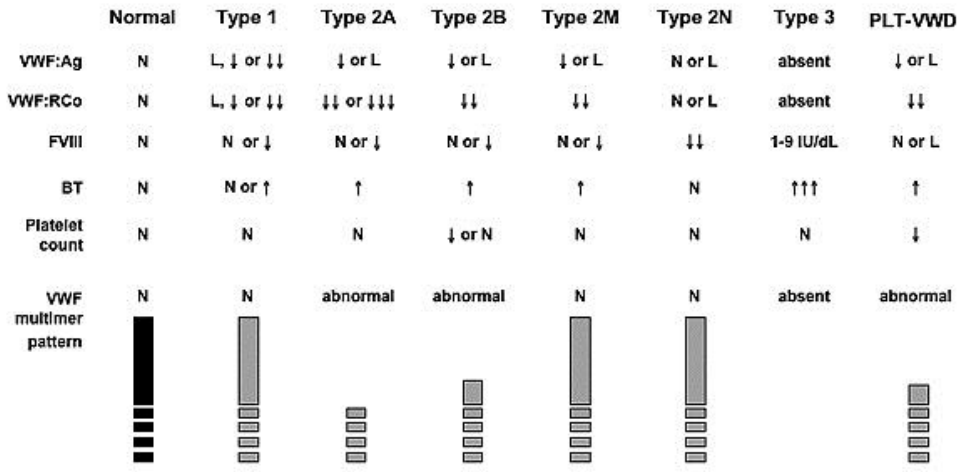

Figure 11: L, 30—50 IU/dL; ↓, ↓↓, ↓↓↓, relative decrease; ↑, ↑↑, ↑↑↑, relative increase; BT, bleeding time; FVIII, factor VIII activity; N, normal; VWF:Ag, VWF antigen; VWF:RCo, VWF ristocetin cofactor activity. (Montgomery RR; http://www.nhlbi.nih.gov/guidelines/vwd/3_diagnosisandevaluation.htm)

Aim of the PhD thesis

My PhD research activity has been focused on the molecular mechanisms leading to severe deficiency of two proteins having key roles in the coagulation cascade (Factor IX) or in the primary Hemostasis (von Willebrand factor).

In particular, I investigated mechanisms due to three different molecular defects such as nonsense and missense mutations in F9 gene, associated with type I hemophilia B, and an in-frame deletion in the VWF gene, displaying a dominant-negative effect.

Hemophilia B is a rare disorder with a incidence of 1:35000 live male births that is associated with hemorrhagic tendency. Current treatment is based on the infusion of FIX. The replacement therapy either plasma derived or recombinant still have limitations that encourage research towards alternative therapeutic approaches. Moreover, the administration of a foreign protein, in a long term therapy, can result in the development of neutralizing FIX antibodies.

The study of FIX nonsense mutations, was triggered by the observation that nonsense mutations are associated with a risk of developing inhibitors lower that deletion. We therefore studies whether certain nonsense mutations, depending on the sequence context, undergo ribosome readthrough and are associated with trace levels of full-length FIX molecules. Moreover, we studied whether the readthrough can be induced by aminoglycosides, an approach that can have therapeutic implications.

The study of the FIX Tyr450Cys missense mutation was aimed at investigating the interplay between mechanisms impairing protein biosynthesis and function that is poorly defined, particularly in relation to specific protein regions.

Von Willebrand Factor is multimeric glycoprotein that play a major role in hemostasis. Von Willebrand Diseases are a cluster of genetic inhered disorder characterized by deficient or defective VWF and are considerate one of the most common inherited coagulation disorder in humans (1.3%) however only around 1:1000 displays disease symptoms. Dimerization and multimerization are distinct property of VWF biosynthesis both necessary to guarantee VWF production, activity and function.

In last part of the PhD, I focused my attention to the elucidation of the dominant-negative mechanisms leading to a VWF disease form caused by the P1105_C1926delinsR mutation in heterozygous condition. The approach was based on the evaluation of the VWF expression and maturation, in the presence of the mutation alone or in combination with a missense change impairing dimerization, both in cellular and mouse models.

Chapter 1

Ribosome Readthrough Over Nonsense Mutations influences the Residual FIX expression

1.1 Ribosome Readthrough Accounts for Secreted Full-Length Factor IX in Hemophilia B Patients with Nonsense Mutations

Mirko Pinotti, Pierpaolo Caruso, Alessandro Canella, Matteo Campioni, Giuseppe Tagariello, Giancarlo Castaman, Sofia Giacomelli, Donata Belvini, Francesco Bernardi

Based on: Hum Mutat. 2012 Sep;33(9):1373-6

Introduction

The mechanism through which nonsense mutations impair gene expression and cause human genetic disease (Mort, Ivanov et al. 2008) consists of premature translation termination, and synthesis of truncated proteins, with loss-of-function features. Moreover, these mutations can trigger nonsense-mediated mRNA decay (NMD) (Khajavi, Inoue et al. 2006). With this as background, they are commonly believed as responsible for null genetic conditions.

However, the mechanism of ribosome readthrough, consisting of mis-recognition of the premature stop codon by an aminoacyl-tRNA instead of the termination factors (Rospert, Rakwalska et al. 2005), could restore translation impaired by nonsense mutations. Even if this process is expected to occur at low rate, it might account for minimal full-length protein biosynthesis.

Translation termination

It has long been known that termination of translation is an essential process in cell physiology since it permits the release from the translational machinery of the neo-synthetized protein of the proper size.

The translation termination is encoded on mRNA by codons called stop or nonsense codons (Brenner et al. 1965, 1967), most part of species on earth use three codons to mediate the signal of end of translation: UAA, UAG and UGA. In eukaryotes all three stop codon are recognized by eRF1 (class I release factor), this protein play the key role to recognize with high fidelity the stop codon and recruit eRF3 (class II release factor), a GTPase, and together these two factors collaborate to hydrolyze the bound between the nascent protein and the t-RNA present in the site P of the ribosome(Alkalaeva, Pisarev et al. 2006), releasing the protein and the whole translational machinery guaranteeing the recycle of all different components from ribosome to mRNA (Dever and Green 2012).

Nonsense mutations

Inspection of the Human Gene Mutation Database strongly highlights the relevance of nonsense mutations, which account for ≈20% of the pathogenic single point mutation (www.hgmd.org).

A bio-statistical analysis of human genes shows that the three different stop codons occur with different frequency, the most frequent is the codon TGA (49,5% of genes) followed by TAA and TAG with 28,1% and 22,4% respectively (Sun, Chen et al. 2005) (Jacobs, Rackham et al. 2002) (figure 12).

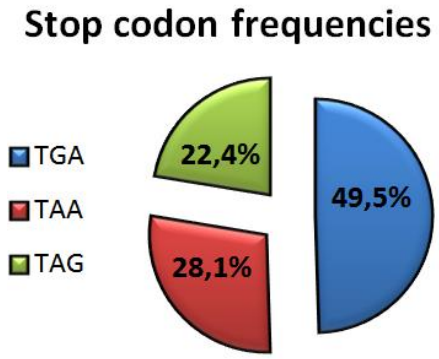

Figure 12: Stop codon frequencies in human transcripts. Data from: Sun, Chen et al. 2005.

When disease-causing stop codons are compared with authentic stop codons it results that the proportion of TAG is significantly higher (40,4 %, p<0,0001) and TGA and TAA proportions are lower (38,5% and 21,1% respectively) (Mort, Ivanov et al. 2008). These discrepancy can be explained in the light of the frequency of most common transition (C→T) that is responsible of 46% of nonsense mutations. As a matter of fact, only 18 codon (10 amino acids) can be directly converted into stop codon; moreover the confirmation of these findings are the two most frequent nonsense mutated codons: CGA (Arg) and CAG (Gln) (Mort, Ivanov et al. 2008) (table 2).

Codon	Amino acid normally encoded	Mutating to:	Codon	Amino acid normally encoded	Mutating to:
CGA	Arginine	TGA	TTG	Leucine	TAG
AGA	Arginine	TGA	TTA	Leucine	TGA / TAA
TGT	Cysteine	TGA	AAG	Lysine	TAG
TGC	Cysteine	TGA	AAA	Lysine	TAA
CAG	Glutamine	TAG	TCG	Serine	TAG
CAA	Glutamine	TAA	TCA	Serine	TGA / TAA
GAG	Glutamic acid	TAG	TGG	Tryptophan	TGA / TAG

GAA	Glutamic acid	TAA	TAT	Tyrosine	TAG / TAA
GGA	Glycine	TGA	TAC	Tyrosine	TAG / TAA

Table 2: Normally occurring amino acids codons that can be converted into stop codon by single nucleotide mutagenesis. Adapted from : (Mort, Ivanov et al. 2008)

When a mutation produces a premature termination codon (PTC) on the genomic DNA, the resulting mRNA can run into multiple different consequences: the first and simplest is the translation into a truncated protein, this protein usually is unable fold and for this reason is retained into the cell and then degraded by the unfolded protein response (UPR). Moreover, the mRNA can undergo degradation by the nonsense-mediated decay process (NMD) (Khajavi, Inoue et al. 2006).

The NMD is a mRNA surveillance system that can lead to degradation of mRNAs harboring a premature termination codon (PTC). NMD allow to eliminate aberrant and abnormal transcripts inside the cell, this process take place outside of the nucleus, during the first translation, called "pioneer round"(Ishigaki, Li et al. 2001). During pioneer round, in normal condition, the ribosome remove all the exon junction protein (EJP), these proteins are left on the junction of the exons by the splicing process, these proteins in fact work as marker of the exons and they play a critical role in PTC recognition process. The ribosome in first translation by simply steric displacement remove EJP proteins till the end of the mRNA and also removing other proteins called Upf which are essential trigger of NMD. If a PTC is present in the mRNA sequence, the ribosome pauses on it and the releasing factors eRF1 and eRF3 associate with the ribosome to start disassembling, then Upf 1-2-3 proteins which are bounded to EJP, take contact with the termination complex triggering NMD and consequently mRNA degradation (Lejeune and Maquat 2005).

Nevertheless, some transcripts can escape the NMD, indeed also in normal transcripts a stop codon is present, normally in the last exon, and for this reason NMD cannot distinguish PTCs present less than ~55bp from the last exon junction. Probably this distance is derived from the dimension of ribosome that displace the EJP before recognize the stop codon (figure 13) (Le Hir, Izaurralde et al. 2000).

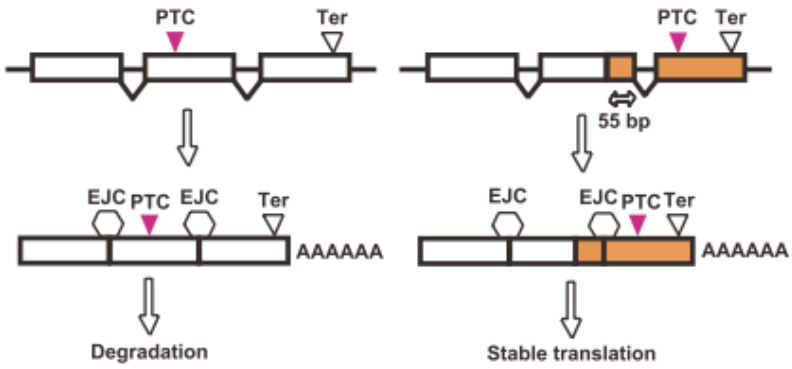

Figure 13: simplified model of NMD discrimination in case of PTC in different position (Khajavi, Inoue et al. 2006)

Not only PTC activate NMD. Indeed, another source of PTC are the errors due to high processivity of the ribosome that can slip on mRNA and result in frame-shift, out-of-phase or "drop off" PTC (Dong and Kurland 1995).

Having this as background, the NMD process is extremely critical and it is important to remind how NMD protect limits the synthesis of dominant-negative truncated proteins, or of gain-of-function dangerous proteins and, last but not least, the accumulation of protein aggregates and cell death due to UPR.

Readthrough

Notwithstanding the conservation along the evolutive tree and the critically role of this process, the termination of translation can misrecognizes the stop codon through a process called "ribosome readthrough". Although known since 1974, this phenomenon is still poorly explored. As a matter of fact, the first explicative paper on this topic was written in 2000 from Manuvakhova.

The readthrough process consists in the misrecognition of the stop codon by an aminoacyl-tRNA instead of eRF1, this event entail the skipping of the stop codon and the prosecution of the translation till the successive stop codon. This event occurs when a cognate tRNA successfully competes with the termination factors, and an amino acid is incorporated into the protein sequence. This type of readthrough hits all three stop codons and is important to discern this kind of readthrough from the selective readthrough, resulted from an aa-tRNA that decode a stop codon when only one termination codon is suppressed (Stansfield and Tuite 1994).

The three different stop codons (TGA, TAA and TAG) show strong differences from the point of view of the readthrough efficiency. The different readthrough efficiency observable among the literature, is due to the impact of type of stop codon and the surrounding sequence. As a first step just observing the three stop codon we can appreciate differences of readthrough from 0,2% to 3,8% (see table 3 for details) (Manuvakhova, Keeling et al. 2000).

Stop codon	Spontaneous readthrough
UGA	0,6 - 3,8 %
UAG	0,8 - 1,6 %
UAA	0,2 - 0,5%

Table 3:Spontaneous readthrough of different stop codon (Manuvakhova, Keeling et al. 2000)

These strong differences (obtained by reporter gene system) underline the complexity of this scenario, and pose questions concerning the cause of this differences; in the same study, analysis of the first base after the stop codon reveals how much just a single base can influence the readthrough process (table 3).

Codon		Readthrough		Codon		Readthrough		Codon		Readthrough	
UGA	A	1,0	%	UAG	A	0,9	%	UAA	A	0,2	%
UGA	C	3,8	%	UAG	C	1,1	%	UAA	C	0,5	%
UGA	G	0,6	%	UAG	G	0,8	%	UAA	G	0,4	%
UGA	U	0,7	%	UAG	U	1,6	%	UAA	U	0,2	%

Table 4: Spontaneous readthrough of different stop codon and the sequence context (Manuvakhova, Keeling et al. 2000)

Several studies indicated that the differences on readthrough depend on the nonsense triplet and its sequence context, and demonstrated that the downstream sequence context can influence the "score of readthough" of each stop codon. In yeast, the presence of a peculiar consensus sequence appears to promote more than 5% of readthrough (figure 14) (Namy, Hatin et al. 2001).

Figure 14: Downstream sequence for high readthough levels in yeast (sequence from: Namy, Hatin et al. 2001)

The readthrough is directly connected to the translational fidelity, for this reason everything that impairs fidelity can change readthrough occurrence. The signs of this double linkage, appear clearly events that involve readthrough and cytoskeleton; indeed actin mutants shown increased readthrough of stop codon (Kandl, Munshi et al. 2002) and moreover low levels of eRF3 increase readthrough and impairs the cytoskeleton (Valouev, Kushnirov et al. 2002); despite different studies on this field, significance of these interconnections still unclear.

Moreover, readthrough efficiency can be influenced by drugs impairing ribosome fidelity such as the antibiotic class of aminoglycosides. Eukaryotic cells are enough resistant to the toxic effect of aminoglycosides due to the 20-50-fold lower affinity of this family of drugs with human ribosome than bacteria ribosome, nevertheless our ribosome still susceptible to the misreading effects of these drugs (Chattoo, Palmer et al. 1979) and this opportunity opened the studies on readthrough induction (see below).

Readthrough in human disease

As previously described the readthrough process physiologically occurs at low rate (10^{-4}), thus providing the rationale for defining the nonsense mutations as associated "null genetic condition". However, by investigating nonsense mutations in *LAMA3* gene, it has been recently demonstrated that the phenomenon of readthrough can occur *in vivo* and produce appreciable amounts of full-length protein, thus potentially influencing the clinical phenotype of patients (Pacho, Zambruno et al. 2011). In this study, a child was found to be compound heterozygous for two different nonsense mutation R943X and R1159X, but manifested a very mild form of Junctional Epidermolysis Bullosa. It turned out that the ribosome readthrough accounted for the presence of full-length laminin-332 α3 chain and accumulation of lamini-332. The evidence of readthrough in human is easy to demonstrate

for protein like LAMA3, which is a structural protein (laminin-332 α3 chain) accumulating over time in cells. While this feature magnifies the readthrough effects, it does not favor the proper assessment of mutation-dependent readthrough rate. So far, no data have been provided on secreted proteins with limited half-life such as coagulation factors (from few hours to few days) (Furie and Furie 1992), which would better reflect the spontaneous ribosome readthrough efficacy *in vivo*.

Aim of the study

Among the molecular defects responsible for FIX deficiency, single point mutations leading to missense and nonsense mutations represent the 85,0% of all pathological mutations (figure 8) (Rallapalli, Kemball-Cook et al. 2013).

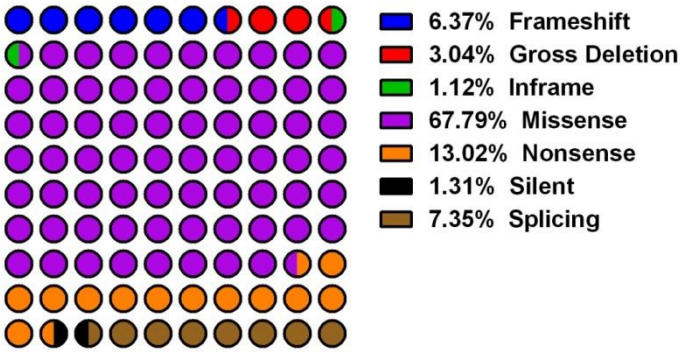

Figure 15: Whole FIX mutation present in global database. Total cases reported: 3580

Aim of the study was to investigate the occurrence of ribosome readthrough over nonsense mutations in *F9* gene and the presence of trace levels of full-length FIX protein in HB patients. We planned to investigate three nonsense mutations in *F9* gene (MIM# 300746; GenBank accession number K02402.1) differing in position and sequence context, which are candidate determinants of ribosome readthrough. Studies in plasma from HB patients and *in vitro* were undertaken to evaluate their differential impact on mRNA and protein biology.

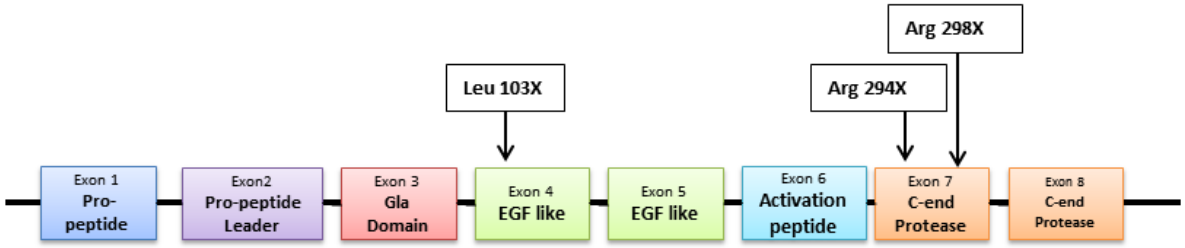

Figure 16:Patients' scheme of position of different FIX stop mutation in this study

Patients' data and analysis

Plasma samples from severely affected HB patients bearing the Leucine 103 Stop (P-103X), Arginine 294 Stop (P-294X) and Arginine 298 Stop (P-298X) nonsense mutations (Belvini, Salviato et al. 2005), and also reported in the Human Gene Mutation Database,

http://www.hgmd.cf.ac.uk] were exploited to investigate the impact of ribosome readthrough *in vivo* (table 5).

Patient	P-103X	P-294X	P298X
Mutation	Leu 103 Stop	Arg 294 Stop	Arg 298 Stop
Sequence context	TGTTAAAA	AAGTGAAA	ATTTGAAT

Table 5: Patients' data, nonsense mutation and sequence context

Plasma samples of patients P-103X and P294X were collected after a wash-out period of one week, plasma of patient P-298X upon a 70 hour wash-out period. The half-life of the infused recombinant FIX (BeneFix, Wyeth, Taplow, UK) is around 20 hours, thus not allowing us to ruled out the presence of confounding residual FIX protein levels in P-298X plasma.

Patient	P-103X	P-294X	P-298X
Mutation	Leu 103 Stop	Arg 294 Stop	Arg 298 Stop
Sequence context	TGTTAAAA	AAGTGAAA	ATTTGAAT
FIX:Ag	<1%	<1%	1%
FIXc	<1%	<1%	1.5%

Table 6: Patients' antigen and activity levels.

Antigen and activity were undetectable in plasma of patient P-103X and P-294X. In plasma from P-298X we revealed traces of circulating FIX antigen (1.5% of PNP) that were associated with measurable FIX activity (1%) (table 6).

To verify the presence of the transcript or the activation of NMD we investigated the presence of the FIX mRNA in patients, trough analysis of leukocyte mRNA by reverse transcription followed by polymerase chain reaction (RT-PCR) (Pinotti, Toso et al. 1998).

While the housekeeping GAPDH mRNA was clearly detected in all samples, the correct amplified FIX fragments were identified in P-294X and P-298X only (Figure 17).

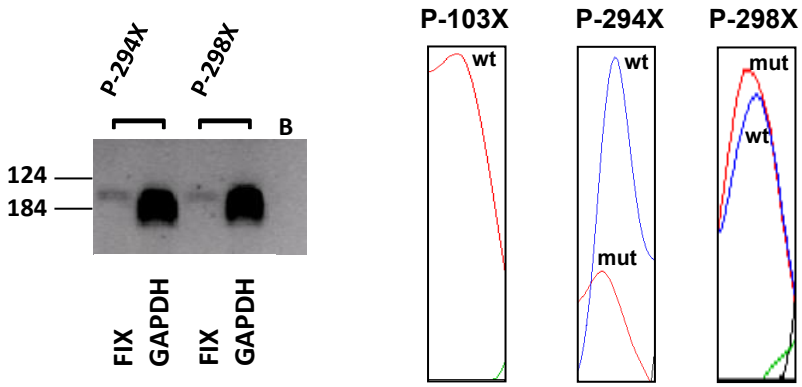

Figure 17:RT-PCR products and chromatograms of mRNA from leukocytes of female carrier. B:Blank

Moreover, RT-PCR and sequencing was exploited for a semi-quantitative estimation of the mutant *versus* normal FIX mRNA forms in female mutation carriers. The expression of the mutated FIX mRNA was appreciable in carriers of the P-294X and P-298X mutations, but not in the P-103X carrier, these findings suggest that being L103X mutation an early stop codon, was expected to trigger major NMD (Figure 17); opposite the data obtained at the ectopic mRNA level, do not support major NMD for the P-294X and P-298X mutations.

Subsequently we analyzed patients' plasma trough western blotting, optimized to investigate low levels of FIX molecules in plasma, undetectable with other methods.

Evidence for the occurrence of readthrough *in vivo*

Patients' plasma samples were diluted 1:30 in PBS buffer, and pooled normal plasma (PNP) diluted 1:100 were used as internal reference. Plasma patient's P-103X, in which NMD prevents the synthesis of FIX, was used as negative control. Commercially available FIX deficient plasma was also used as negative control in setup experiments but, being immuno-depleted, it might contain traces of FIX protein that could have confounding effects in our assays aimed at evaluating very low protein amounts.

Western blotting analysis (figure 18) clearly shown a band corresponding to full-length FIX (57kD) in P-298X plasma, and upon film over-exposure, in P-294X plasma. This band was undetectable in P-103X's plasma, which as mentioned before provided us with an internal negative control and validated the specificity of the antibody used. We have no interpretation of lighter bands (≈50kDa) present in samples but not in PNP. However this band is also present in patient P-103X in which we have demonstrated activation of NMD. This led us to hypothesize that the extra-band is not FIX-related.

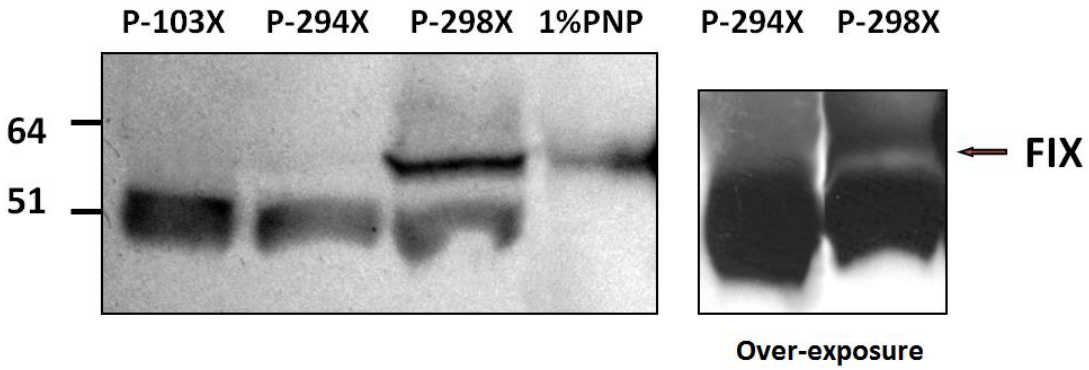

Figure 18: Western blotting of patients' plasma; left panel 1 h exposure, right over-night exposure.

Evidence for the occurrence of readthrough *in vitro*

To validate our results on plasma samples we conducted expression studies in eukaryotic cells to investigate the occurrence of readthrough over the different nonsense triplets, and its rate.

As mentioned before several studies have been conducted *in vitro* with different intents and exploiting reporter genes. In our study, we inserted the nonsense mutations into the full-length human FIX cDNA and investigated the proteins secreted in medium, thus favoring the comparison of truncated and full-length molecules, and therefore the evaluation of readthrough effects in the proper nucleotide (table 7) and protein context (figure 19).

Mutation	Leu 103 Stop	Arg 162 Stop	Arg 294 Stop	Arg 298 Stop
Sequence context	TGTTAAAA	TATTGACTT	AAGTGAAA	ATTTGAAT
Predicted Readthrough	<0,5	3-4%	1%	1%

Table 7: Mutation, sequence context and predicted readthrough of different mutations

Ee expressed these four nonsense FIX mutants and analyzed the secreted FIX protein in media through ELISA and Western Blotting

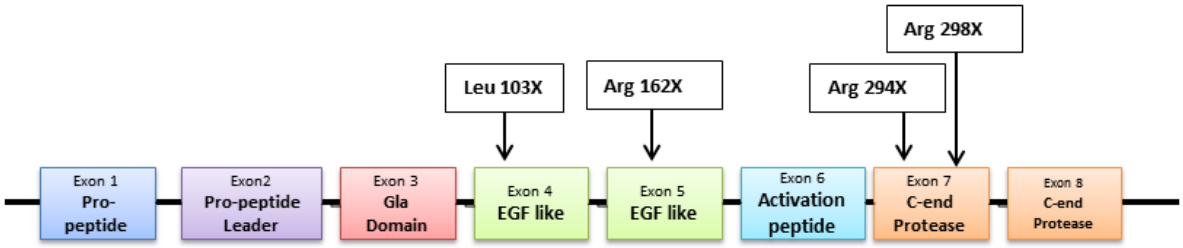

Figure 19: Position of different FIX nonsense mutations

In this experimental model, the recombinant rFIX-294X and rFIX-298X molecules were secreted at appreciable level respectively the 3.1±1.1% and 2.5±0.7% of rFIX-wt, whereas

not surprisingly rFIX-103X antigen was undetectable in medium (figure 20). However antigen levels obtained through ELISA cannot discriminate between truncated and full-length form of the protein, for these reason western blotting analysis is a forced analysis to verify the presence of full-length protein.

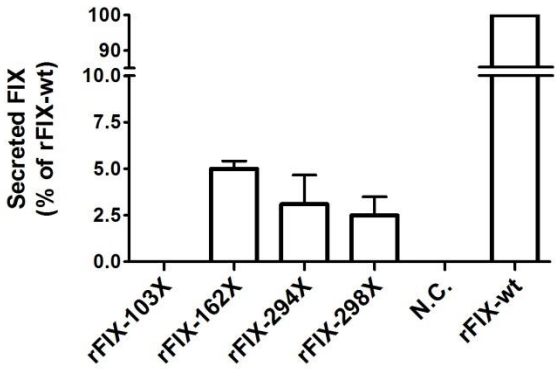

Figure 20:Media antigen levels of recombinant FIX variants expressed as percentage of rFIX-WT

Western blotting of medium from the rFIX-294X and rFIX-298X expressing cells revealed a large proportion of truncated FIX forms (figure 21), which were not detected in patients' plasma probably because of removal from circulation of this partial forms of the protein. As expected, FIX was not detected in medium from cells expressing the rFIX-103X.

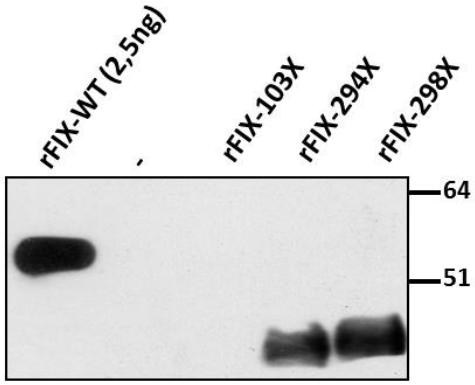

Figure 21: Western blotting analysis of conditioned medium from recominant FIX variants. "-" :Negative control

Comparison of results from ELISA and Western blot indicated that the truncated variants were secreted with lower efficiency than rFIX-wt, which is consistent with the essential role of the FIX carboxyl-terminal region for secretion (Kurachi, Pantazatos et al. 1997).

Noticeably, overexposure of films (figure 22) showed a form compatible with full-length FIX, with an intensity of approximately 0.2% of rFIX-WT in rFIX-294X and rFIX-298X media.

Moreover the band corresponding to full-length FIX was absent, even upon overexposure, in rFIX-103X and in the empty pCMV5, thus emphasizing the specificity of the signal detected. This differential readthrough efficiency might have contributed to appreciate mutated mRNA in carriers (figure 17).

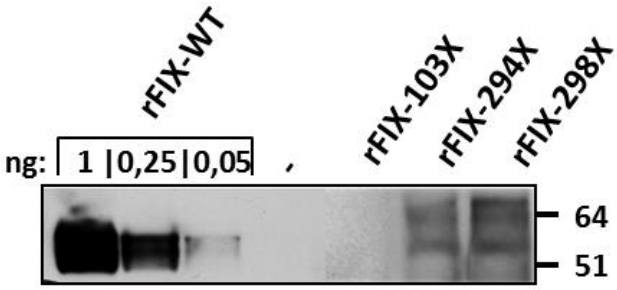

Figure 22: Western blotting analysis of conditioned medium from recominant FIX variants. "-" :Negative control

It is worth noting that ribosome readthrough often leads to insertion of amino acids other than the natural one at the nonsense mutation position (Rospert, Rakwalska et al. 2005), this event potentially impair the intracellular protein biosynthesis and might vanish the effects of readthrough itself. However, the poor conservation of arginine 294 and arginine 298 among serine-proteases (Greer 1990) would make tolerable most substitutions at these positions, in agreement with the observed residual FIX biosynthesis.

Altogether, these findings in patients' plasma and with recombinant proteins support the occurrence of ribosome readthrough over the Arg294X and Arg298X nonsense mutations and the synthesis of traces of full-length FIX. These data support the investigation of the readthrough-mediated full-length FIX synthesis, as additional determinant of clinical phenotype, and particularly of anti-FIX antibody development.

Interestingly, the efficiency through which the nonsense mutations underwent readthrough (i.e. P-298X ≈ P-294X >>> P-103X) in the proper protein context was roughly consistent with the score (table 7) derived from reporter gene assays (Manuvakhova, Keeling et al. 2000).

To provide additional insights into the key role of the nonsense triplet sequence context for readthrough, we also expressed and investigated the naturally occurring Arg162Stop mutation that, based on the above mentioned score, is predicted to undergo readthrough with a 3-4 times higher efficiency than other mutations (table 7).

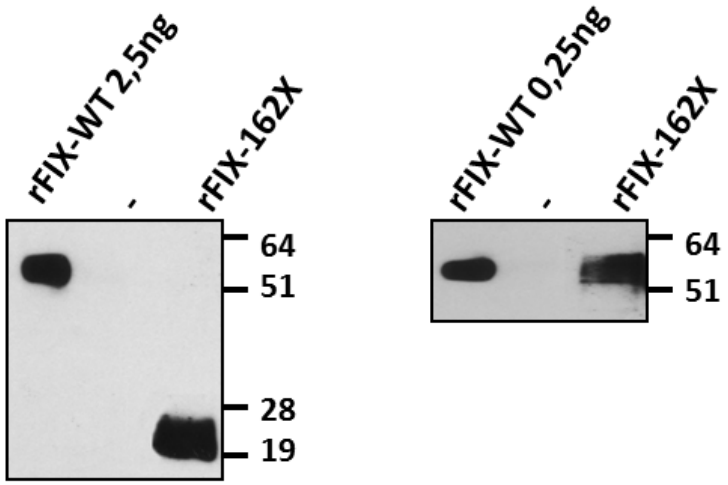

Figure 23:western blotting analysis on rFIX-162X media.

Secreted rFIX-162X antigen levels, even if cannot distinguish between truncated and full-length, were 5±0.3% of rFIX-WT (figure 20) and, accordingly in western blotting the band of truncated form is clearly appreciable but also the band corresponding to full-length FIX was much more appreciable (≈0.5% of rFIX-wt) than that from the other nonsense variants (figure 23, right film). This observation suggests a direct relationship between the amount of full-length proteins and of truncated forms that are the large majority of the secreted molecules.

Noticeably, the efficient readthrough over the *F9* p.R162X mutation, associated to severe HB, was consistent with that over the *LAMA3* Arg943Stop nonsense mutation (Pacho, Zambruno et al. 2011), which displays an identical sequence context (TTGACT) and a mild clinical phenotype. Differently from FIX, a circulating enzyme with a 1 day-half-life, the structural features of the LAMA3 encoded protein would permit its accumulation over time in the basement membrane and render its function less vulnerable to amino acid substitutions normally occurring in readthrough events. These observations underscore the interplay of nucleotide sequence, the determinant of ribosome readthrough, and structure-function features of proteins in determining the relationships between nonsense mutations and clinical phenotypes.

Conclusion

In conclusion, these data in patient's plasma and with recombinant proteins obtained in a panel of selected *F9* gene nonsense changes demonstrate for the first time for a secreted protein with short half-life a gradient of spontaneous and productive ribosome readthrough, consistent with its predicted determinants. These results have potential pathophysiological implications.

Current treatment of Hemophilia B consist of infusion of plasma derived or recombinant FIX. The therapeutic dose is adjusted for each patient from 25 to 100 Unit of FIX per Kg every 12 or 24 hours according to the patient's severity (Santagostino, Mannucci et al. 2000). This

high doses of exogenous protein in patients with no, or very low, circulating FIX antigen levels can trigger the immune response and the development of inhibitory antibodies.

Causes of inhibitor development in HB are not well defined and investigated, mainly caused by the low data on patient present in FIX global database (Lozier, Tayebi et al. 2005).

Development of inhibitor antibodies impairs therapy with less protection against bleeding, actually the protocols in therapy take in consideration: I) change of treatment from FIX to recombinant FVII (VB), II) increase of amount of FIX infused III) immune suppression protocols to decrease the immune response (Brackmann 1984, Nilsson, Berntorp et al. 1986) or IV) immune tolerance protocols to try to revert immune response (Freiburghaus, Berntorp et al. 1999).

Intriguingly patients with truly null mutations such as large deletion/insertion or total gene deletion appears to be more prone to develop inhibitors antibodies than patients with nonsense mutations, which are also commonly considered to be associated to “null genetic conditions”. Moreover, patients with complete gene deletions show significantly higher risk of anaphylaxis than patient with nonsense mutation and small insertion or deletion (Thorland, Drost et al. 1999). This lower frequency in patients with nonsense mutations might underlie the occurrence of readthrough over certain mutations and explain the presence of traces levels of full-length FIX protein that, even if not properly functional, can strongly reduce the immune response.

Therefore, our results encourage the investigation of ribosome readthrough over the several nonsense mutations identified in F9 gene and its association to the immunologic complication in the treated patients. This might unravel a novel determinant of the HB phenotype.

1.2 Induction of Ribosome Readthrough Over F9 Nonsense Mutations by Aminoglycosides

The state of art of ribosome readthough induction

In the last decades, enormous efforts have been pushed toward the induction of ribosome readthrough over nonsense mutations as a therapeutic strategy for human genetic disorders (Bidou, Allamand et al. 2012).

The first compounds used for PTC readthrough were the aminoglycosides, commonly used as antibacterial but that can also bind to minor extent to the human ribosome small-subunit and induce PTC suppression. Among aminoglycosides, Paromomycin and G418 (figure 24, panel A and B) are known as the best compounds. Nevertheless the only compound in clinical trials for nonsense mutation treatment is Gentamicin (figure 24, panel C) (Malik, Rodino-Klapac et al. 2010). Aminoglycosides compounds have a strong limitation consisting on their reversible nephrotoxicity and irreversible ototoxicity (Swan 1997, Forge and Schacht 2000), which encouraged research toward other drugs triggering readthrough.

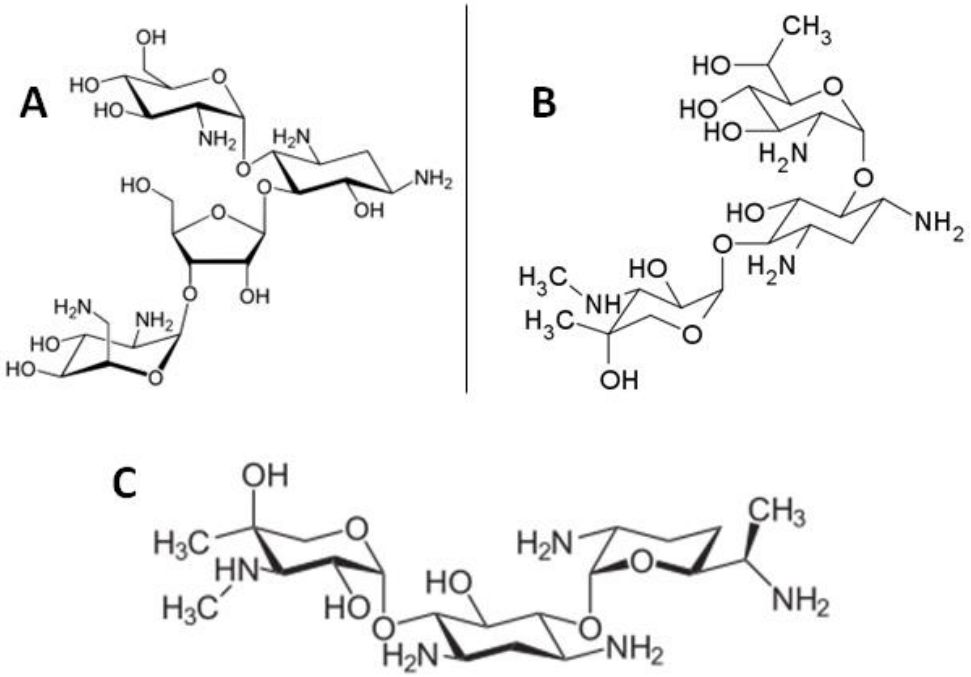

Figure 24: common aminoglycosides. Panel A: Paronomycin; Panel B: G418 called also Geneticin; Panel C: Gentamycin

The compound PTC124 (PTC therapeutics, South Plainfield, NJ), also known as "Ataluren®" (figure 25) can induce PTC suppression without significant antibiotic activity and can be administrated orally and so far appears to be safe. Albeit some doubts still remains on PTC124 efficacy, there are currently on-going clinical trials on different pathologies such as Duchenne muscular dystrophy, cystic fibrosis and hemophilia (Drake, Dunmore et al. 2013, Peltz, Morsy et al. 2013, Zhou, Jiang et al. 2013).

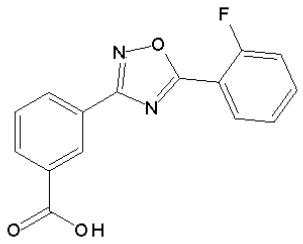

Figure 25: "Ataluren" or PTC124 chemical structure.

Even unexpected compounds can promote nonsense suppression. It was recently discovered a new function of Amlexanox (figure 26), a well know anti-inflammatory anallergic immunomodulator drug commonly used for treatment of ulcers, bronchial asthma and other allergic condition. In a single study, this compound was demonstrated to promote readthrough *in vitro* on three different cell lines (Gonzalez-Hilarion, Beghyn et al. 2012) opening great new prospects of therapies.

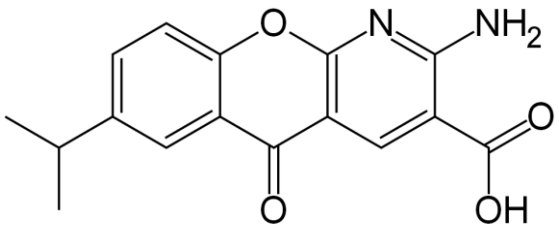

Figure 26: Amlexanox chemical structure.

Similarly to spontaneous readthrough, the extent of induced ribosome readthrough appear to be strongly influenced by the sequence determinants. Recent studies combining bioinformatics and in vitro assays with reported genes defined a candidate consensus sequence that would predict the expected readthrough efficiency induced by gentamicin drugs (figure 27) (Floquet, Hatin et al. 2012).

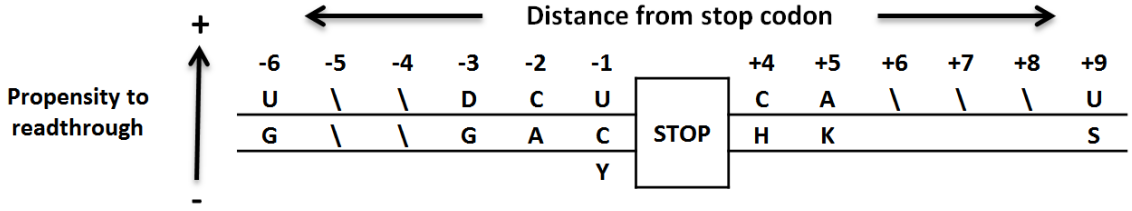

Figure 27: Consensus sequence for readthrough induction by aminoglycosides(Floquet, Hatin et al. 2012).

Rationale and Aim of the study

The study of spontaneous readthrough provided us with optimized experimental protocols to investigate even very low levels of full-length FIX arising from readthrough over nonsense mutations. This prompted us to investigate the aminoglycosides-induced readthrough over a panel of naturally occurring *F9* nonsense mutations.

To this purpose, beside the above described mutations, we selected five additional nonsense mutations from the hemophilia B Italian database (Belvini, Salviato et al. 2005). The rationale behind choosing these was that they display different i) nonsense triplet and ii) sequence context as well as iii) aminoacid and position into the protein sequence. Based on previous data the mutations are predicted to undergo induced readthrough with different efficiency (Manuvakhova, Keeling et al. 2000)(table 8).

We also selected the Arg333X mutation that is associated with an extremely variable coagulation and clinical phenotype, from severe to mild conditions. Analysis of its sequence context predicts a low readthrough efficiency even upon induction. To shed light on this observation, we also created and expressed an artificial variant called 333-i, characterized by a four time fold increase score of readthrough, making it comparable with Arg116X readthrough.

Mutation	Sequence context	Readthrough	
		Basal	Induced

Arg 75 stop	GCA	TGA	GAA	0,6	40,0
Leu 103 stop	TGT	TAA	AAT	0,2	5,9
Arg 162 stop	TAT	TGA	CTT	3,8	63,2
Arg 294 stop	AAG	TGA	AAT	1,0	41,0
Arg 298 stop	AAT	TGA	ATT	1,0	41,0
Tyr 330 stop	AGC	TAA	GTT	0,4	8,5
Gln 370 stop	CTT	TAG	TAC	1,6	48,6
Arg 379 stop	GAC	TGA	GCC	0,6	40,1
Arg 384 stop	CTT	TGA	TCT	0,7	27,0
Arg 379-i stop	GAC	TGA	CCC	3,8	63,2

Table 8: panel of ten mutations selected for induction studies

Investigation of readthrough induced by G418 in vitro

We completed the entire panel of vectors for the FIX nonsense variants and expressed them in eukaryotic cells (Hek293). Due to higher number of samples, we changed our experimental setup into 12 wells and transfection were adjusted with 2 µg of plasmid for each well. To evaluate readthrough induction, four hours after transfection, cell media were changed with Optimem ® with 100 µg/ml of G418, inductor concentration were assessed by previous experience in readthrough induction in our laboratory (Pinotti, Rizzotto et al. 2006).

During previous analyses we demonstrated the ELISA is not appropriate to correctly evaluate FIX readthrough due to the confounding effects of the truncated protein variants. Therefore, in this preliminary study we directly tested the FIX form in conditioned media from cells expressing the nonsense variants, treated or untreated with G418.

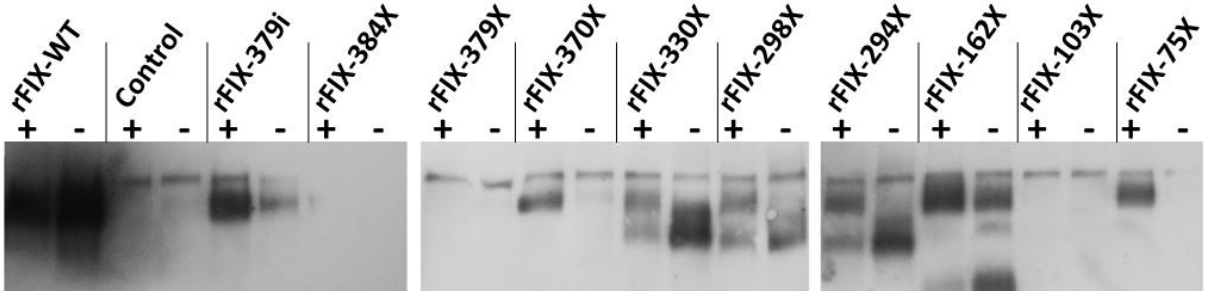

Figure 28: Western blotting of FIX in media from cells expressing the nonsense variants without (-) or after treatment (+) with 100ug/ml G418

The truncated FIX variants were appreciable only for the R162X, R294X, R298X and Tyr330 mutations but not in the others, a finding that could rely on the differential impact of alterations on protein folding and on their ability to escape the quality-control in the ER.

Interestingly, treatment with G418 clearly induced the appearance of protein isoform compatible with the full-length FIX in the presence of several mutations (Arg75X, Arg162X, Arg294X, Arg298X, Tyr330X, Gln370X), and significantly increased the readthrough efficiency in those previously shown to undergo spontaneous readthrough such as the Arg294X and Arg298X mutants.

The data from the Arg379Xi that, at variance from the natural Arg379X, underwent an appreciable spontaneous and induced readthrough, clearly indicated that the nucleotide sequence context plays a major role.

Taken together these preliminary results suggest a differential readthrough efficiency over nonsense mutations that can be easily tested in cellular model created by expression of the nonsense variants.

At variance from bioinformatics tools or consensus sequences generated from data with reporter genes, our findings have been obtained in the proper sequence and protein context and therefore should better mimic the in vivo situation. It must be noticed that ribosome readthrough at the nonsense codon position leads to the insertion of aminoacids other than the natural one, which might have strong detrimental effects on protein biology. This point cannot be assessed with reporter genes assay; conversely, our data demonstrating the presence of full-length FIX in medium at least indicate that the protein arising from readthrough is processed and secreted.

The results from this currently ongoing study will further indicate whether this full-length variants are characterized by an appreciable procoagulant properties, an additional open issue in the field of interventions at the termination translation for therapeutic purposes.

Chapter 2

FIX Tyr450Cys mutation

Replacement of the Y450 (c234) phenyl ring in the carboxyl-terminal region of coagulation factor IX causes pleiotropic effects on secretion and enzyme activity.

*Branchini A, *Campioni M, Mazzucconi MG, Biondo F, Mari R, Bicocchi MP,Bernardi F, Pinotti M.
**Both authors contributed equally to this study*

Based on: FEBS Lett. 2013 Oct 1.

Missense mutations

Missense mutations, introducing amino acid changes into the primary sequence of the protein, are one of the common causes of pathology. Depending on the role of the specific amino acid and of the protein region involved, the effects on protein biology of a secreted molecule such as coagulation factors can be different, ranging from impaired biosynthesis and intracellular degradation/accumulation to secretion of dysfunctional variants. With this as background, missense mutations represents ideal models to elucidate the relationship between the structure and function of proteins.

We focused our attention on the c. 1349 A > G mutation in F9 exon 8, which results in the Tyr450Cys amino acid substitution. This mutation was identified in a young boy (4 years old) affected by a clinically severe Hemophilia B form (table 9) that requires weekly infusion of recombinant FIX to prevent bleeding.

Assay	Levels
FIX antigen	0,6% of PNP (≈30ng/µl)
FIX activity	> 1%

Table 9: Clinical data of propositus Y450C.

Aim of the study was to characterize the biochemical mechanisms leading to the FIX deficiency through the expression of FIX variant in mammalian cells and investigation of FIX protein levels

In Vitro Expression of the rFIX-450Cys variant

To demonstrate the causative nature of the mutation we transiently expressed the rFIX-450Cys in eukaryotic cells and evaluated the intracellular and secreted FIX levels. In our experimental system, the p.Y450C mutation resulted in markedly reduced secreted amounts of rFIX, as indicated by the protein concentration in medium of 18.9±6.2 ng/ml, corresponding to 4.9±1.1% of those of rFIX-WT (373.8±119.6 ng/ml) (Figure 29).

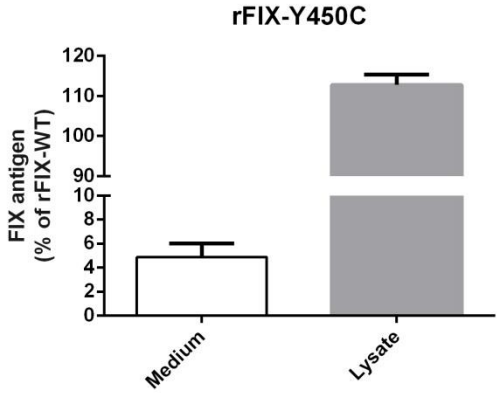

Figure 29:rFIX-450Cys levels in medium and cell lysates. Values are expressed as % of rFIX-WT

The mutation leads to the introduction of a cysteine on the catalytic domain, which could participate in the formation of illegitimate disulphyde bonds, and affect folding, or trigger protein dimerization. In both case this could account for altered biosynthesis, protein degradation by the ER quality control and eventually poor secretion. To investigate this issue we treated transfected cells with a reducing agent such as N-acetyl cysteine, a pharmaceutical compound commonly used in clinics as antioxidant, mucolytic and as antidote for Paracetamol intoxication.

N-acetyl cysteine is considered safe (Oral Lethal dose 5050 mg/ml in mouse and rats) and displays protection also against heavy metals and oxidative stress (Yedjou, Tchounwou et al. 2010, Zhang, Liu et al. 2010). Furthermore N-acetyl cysteine shown the ability of interact with intact cells and change apparently without side effects the redox status of membrane receptor such as insulin receptor (Garant, Kole et al. 1999), moreover this status in reversible, give rise to the real possibility of treatment trough this compound.

However, treatment of transfected cells with increasing concentrations of N-acetyl cysteine did not result in appreciable effects on rFIX-Y450C secreted or intracellular levels, thus not supporting our hypothesis.

The observation that protein concentration of the secreted rFIX-450C variant (≈5% of rFIXwt) was higher than that measured in patient's plasma (≈30 ng/ml, 0.6% of normal plasma) might underlie a preferential removal of the FIX mutant molecules in vivo or shorter half-life in blood of this variant, which cannot be properly assessed in cellular models. On the other hand, the natural accumulation in medium might of the rFIX-450C due of experimental setup have led to overestimate the secreted levels (figure 30).

We therefore conducted a time-course experiment to evaluate the rFIX accumulation in medium over time.

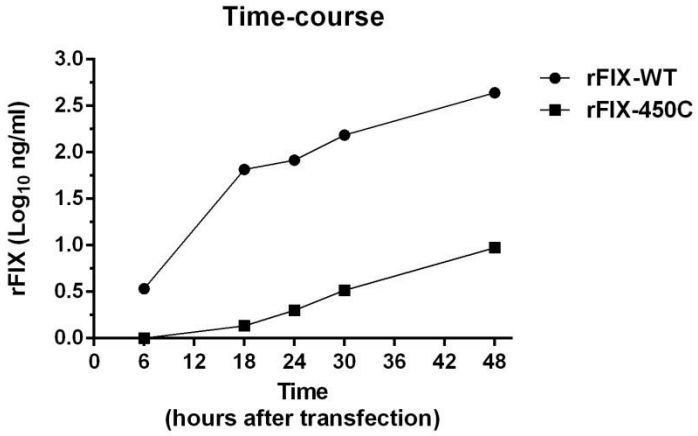

Figure 30: ELISA assay on media of rFIX-450C recombinant protein in time course experiment, for clarity data were expressed as logarithm of FIX concentration.

While the rFIX-wt was clearly appreciable in medium even at 6 hours post-transfection (3.4±0.2 ng/ml), the levels of the rFIX-450Cys variant became barely detectable only at 18 hours and slowly increased over time (figure 30). The rFIX-Y450Cys concentration indicates a remarkable delayed secretion of the recombinant protein and if we take into account the one day half-life of FIX (Furie and Furie 1992), this findings provides a plausible explanation for the very low amount of circulating FIX in the patient (0,6% of PNP).

Investigation of the role of the Tyr450 side-chain

Inspection of the crystallographic structure of FIX reveal that tyrosine 450 is partially buried in the catalytic domain (Figure 10) and appears to be inserted in an aliphatic region. This model suggests that the introduced cysteine can hardly participate in S-S bonds, in accordance with our finding in vitro. .

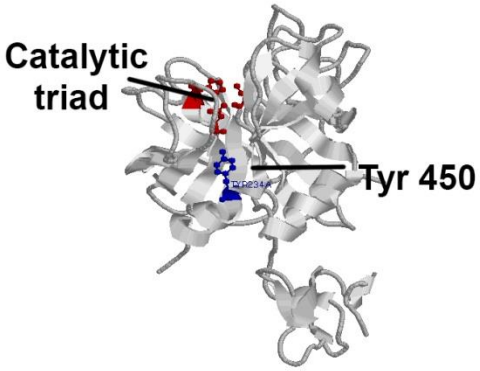

Figure 31: RasMol 3D view of the tyr450 residue and of the catalytic triad in the FIX serine protease domain (FIX ID 1RFN)

To gain insights into the detrimental role of the Tyr to Cys substitution we investigated the effects on FIX biology of the introduction of phenylalanine or of serine (Figure 32).

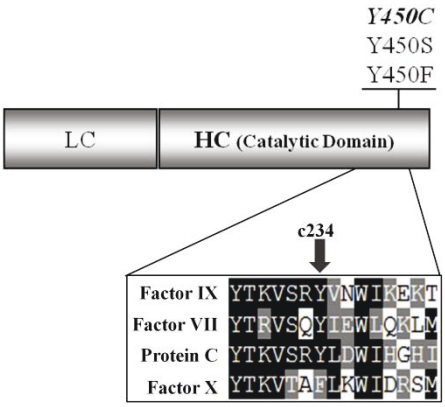

Figure 32: Whole panel of FIX mutation

These different changes have peculiar features (figure 33, in green similarity, in red differences). The variant with serine (rFIX-Y450S) mimics the polarity of the cysteine without the capability of dimerization through S-S bond (figure 33 panel A and B). On the other hand, the variant with phenylalanine mimics tyrosine for its aromatic ring but cannot allow hydrogen bond formation (figure 33 panel C and D).

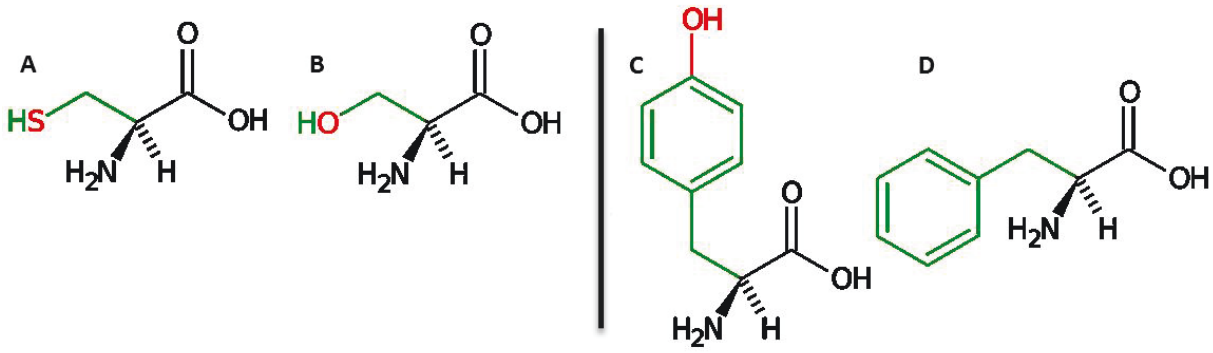

Figure 33: chemical structures of different amino acids for analysis of position 450.Panel A: Cysteine, B: Serine, C Tyrosine, D Phenylalanine. Color legend: green: similarity, red: differences

Alignment of Factor IX,VII, X and protein C shown that tyrosine 450 (c234, in chymotrypsin numbering) is highly conserved but in Factor X is substituted by a phenylalanine, thus strengthening the hypothesis of a structural role of tyrosine 450. Moreover, previous studies on the recombinant FIX-Y450H and Y450P variants, whose secretion levels were 7% and undetectable (Kurachi, Pantazatos et al. 1997), respectively, further support the detrimental impact of amino acid changes at this position.

We therefore conducted a time-course experiment on the whole panel of rFIX variants to evaluate the differential impact of substitutions.

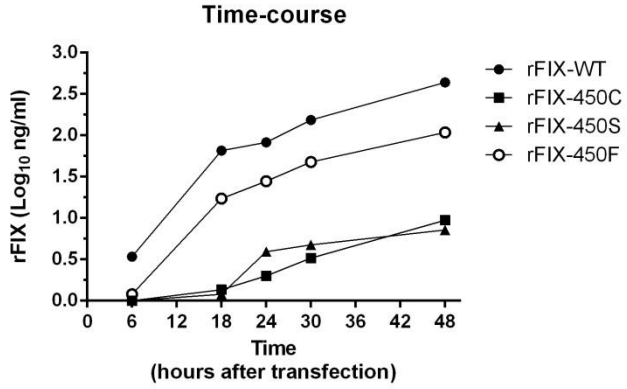

Figure 34: ELISA assay on media of different recombinant proteins in time course experiment, for clarity data were expressed as logarithm of FIX concentration.

Similarly to the natural rFIX-450C variant, the secretion of the rFIX-450S was markedly reduced (5.5±0.2% of rFIX-wt) and delayed. At variance, the rFIX-450F was secreted in medium at appreciable levels (25.3±2.3%) and its time course was comparable to that of rFIX-WT secretion (Figure 34).

To evaluate whether the different substitutions affect the procoagulant properties of FIX we exploited functional aPTT-based assays by supplementing FIX depleted plasma with the rFIX-containing medium. As positive and negative controls we chose a standard curve of the rFIX-WT and mock-medium, respectively.

Sample	Protein Levels (% of rFIX-WT)		aPTT (% of rFIX-WT)		Specific Activity (%)	
rFIX-450C	4,89	±1,08	0,86	±0,13	14,28	±0,58
rFIX-450S	5,53	±0,18	0,88	±0,31	15,24	±5,00
rFIX-450F	25,26	±2,33	19,12	±3,18	78,30	±19,06

Table 10: Antigen, aPTT levels and specific activity for the different rFIX variants

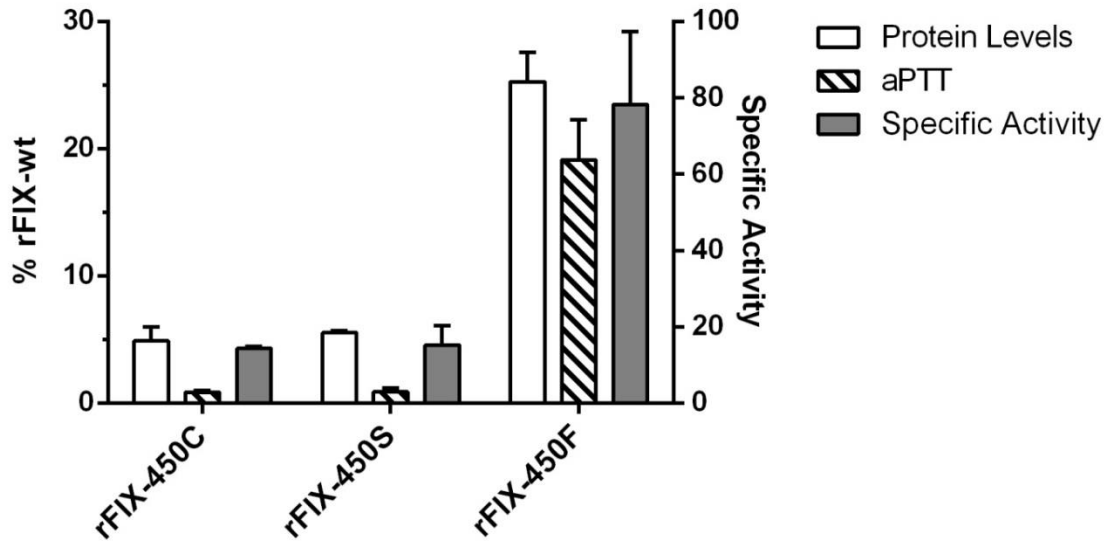

Figure 35: Antigen, aPTT levels (expressed in percentage of WT) and interpolated specific activity for different FIX variants (expressed as percentage of activity of each variant)

The activity of the rFIX-450C (0.86±0.13%) and and rFIX-450S (0.88±0.31%) was remarkably reduced as compared to rFIXwt. Taking into account the antigen levels, these activity values correspond to a specific activity of 14.28±0.58 for rFIX-450C and 15.24±5.00 for rFIX-450S, thus indicating that the introduction of a polar aminoacid at position 450 (c234) severely impairs not only biosynthesis but also procoagulant function.

On the other hand, the rFIX-450F variant was efficiently secreted and displayed a virtually normal specific activity (78.30±19%), to indicate the key role of the phenyl aromatic group in the 450 position of the carboxyl-terminal domain of FIX (figure 35).

The present findings on FIX differ substantially from previous observations found in literature of other coagulation factors, in particular to findings on FVII, and from those obtained in protein C (figure 36).

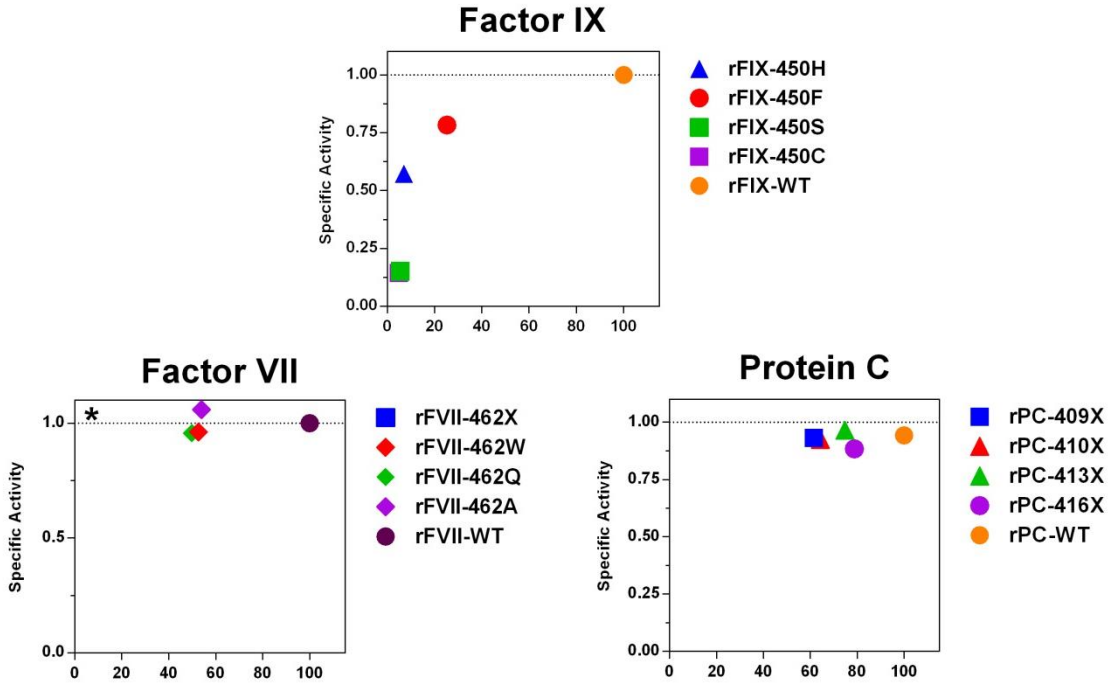

Figure 36: Relationship between secreted protein and specific activity of FIX, FVII and PC for different carboxyl-terminal variants, specific activity was calculated as activity and antigen ratio.

*Wild type was referred as 1.00 of specific activity. *: rFVII-462X variant has 2.70 of specific activity*

Indeed, substitutions of FVII Arginine 462 (c253) or short deletions at the FVII carboxyl-terminus impairs biosynthesis of the protein causing reduction of secreted levels, but they do not affect specific activity that result normal (figure 36 Factor VII panel); Paradoxically FVII R462X displayed gain-of-function features with a specific activity of 2.70 producing an asymptomatic FVII deficiency form (Tanaka, Nakashima et al. 2010, Branchini, Rizzotto et al. 2012).

On the other hand, in PC deletion scanning of the carboxyl-terminal region (figure 36 protein C panel) revealed that alterations of this protein region have a minor impact on secretion as indicated by antigen levels that stay above the 60% of WT; moreover the specific activity of the secreted truncated variants substantially is not affect by truncation; this effect is constant till aspartic acid 409, where further truncation result in impaired biosynthesis and activity with undetectable activity and antigen levels (Katsumi, Kojima et al. 1998).

Noticeably, these observations indicate additive or compensatory pleiotropic effects elicited by some mutations in the carboxyl-terminal of different coagulation factors that although with high homologies can take different destinies; FIX and PC does not admit strong changes or reduction of length without affecting synthesis or activity, FVII can tolerate deletion and missense mutation, that affect synthesis but creating overpower activity. Moreover these information suggest that the carboxyl-terminal region of these proteins does not only represent a secretion determinant, but has a still undefined role for FIX and FVII function.

These differences in behavior can also explain a part of the heterogeneity of different phenotypes, form mild to life-threatening that occur in hemophilic disorder.

Conclusions

The study of model mutations in the carboxyl-terminus of FIX is particularly informative to elucidate the interplay between pathogenic molecular mechanisms impairing protein biosynthesis and function. We provide evidence for a dual role of the FIX carboxyl-terminus both for secretion and procoagulant activity and for additive effects of the p.Y450C mutation, which explain a particularly severe Hemophilia B form. Comparison of findings in the highly homologous coagulation serine protease family members suggests that variations in this protein region might have contributed to the evolution of this protein family sub-group.

Chapter 3

Molecular mechanisms in VWD

Dominant negative effects in Von Willebrand Factor biosynthesis

Unpublished

The dominant negative effect

Dimerization and multimerization are distinct property of VWF biosynthesis both necessary to guarantee the production of extremely large and adhesive molecules, which assure the correct functionality of this protein. The rationale of the dominant inheritance in VWD is the interaction of wild type and mutant monomers during dimerization and multimerization, which impairs the VWF adhesive function. The strength of the negative effects produced by dominant variants would be associated with the ample variation of residual VWF levels and function, and participate in phenotypic penetrance and severity of inherited VWD.

Previous knowledge

Long time ago, in our laboratory, we described a large *de novo* and heterozygous deletion in *VWF* gene associated to a variant of type 2 VWD. The patient showed a severe VWF deficiency, with prolonged bleeding time (20 minutes) and extremely reduced ristocetin cofactor activity (3%) (table 11).

Patient displays altered multimers pattern characterized by reduced amount of intermediate and almost complete absence of HMWMs in plasma and platelets. VWF antigen levels and FVIII coagulant activity were also reduced. The gene deletion between exons 25 and 35 codifies at protein level for a deleted protein where proline codon 1104 is connected with cysteine codon 1926, this new in-frame junction eliminates proline and arginine junction, inserting an arginine at position 1926 (Bernardi, Marchetti et al. 1990).

Analysis	PNP	Patient
bleeding time (min)	5-8	20
FVIII:C	60-170	29
VWF:Ag	60-150	24
Ri:Cof	60-150	3

Table 11: Hemostatic parameters in members of the propositus's family as in Bernardi et al. 1990 Blood. PNP: Pool Normal Plasma

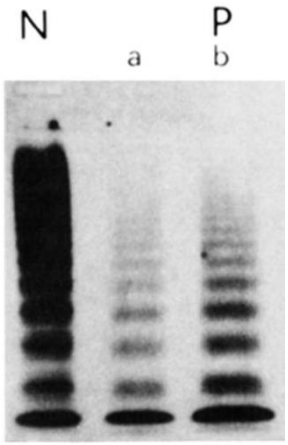

Figure 37: Multimers analysis of plasma (a) and platelet (b) reported by (Bernardi, Marchetti et al. 1990)

The finally encoded protein indeed, the deleted protein does not contain the C-terminal portion of D3 domain and the N-terminal part of the D4 domain, moreover the A1, A2 and A3 modules were completely absent; Among the inferred effects, the deletion abolishes the adhesive functions (A domains) of the protein and impairs interdimer disulphide bond formation (deletion of cysteine 1142 in the D3 domain) and therefore correct multimerization (figure 37 e 38).

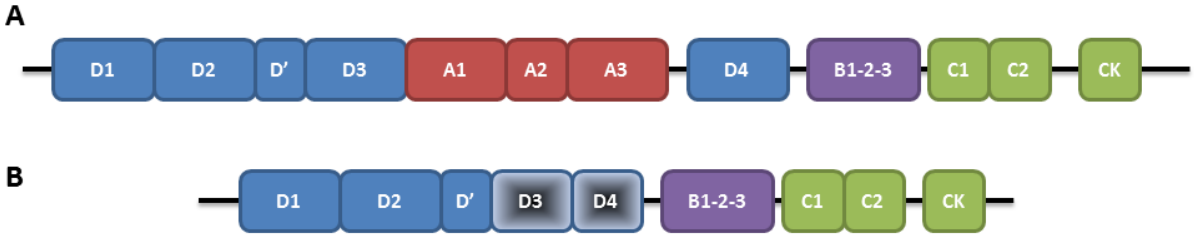

Figure 38: Schematic representation of the wild type and deleted VWF protein domains. Dark-grey motifs (1105-1925 amino acids) are missed in the deleted VWF.

In the recent past (2010) Casari and collaborators created a cellular model to evaluate the main biosynthetic steps of the deleted VWF and its interaction with wild-type protein. This model enabled the authors to better interpret the disease at the macromolecular level.

The "heterozygous" cellular model, displayed intermediate phenotypes than that observed in patient plasma both at qualitative and quantitative levels.

The presence and proportion of heteropolymers "WT – Deleted" play a key role in the dominant-negative behavior; indeed the properly folded cysteine knot domain, correctly encoded by the in-frame deleted VWF, enables a correct dimerization process, even if in the absence of all the A domains. However the successive phase in VWF maturation, the multimerization step, is certainly abolished because of the absence of the Cys 1142, which is involved in interdimer disulfide bond formation.

Casari et al demonstrated the "terminator effect" of the heterodimers, by acting as terminators of the growing polymer, the heterodimers containing the deleted VWF severely impairs VWF multimers size and activity (figure 39).

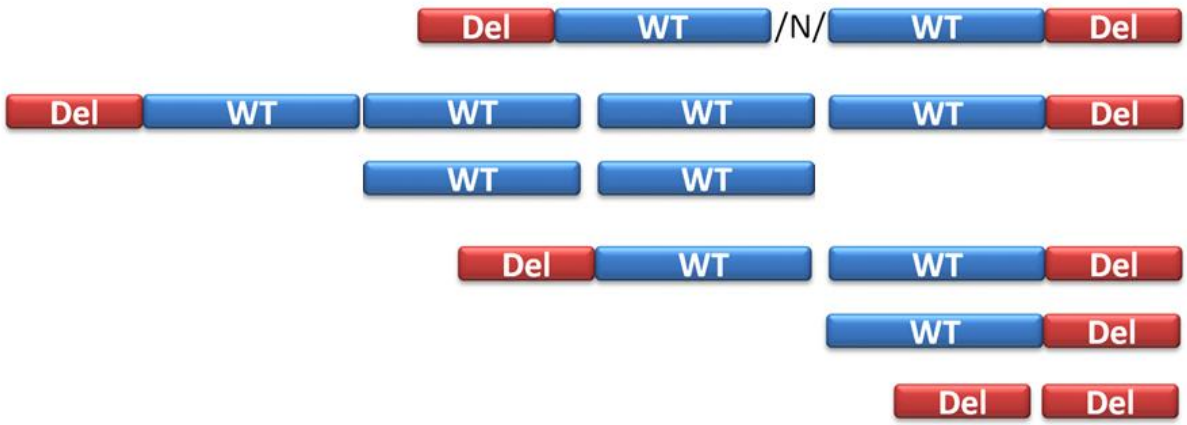

Figure 39: polymerization, interaction with WT and terminator effect of the deleted VWF

In the same study, modulation through the use of siRNAs selectively targeting the deleted RNA, resulted in decreased expression of the deleted molecule, increased VWF antigen levels, partial restoration of and increased collagen-binding activity (Casari, Pinotti et al. 2010). However this strategy, acting at the mRNA level, decrease the amount of deleted protein and thus the rate of heterodimer formation. Although largely improved, VWF function was not completely restored due to the small amount of deleted protein still present after the siRNA treatment.

Moreover is necessary to underline that the obtained restoration effect is simply due to removal of deleted construct mRNA and therefore to reduced availability of deleted protein and decreased rate of heterodimer formation. Indeed, the small amounts of the deleted VWF, still present after the RNAi treatment, are able to dimerize with the WT VWF and thus stop multimerisation.

In vivo P1105_C1926delinsR

The first step for analyze in vivo the deletion was the creation of plasmids for the mouse model, indeed due to interspecies-barrier human VWF cannot bind to murine GP-I-bα, for this reason to make a correct moue model of the pathology we need to replicate our deletion in murin VWF. Therefore we aligned human and mice VWF coding sequences to find any differences that could impede correct replication of the mutation. The alignment of VWF coding sequences highlighted high similarity the regions of interest (exons 25 and 35

boundaries) suggesting that it would be possible to reproduce the human deletion into the mouse VWF (figure 40).

```
human AGGACGGCCACATTGTGCCCCCAGAGCTGCGAGGAGAGGAATCTC
mouse AGGACACCCACACTGTGCCCCCAGAGCTGTGAAGAAAAGAATGTT
cons  *****  ***** ********************** * **** *

human GAAGAGACCTGTGGCTGCCGCTGGACCTGCCCCTGCGTGTGCACA
mouse GAGGAGACGTGTGGCTGCCGCTGGACCTGCCCTTGTGTGTGCACG
cons  ** ***** ************************ ** ********

human GGCAGCTCCACTCGGCACATCGTGACCTTTGATGGGCAGAATTTC
mouse GGCAGTTCCACTCGGCACATCGTCACCTTCGATGGGCAGAATTTC
cons  ***** ***************** ***** ***************
```

Figure 40: preliminary analysis of human and murine VWF cDNA to reproduce P1127_C1948delinsR mutation. Underlined the new junction

We used the hydrodynamic gene transfer technique to create the mouse model of the VWD. This procedure allowed protein expression by hepatocytes and its subsequent release into the circulation (Casari, Lenting et al. 2013).

To assure efficient ectopic expression in the liver, we cloned the sequence of murine VWF cDNA either wild type or carrying the deletion into the pLIVE vector (Mirus BIO, Madison, WI), which contains an hepatic specific-promoter (murine albumin minimal promoter).

VWF deficient mice (C57BL/6J vwf -/- (Denis, Methia et al. 1998)) displayed undetectable VWF antigen levels, reduced FVIII activity (27.6% of WT) and bleeding time over 500 seconds. For these reasons the VWF protein detected after the hydrodynamic procedure is exclusively derived form the hepatic expression of the foreign recombinant plasmids.

Mice were hydrodynamically injected with 50 and 25 µg of WT plasmid to mimic homozygous or hemizygous WT mice respectively. To mimic the pathologic heterozygosis condition we injected 25 µg of WT- and 25 µg of DEL- plasmid together into the same mouse. Plasma samples were collected 4 days after injection and antigen levels were analyzed trough ELISA.

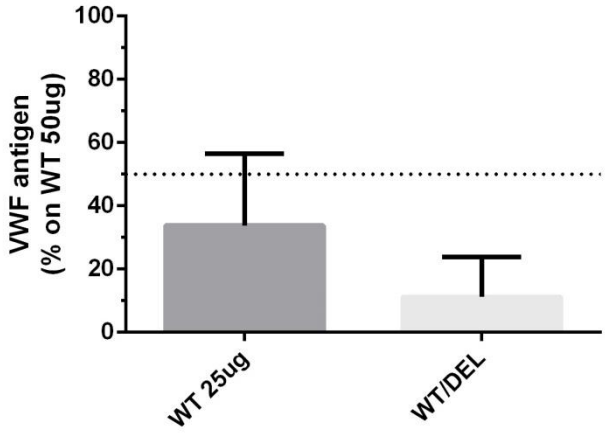

Figure 41: plasmatic levels of VWF hydrodynamic injected mice.

VWF antigen levels clearly showed results similar to that obtained in the cellular model. Consistent with the hemizygous condition, injection of 25 µg of WT plasmid results in VWF

antigen levels of 33.83±22.72% (compared to the 100% expressed after 50 µg injection) (figure 41). Coinjection of both plasmids results in VWF antigen levels of 11.23±12.53% that is even less than that obtained in the *in vitro* system (24%)(Casari, Pinotti et al. 2010).

Although the VWF antigen levels are a good indicator of the dominant-negative effect of the deleted protein we perform the multimer analysis of the same plasma samples. This assay allow us to appreciate the degree of VWF multimerization, which directly correlates with its functional activity.

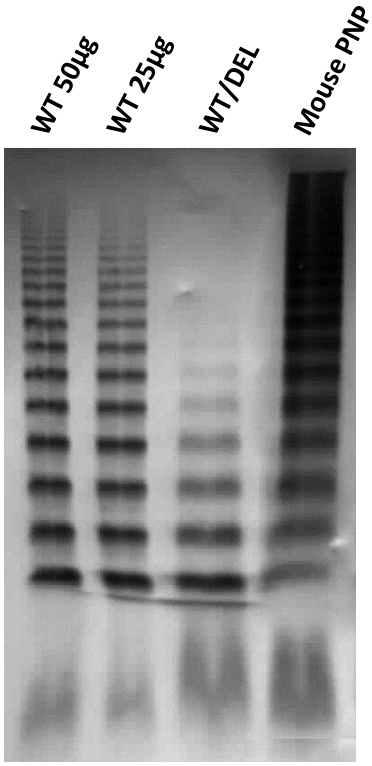

Figure 42: multimer assay on mouse plasma.

Plasma from mice coinjected with the WT and the DEL plasmids clearly exhibits a multimerization defect and provides in vivo evidence for the dominant effect of the P1105_C1926delinsR deletion (figure 42).

"Double mutant" strategy

The reproducibility *in vitro* and *in vivo* of the dominant-negative effect enable us to further investigate the molecular aspects of the dominance, particularly to deeply understand the dominant negative effects in VWD.

We have demonstrated that both the previously described in vitro system and the proposed in vivo strategy can be used to successfully reproduce the dominant-negative effect of the deleted molecule comparable with patient's clinical phenotype and we applied these models to further investigate molecular aspects of dominant negative effects occurring in VWD.

For this purpose we planned to combine the deletion, impairing multimerization, with a mutation, well known to impair dimerization and localized in the CK domain: the substitution of the Cysteine 2773 to Arginine (C2773R).

The C2773R mutation was described for the first time in 1996, as type 2 D VWD. Molecular studies on this protein variant showed the inability of the mutated protein to correctly produce dimers in the endoplasmic reticulum (figure 43, panel A)(Schneppenheim, Brassard et al. 1996). Alignment of different mucine-like domains from different proteins showed an high conservation of the cysteine residue in this specific position of the domain (figure 43

panel B)(Katsumi, Tuley et al. 2000). Further studies focused on the C2773S mutation confirmed the essential role of cysteine 2773 in dimer formation. Moreover, recent studies on Weibel-Palade bodies demonstrated that the C2773S VWF variant is properly stored in these specialized compartments, the formation of which is not affected by the mutation (Wang, Groeneveld et al. 2012).

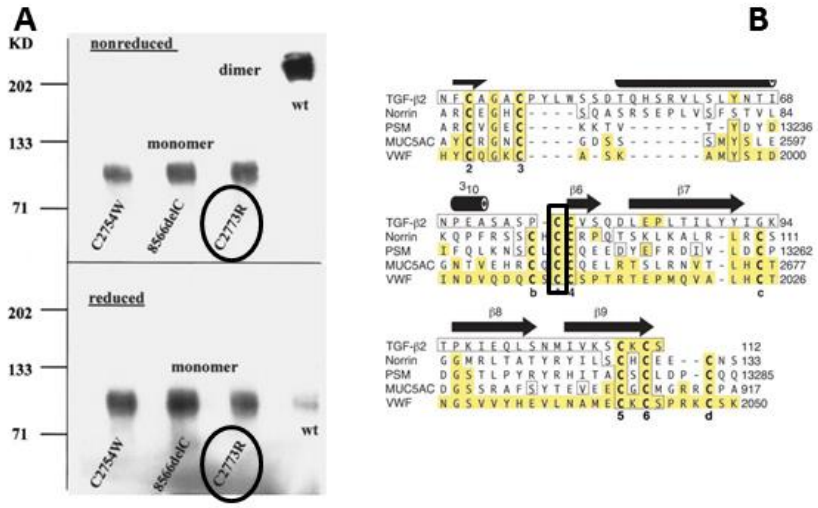

Figure 43: Panel A: (Schneppenheim, Budde et al. 2001) panel B: (Katsumi, Tuley et al. 2000)

We used the P1127_C1948delinsR (DEL) variant and the C2773R mutation to investigate our hypothesis: combination of two mutations with dominant-negative effects, one impairing dimerization and the second one compromising multimerization, should abolish the dominant effect of the latter, thus enabling expression of normal VWF (figure 44).

This experiment would confirm the terminator effect of the P1127_C1948delinsR (DEL) variant provide us with a detailed picture of the molecular mechanism underlying the disease.

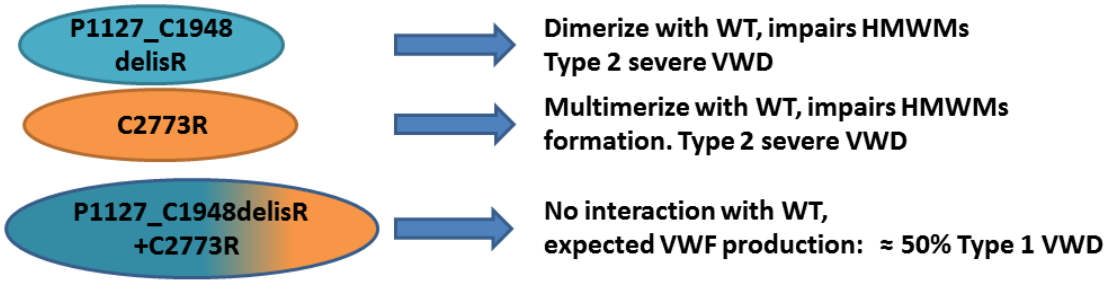

Figure 44: variants used in the study and effect on VWF biosynthesis

in vitro investigation of the DEL+C2773R variant

First, we performed *in vitro* assays to verify our hypothesis. COS-1 cells were transfected with 7µg of different combination of plasmids to mimic homozygous and heterozygous conditions (table 12)

Sample name	Plasmid combination (µg)				Mimed condition
	pWT	pDEL	pC2773R	pDEL+C2773R	
WT	7	0	0	0	WT Homozygous
DEL	0	7	0	0	DEL Homozygous
WT/DEL	3,5	3,5	0	0	Del Heterozygous
C2773R	0	0	7	0	C2773R Homozygous
WT/C2773R	3,5	0	3,5	0	C2773R Heterozygous
DEL+C2773R	0	0	0	7	Del+C2773R Homozygous
WT/DEL+C2773R	3,5	0	0	3,5	Del+C2773R Heterozygous

Table 12: Plasmids combination for mimic different condition.

4 hour after transfection, culture media were replaced with fresh Opti-MEM® and 72 hours after, media were collected, briefly centrifuged to discard debris and analyzed at protein levels through ELISA and Western blotting.

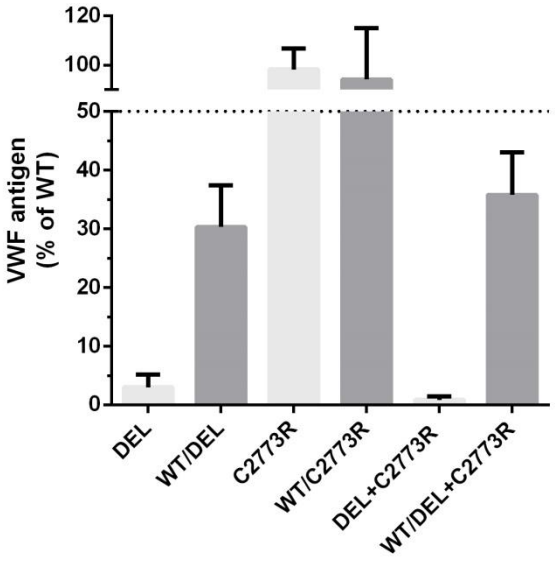

Figure 45: VWF antigen levels in conditioned media.

We observe extremely low VWF antigen levels for DEL and DEL+C2773R samples, 2.99±2.15% and 0.85±0.57% of WT, respectively. C2773R variants in homozygous conditions or in combination with the WT molecule, displays VWF antigen levels similar to WT with concentrations of 98.26±8.54% and 94.22±20.92%, respectively. These results are consistent with those reported for a patient carrying the same mutation and described as indistinguishable form normal VWF levels (1,19 U/ml) (Schneppenheim, Brassard et al. 1996).

In our experimental system antigen levels of WT/DEL and WT/DEL+C2773R are significantly different (P<0,0001) when compared to WT but they did not significantly differ when compared to each other.

Although the absence of dominant effects would imply to rise up the WT/DEL+C2773R antigen level to ≈50% of WT, we measured lower antigen levels (35.79%±7.23%). However, the ELISA assay does not give us information about the quality of the VWF produced by cells and thus does not enable us to verify the hypothesis about the presence/absence of interaction between WT and the DEL+C2773R variant.

Western blotting analysis of media

To provide useful information on secreted media, we performed Western Blotting experiment on they with the antibodies M13 an M31, those display specificities for different protein domains (figure 46).

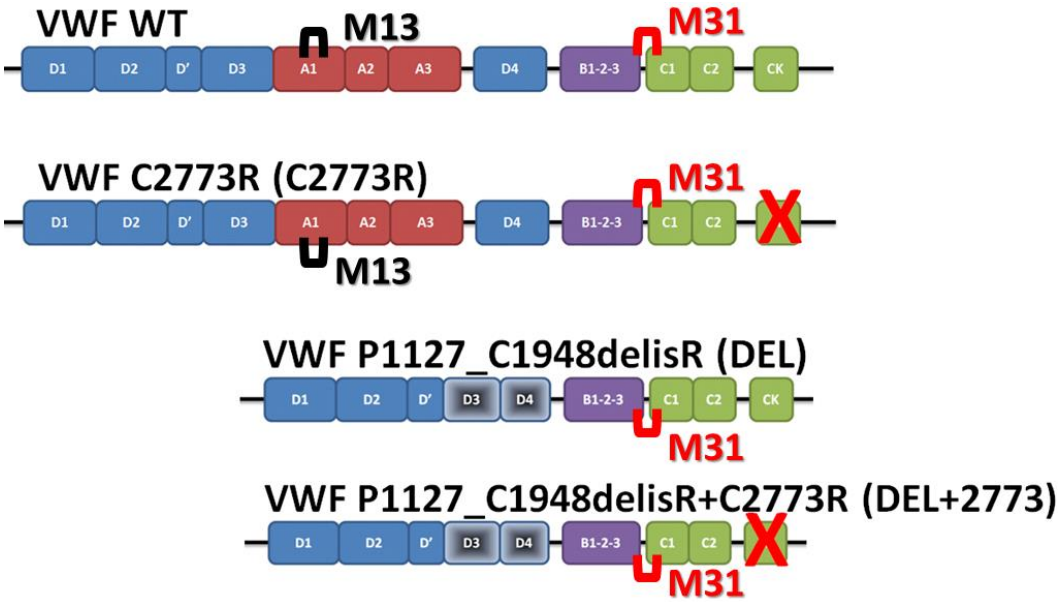

Figure 46: Scheme of different epitope recognized by M13 and M31 antibodies

The M13 antibody binds to the A1 domain, not present in deleted forms, which and allows us to recognize the WT and C2773R forms; the M31 antibody binds to a region that includes the B3 and C1 domains and thus recognizes all VWF variants. Analysis of Western blots will enable us to evaluate the ratio between secreted full-length and deleted VWF. Although indirectly, these experiments will provide information about formation of heteropolymers.

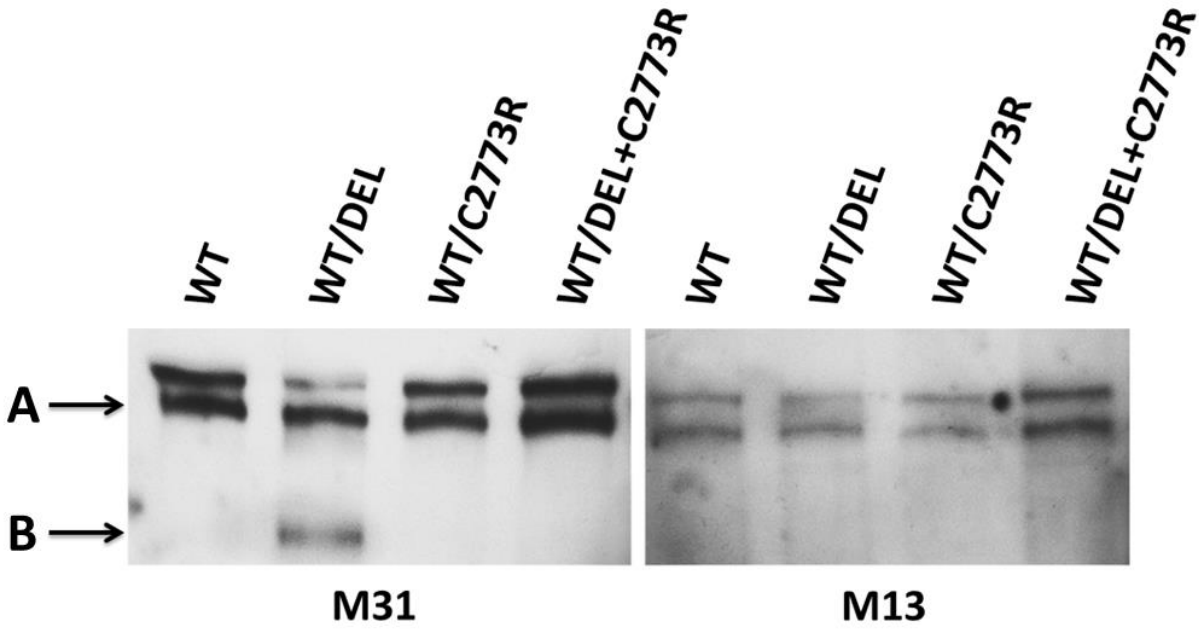

Figure 47: Western Blotting analysis with M31 and M13 antibodies, A: full length mature VWF, B: Deleted VWF

Western Blotting analysis (figure 47) showed the presence of two distinct bands in all samples and with both antibodies, although in different relative amounts. They correspond to the full-length molecules of VWF (figure 47, A), the mature protein and a non-completely processed form still containing the large propeptide. Both are expected due to the specific in vitro system (COS-1 cells).

Interestingly, the band corresponding to the deleted form of VWF is detected by the M31 antibody and not by the M13 antibody, only in media from cells expressing the DEL plasmid (figure 47,B). This result confirms that the deleted protein is expressed, co-secreted and probably could interact with the WT VWF.

Most important, this lower size band is not appreciable into the WT/DEL+C2773R medium clearly indicating that the DEL+C2773R variant cannot be secreted alone or more likely does not form secreted homo and heterodimers with WT. These results support the notion that the C2773R prevents the interaction of the deleted VWF with WT.

Multimer analysis of conditioned media

We performed the multimer analysis of media studied by Western blot to verify if HMWM are affected or not by the expression of the DEL+C2773R plasmid.

Multimer analysis indicates an altered pattern both in WT/DEL and WT/C2773R media, compatible with the dominant nature of both variants. Interestingly the WT/DEL+C2773R media contains an ample series of HMWM, supporting our hypothesis. Indeed, the "double mutant" VWF does not exhibits dominant-negative features, and the resulting WT/DEL+C2773R multimeric pattern is similar to that of a quantitative, type 1 VWD form.

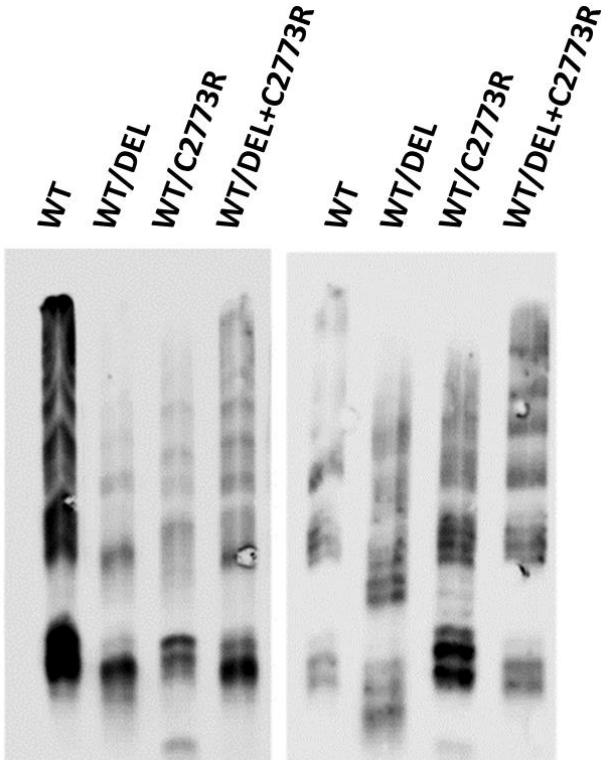

Figure 48: Multimer analysis on conditioned media.

Results obtained by Western blotting and multimer analysis on media are coherent and support that the "double mutant" does not possess the ability to form neither dimers nor multimers with WT VWF thus implying that its dominant-negative feature has been abolished.

Investigation of DEL+C2773R variant in mouse model

We next translated *in vivo* the experiments conducted in cells in order to verify also in vivo our hypothesis and appreciate bleeding phenotype of ours models.

Mice were hydrodynamically injected with 50 and 25 µg of WT plasmid to mimic hemizygous and homozygous WT as done before. The coinjection of mice with 25 µg of WT plasmid and

25 µg of the plasmid carrying the deletion or the double mutation (DEL or DEL+C2773R, respectively) was aimed to mimic the heterozygous conditions.

Plasma samples collection and tail-clip experiments were performed 4 days after injection. In accordance with the experimental setup, bleeding-time exceeding 600 seconds (10 minutes) was considered as inability to perform blood coagulation. ELISA assays were also performed to investigate VWF antigen levels.

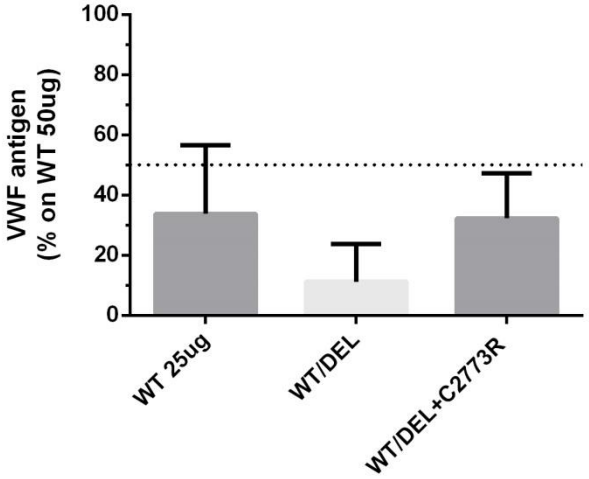

Figure 49: plasmatic levels of VWF hydrodynamic injected mice.

Antigen analysis showed a small but significant difference between WT/DEL and WT/DEL+C2773R antigen levels (11.23±12.53 for WT/DEL and 32.29±14.97 for WT/DEL+C2773R; P value P=0.0315 two-tailed t-test; P=0.0157 one-tailed t-test). Moreover, no significant differences are appreciable between WT 25µg and WT/DEL+C2773R. Although these findings are compatible with reduction of the dominant negative effects of the DEL+C2773R plasmid, anyway they do not give us information about the haemostatic function of the VWF molecules. For this purpose we evaluated through a tail-clip assay, the bleeding time in the corresponding animal models.

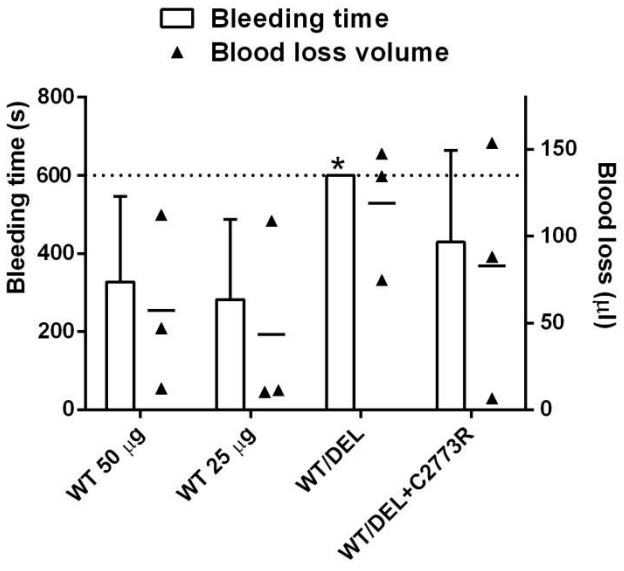

Figure 50:Bleeding time and amount of blood loss, dotted line indicate time limit of bleeding time analysis; solid bar in blood loss volume data: mean.

Whereas “homozygous” and “hemizygous” WT VWF expression permitted hemostasis, we observed that mice expressing the “heterozygous” WT/DEL plasmids did not stop to bleed and exceeded the experimental limit of 600 seconds with continuous blood loss (figure 50, white histograms).

Bleeding time measurement in mice coexpressing VWF WT and the DEL+C2773R variant did not provide statistical evidence for haemostatic improvement compared to mice coexpressing WT and DEL VWF and differently from what expected by the VWF antigen levels (figure 50, triangles). Although not statistically significant, bleeding was efficiently stopped in two out of three mice expressing WT/DEL+C2773R VWF.

Plasma samples were evaluated in multimer analysis to understand if data obtained from the tail-clip assay are affected by the low number of available mice.

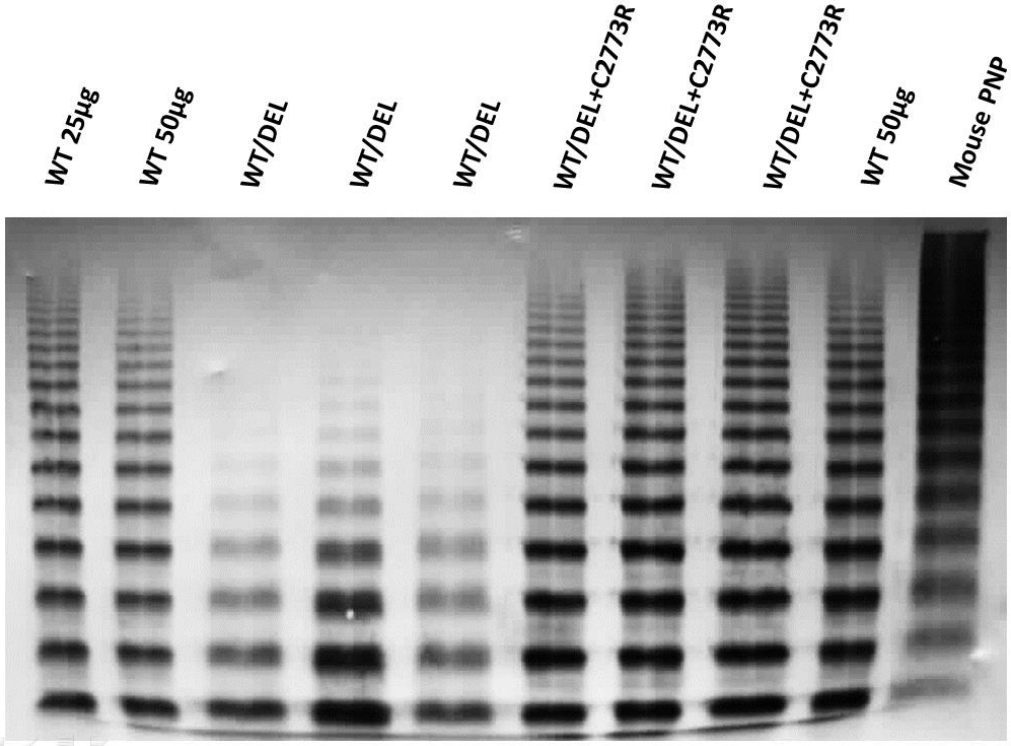

Figure 51: Multimer analysis on mice plasma.

Multimer analysis of plasma collected form WT/DEL mice confirmed the strong reduction of HMWM, as previously observed in the first set of experiments (figure 51).

Interestingly, plasma collected form WT/DEL+C2773R mice showed a multimer profile comparable with both WT 50µg and WT 25µg, thus having almost normal HMWMs. These data provide in vivo evidence for the inability of the VWF DEL+C2773R variant to dimerize and multimerize with WT-VWF

We do not offer yet a clear explanation for the discrepancy between the prolonged bleeding time measured in tail-clip assay for one mouse and the high degree of VWF polymerization observed in multimer analysis observed in all the 3 animals.

Conclusion

The molecular mechanisms of dominant VWD types play a key role to produce the relatively high incidence of VWD, and their understanding would help us to investigate new therapeutic strategies for the most frequent inherited bleeding disorder (Ginsburg and Sadler 1993, Keeney and Cumming 2001). The reported (Casari, Pinotti et al. 2010) cellular model of the in-frame deletion was used to understand the dominat negative effects,

hypothesized when the deletion was discovered and characterized (Bernardi, Marchetti et al. 1990).

Casari and collaborators clearly demonstrated that formation of dimers between normal and deleted VWF (heterodimers) constitutes a critical step in the dominant-negative behavior, especially because this interaction occurs in the "cysteine knot" domain of the protein resulting in an indissoluble bond between WT and deleted form; moreover, other studies (Schneppenheim, Budde et al. 2001, Wang, Groeneveld et al. 2012) demonstrated a similar mechanism for mutations that impair dimerization of the CK domain but not multimerization, producing similar alteration on VWF biosynthesis.

We reproduced in vivo trough hydrodynamic injection the dominant-negative effect due to the P1127_C1948delinsR (DEL) showing a reduction in antigen levels and HMWM corresponding to that observed in the cellular model.

To deeply investigate the multimerization mechanism as the cross-road between HMWM impairment and dominant-negative effect, we took advantage of two mutations, both of which able to impair two main steps of VWF multimer formation, with dominant-negative effect. This novel experimental setup, trough combination of two dominant-negative effects, allowed us to verify the hypothesized dominant features at the protein level without any change or interference in transcripts ratio due to the siRNA approach.

In vitro expression of the P1127_C1948delinsR (DEL), Cys2773Arg (C2773R) and P1127_C1948delinsR-Cys2773Arg (DEL+C2773R) single/double mutations or their co-expression with WT to mimic the heterozygous condition, showed comparable levels of antigen in WT/DEL and WT/DEL+C2773R mutations, while WT/C2773R and C2773R mutations showed similar or higher levels than WT (FIGURE 45).

However, Western blotting analysis of media, with antibodies enabling to distinguish the DEL protein form, indicated the and joined secretion of the WT and DEL protein, and probably their hetero dimerization; differently the DEL+C2773R variant did not displayed interaction with WT or joined secretion (figure 47). Multimer analysis of media (figure 48) clearly showed relevant differences among samples: whereas in WT/DEL and WT/C2773R media multimerization was impaired and HMWM decreased, in WT/DEL+C2773R this effect was not appreciable at all, with HMWM pattern superimposable to that of WT.

These in vitro data confirmed the hypothesized molecular mechanism of negative dominance based on molecular interaction of mutant proteins with WT, and particularly their role as terminator molecules on dimerization or multimerization.

We translated our experimental system in vivo through hydrodynamic injection to validate data obtained in vitro, also aiming to appreciate effects on hemostasis.

Most important, the WT/DEL mice confirmed the dominant features of the deletion both in plasma assays and the tail-clip. It could not stop bleeding at all before the end of the experiment (600 s, figure 50).

Concerning the DEL+C2773R model, antigen analysis showed significant differences between WT/DEL and WT/DEL+C2773R plasma samples, that were coherent with information obtained in the cellular model.

Interestingly, in the multimer analysis of plasma samples, the WT/DEL+C2773R mice displayed high degree of polymerization and HMWM comparable with both WT mice. These data confirmed in vivo that the DEL+C2773R variant is unable to dimerize and multimerize with WT and does not exhibits the dominant-negative features (figure 51).

However, we could not appreciate statistically significant differences among samples in bleeding measurement. In particular, among the three WT/DEL+C2773R mice we observed discrepant bleeding phenotypes, ranging from normal to absence of coagulation at the end of measurement (figure 50).

Although the bleeding phenotype needs to be evaluated in a larger number of animals, these data provide the proofs of the dominant-negative effect of the in frame deletion, and experimentally supported a molecular mechanism substantially based on the capability of the mutant VWF to dimerize with the WT molecules and to exert a terminator effect on multimerization. Prevention of the dimerization through the association with a specific mutation not only prevented the dominant effect but also restored virtually normal mutimerization of the WT molecules, reverting type II VWD in a type 1 VWD

We believe that our finding have general implication for the dominant forms of VWD, which is the most frequent inherited bleeding disorders in humans.

General Methods

Transformation of bacteria

Transformation of clones was carried out using 10 ng of the plasmid DNA. The DNA was incubated with 50 µL of competent cells for 20 min on ice and at 42°C for 45 sec. After the step of the heat shock, 200 µL of LB were added and the bacteria allowed to recovery for 60 min at 37 °C. The cells were then spread onto agarose plates containing the appropriate antibiotic. The plates were then incubated for 12 hours at 37 °C.

Preparation of bacterial competent cells

Bacterial chemical competent cells were prepared as follow: E. coli strains were grown overnight in 10 mL of LB at 37°C. The following day, 140 mL of fresh LB were added and the cells were grown in the shaker at room temperature for 30-45 min until the OD600 was 0.3-0.38. The cells were transferred into a Falcon 50ml tube and then placed in ice and centrifuged at 4 °C and 1000g for 10 min. The pellet was resuspended in 12 mL 50mM $CaCl_2$ then left on ice for 90 minutes . The cells were centrifuged at 4 °C and 1000g for 10 min resuspended in 12 ml of 50mM $CaCl_2$, 10% glycerol and then aliquoted and stored at –80°C. Competence was determined by transformation with 0.1 ng of pUC19 and was deemed satisfactory if this procedure resulted in more than 100 colonies.

Plasmid DNA purification

Rapid isolation of plasmid DNA from 5 ml of E. coli culture grown over night was achieved by using the Wizard® Plus Minipreps DNA Purification System (Promega Corporation, Madison, WI). Bacterial culture was harvested by centrifugation for 5 min at 10,000 x g, and the pellet resuspended in 250 µl of Cell Resuspension Solution. Cell Lysis Solution (250 µl) was then added and the tube was inverted 4 times. After adding 10 µl of Alkaline Protease Solution and inverting the tube 4 times, the sample was let incubate at room temperature for 5 min. Neutralizing Solution (350 µl) was then added and the tube was inverted 4 times before centrifuging the bacterial lysate at 14,000 x g for 10 min at room temperature. The plasmid DNA purification unit was prepared by inserting the Spin Column into a 2 ml Collection Tube. After centrifugation, the cleared lysate was transferred to the prepared Spin Column and centrifuged at 14,000 x g for 1 min at room temperature. DNA bound to the Spin Column was then washed with 750 µl of Column Wash Solution and newly centrifuged at 14,000 x g for 1 min at room temperature. The same procedure was repeated using 250 µl of Column Wash Solution. Finally DNA was eluted from the Column into a new tube adding 100 µl of Nuclease-Free Water to the Spin Column and by centrifuging the system at 14,000 x g for 1 min at room temperature.

Rapid isolation of plasmid DNA from 5 ml of E. coli culture grown over night was achieved by using the GenElute™ HP Plasmid Miniprep Kit (Sigma-Aldrich, St. Louis, MO). For transfection experiments were high-quality DNA was required, plasmids DNA was obtained from 100 ml of E. coli culture grown over night and extracted by using the GenElute™ HP Plasmid Midiprep Kit (Sigma-Aldrich, St. Louis, MO).

Direct sequencing

Sequencing of plasmids were performed by an external sequencing service: Macrogen (Macrogen Europe).

Gel electrophoresis

Due to their numerous phosphate groups, nucleic acids are negatively charged at neutral pH and tend to migrate towards the anode if subjected to an electric field. Their migration rate is inversely proportional to the logarithm of their length in bp. These properties make it possible to separate DNA fragments according to their size. At the end of the electrophoretic run, the positions of the DNA fragments in the gel are visualized by ethidium bromide, an intercalating dye that fluoresces when bound to DNA. Agarose gels (able to separate fragments ranging from 200 bp to 50 kb) were prepared by dissolving the desired amount of agarose in 1× TAE buffer (40 mM Tris-acetate, 1 mM EDTA) and heating this mixture in a microwave oven till complete clarification. A 1% agarose gel contains 1 g agarose in 100 ml buffer. Ethidium bromide was added directly to the melted gel before casting, in the proportion of 5 µl of a 10 mg/ml stock to 100 ml gel. Agarose gels were run horizontally in 1× TAE buffer, by applying a voltage of 5 V/cm. Gels were viewed under UV transillumination at 254 nm, the picture was imported with a GelDoc 1000 UV-gel camera (Bio-Rad Laboratories, Hercules, CA, USA) and stored on a computer as an image file. Gel images were manipulated with the software Molecular Analyst™, version 1.3 (Bio-Rad Laboratories, Hercules, CA, USA).

Polymerase chain reaction (PCR)

DNA amplification by PCR (Mullis and Faloona 1987) takes advantage of a natural enzyme (the thermostable DNA-polymerase I of the thermophilic bacterium *Thermus aquaticus*, *Taq* polymerase) to produce a large number of copies of the same DNA fragment.

The PCR reaction (Mullis and Faloona 1987) requires a thermostable DNA-polymerase of the thermophilic bacterium *Thermus aquaticus,* a template (usually purified DNA), two primers (single-stranded oligonucleotides that frame the target sequence) and all four deoxyribonucleoside 5'-triphosphates (dNTPs) in the presence of $MgCl_2$.

The amplification reaction is performed via 25-30 DNA replication cycles, each comprising three steps: 1) denaturation (separation of the two strands of template DNA); 2) annealing (hybridization of the primers to their complementary sequences on the template); 3) extension (elongation of the primers). These steps require different temperatures (denaturation: 95 °C; annealing: 45-60 °C, according to the characteristics of the primers; extension: 72 °C).

Amplification reactions (25-50 µl total volume) were carried out using 1 unit of *Taq* polymerase (BioTherm™ Taq DNA Polymerase, eEnzyme LLC, Gaithersburg, MD) in the buffer provided by the supplier.

Usually reaction conditions were: 1 unit of enzyme, 100 ng template DNA, 272 nM each primer, 68 nM each nucleotide precursor, 50 mM. Negative control (a reaction carried out in the absence of template DNA) was always included to check for reagent contamination. Thermal cycles comprised 5 min of initial denaturation at 95 °C, then 30 cycles of denaturation, annealing, extension as previously described and 5 min of final extension at 72 °C. All PCR reactions were performed with a GeneAmp® PCR System 2400 thermal cycler (Applied Biosystems, Foster City, CA). The qualitative and quantitative outcome of the amplification reaction was checked by running 8 µl of PCR product on agarose gel in parallel to an appropriate molecular weight marker.

Retro trasciption reaction (RT)

RT was exploited using SuperScript III Reverse Trascriptase (Invitrogen ®; Carlsbad, CA), retrotranscription were performed using manufacture specifies and oligodeoxytimine to retrotranscribe all mRNA presents in the sample.

Plasmids

pCMV 5 vector were used for *in vitro* expression of FIX variants. Cytomegalovirus promoter and bGH polyA signal assure high level of recombinant FIX production in the majority of cell lines.

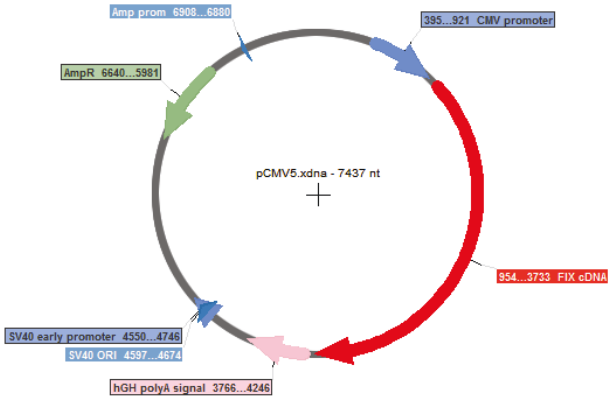

Figure 52: Graphical map of pCMV 5 vector containing FIX cDNA

pSV7d vector were used for *in vitro* expression of VWF variants was a generous gift from Prof J.E. Sadler (Washington University, St Louis, MO), and were also used in previous study for VWF expression {Casari, 2010 #46}.

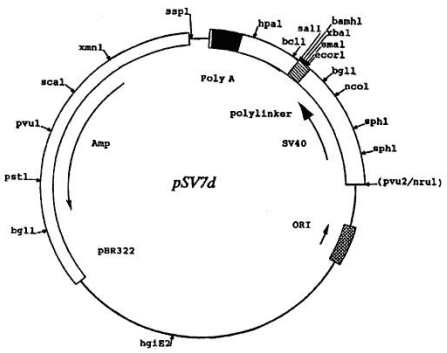

pLIVE vector (Mirus BIO, Madison, WI) were used for *in vivo* expression of VWF variants, due to the presence of Mouse minimal albumin promoter, this plasmid assure specific liver expression of murin VWF transgene.

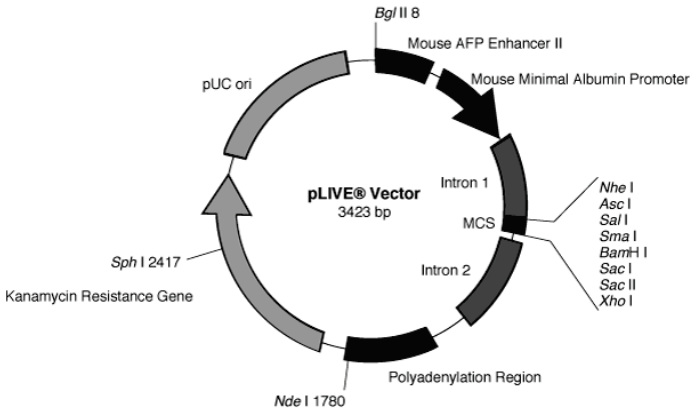

In all plasmids used in these studies utilized the cDNA of FIX (pCMV5) or VWF (pSV7d and pLIVE vector) to produce the corrispettive mRNA to drive protein synthesis.

Site specific mutagenesis

Site specific mutagenesis was performed using QuikChange® XL Site-Directed Mutagenesis Kit (Agilent; Santa Clara, CA); briefly primers were designed 29 bp long perfectly complementary to target DNA except for the singe point mutation that was inserted in the middle of the prmier sequence. The reaction was essentially carried out following manufacture protocol, but with half of volume, 25 µl instead of 50µl. mutagenesis reaction was immediately transformed into competent bacteria cells.

Transfection protocol

HEK 293 (human embryonic kidney) and COS-1 (African green monkey kidney fibroblasts) cells were transiently transfected into 6 or 12 well by using Lipofectamine 2000 (Invitrogen Corporation, Carlsbad, CA). Basically in an eppendorf tube, 4 µl (in ration 1:1 to the amount of DNA transfected) of Lipofectamine were added to 100 µl of serum-free medium (GIBCO-BRL™ OptiMEM®, Gaithersburg, MD) and incubated for 5 min at room temperature. DNA vector (4 µg) was placed in a separate tube with other 100 µl of serum-free medium. The solutions were joined after 5 minutes. The mixture was incubated at room temperature for 20 min and then added dropwise to the cells. The medium was changed 4 hours after transfection to reduce toxicity effects of Lipofectamine. Free FBS- Culture medium (OptiMEM; Invitrogen Corporation, Carlsbad, CA) was supplemented with 5 µg/mL vitamin K (Konakion; Roche, Welwyn Garden City, United Kingdom) to allow proper FIX biosynthesis. Lysis of cells and collection of media for protein studies, were conducted 48 or 72 hours after transfection for FIX or VWF respectively. Cell lysates when necessary were collected using non-reducing lysis buffer (25 mM Tris-phosphate, 10% glycerol, 1% Tryton X-100, pH 7.8) with protease inhibitors cocktail (sigma-aldrich, st. Louis, MO).

Western blot analysis

For Western blotting analysis, 26 µl of conditioned medium were incubated 5 min at 95°C and run on 4–15% Mini-PROTEAN® TGX™ Gel (Bio-Rad Laboratories; Hercules, CA) or NuPAGE Bis-Tris gel (Invitrogen ®; Carlsbad, CA). Proteins were transferred onto a 0.2 µm nitrocellulose membrane (Whatman®, Dassel, Germany), which was blocked overnight with PBS buffer supplemented with 0.1% Tween-20 (PBS-T) and 5% low fat dry milk (Bio-Rad, Hercules, CA). Membranes were then incubated for 3 hours at room temperature with PBS-T 5% low fat dry milk (Bio-Rad, Hercules, CA) with the respective antibody. For FIX analysis were used anti-Human FIX peroxidase conjugated (GAFIX-APHRP, Affinity Biologicals; Ancaster, Canada) in 1:1000 dilution. For VWF analysis membrane were with M13 and M31 and dilution were respectively 1:1000 and 1:3000 , moreover to detect M13 and M31 antibodies, successive incubation with anti-rabbit antibody HRP conjugated were used. The Supersignal® West Femto reagent (Thermo Scientific, Rockford, IL) was exploited for detection.

ELISA

Factor IX antigen levels in conditioned medium were evaluated by ELISA (Factor IX antigen F.IX; Affinity Biologicals, Ancaster, Canada). For VWF antigen levels were used anti-VWF (Dako A0082) 1:600 and anti-VWF-HRP (Dako P0226) 1:3000.

Briefly plates were coated overnight at 4°C with Coating buffer ($NaHCO_3$ 10mM,Na_2CO_3 50 mM pH 9,6), plate was washed 3 times with was buffer (PBS, Tween 0,1%, BSA 0,1%), in WVF elisa after washing plates were blocked with Blocking buffer for 30 minutes at 37°C (PBS,

Tween 0,1%, BSA 3%), then sample were loaded after proper dilution in dilution buffer (for FIX ELISA dilution buffer recipe is available into the kit procedure, for VWF dilution were performed in blocking buffer). After 90 minutes at room temperature samples were removed, plates was washed 3 times and secondary antibody was applied for 90 minutes. After this passage plates was washed again for 3 times and reaction solution (citrate-phosphate buffer, OPD, pH 5) was applied to start color development; reaction was constantly monitored and stopped with H_2SO_4 3M. To calibrate assay PNP serial dilution were used as reference.

Factor IX activity

FIX coagulant activity was assessed by activated partial thromboplastin time (aPTT)-based coagulation assays by exploiting FIX-depleted plasma (HemosIL, Instrumentation Laboratory, Lexington, MA, USA) supplemented with conditioned medium containing recombinant FIX. Coagulation times were measured upon addition of a contact activator (SynthASil, Hemosil) and $CaCl_2$ on a ACLTOP700 (Instrumentation Laboratory) instrument. Coagulation times from serial dilutions of recombinant rFIX-wt were used as standard curve, which was optimized for the determination of low activity. The specific activity of recombinant FIX variants was calculated as the ratio between coagulant activity and protein concentration.

Hydrodynamic injection

Nucleic Acid Preparation:

Determine the required total injection volume by using the following formula: Total volume needed per mouse (in ml) = mouse weight (g)/10 + 0.1 ml Delivery Solution (The addition of the 0.1 ml of Delivery Solution represents the void volume that remains in the syringe and needle after injection). The optimal mouse weight is between 18-25 g, which requires 1.9-2.6 ml of injection volume per mouse.It is recommended to inject 1-50 µg, but adjustments are required for optimal efficacy. Nucleic acid and Delivery Solution can be scaled up for additional mice as needed for replicate injections.Immediately prior to injection, add nucleic acid to a sterile plastic tube. Add the required volume of Delivery Solution pre-warmed to 37°C to the tube containing the nucleic acid and mix well. Inject the nucleic acid/Delivery Solution within 30 minutes of mixing. Connect the needle to the syringe and fill with the entire injection solution, ensuring that no air bubbles are present in the needle or syringe.

Injection Protocol

Preparation of Animal for Injection:

Generally, a laboratory mice of 5-6 weeks old are optimal for gene delivery. Mice that are older or have more body fat may exhibit compromised gene delivery. It is recommend starting with mice that are 18-25 g each. Use of anesthesia is optional and generally not required. To facilitate tail vein visualization and ensure optimal injections, dilate the tail vessels immediately prior to injection by warming the tail of the mouse in warm water (37°C) for 7-10 minutes. As the mouse tail warms up, the vein should dilate and become more visible.

Injection

While working under a light source, locate the dilated vein on the ventral side of the mouse tail, preferably near the distal end (tip) of the tail. Swab the area with an alcohol swab and allow it to air dry to further increase vein visibility and clean the injection site.

Place the syringe needle nearly parallel to the tail with the bevel down (toward the tail). Insert the needle into the tail vein. Check needle placement by injecting a small volume in the vein. If the needle is inserted correctly, the vein should begin to clear of blood. If there is

significant resistance, the needle may not be properly inserted into the tail vein. Improper needle insertion into tail tissue is characterized by discoloration and local swelling

Insert almost the full length of the needle into the vein (to prevent accidental removal of the needle while injecting). Dispense the complete injection volume into the mouse tail vein within 4-7 seconds at a constant rate. A good injection is characterized by a constant resistance that does not increase during the procedure.

Multimer analisys

Mutlimer analysis were performed at INSERM U770 (Paris, FRANCE). Briefly Low melting agarose (Seakem HGT,Lonza) gel was prepared and cooled at 4°C; samples were conditioned in Loading buffer (SDS 5%, EDTA, Tris, Urea pH 6.7) and warmed at 65°C for 15 minutes. Then Sample were loaded and gel starts 21 hours run at 57 V. After run proteins were blotted by capillarity overnight. Revelation of membranes were performed as normal western blotting assay.

Bibliography

Alberio, L. and G. L. Dale (1999). "Review article: platelet-collagen interactions: membrane receptors and intracellular signalling pathways." Eur J Clin Invest **29**(12): 1066-1076.

Alkalaeva, E. Z., A. V. Pisarev, L. Y. Frolova, L. L. Kisselev and T. V. Pestova (2006). "In vitro reconstitution of eukaryotic translation reveals cooperativity between release factors eRF1 and eRF3." Cell **125**(6): 1125-1136.

Arnout, J., M. F. Hoylaerts and H. R. Lijnen (2006). "Haemostasis." Handb Exp Pharmacol(176 Pt 2): 1-41.

Bajzar, L., R. Manuel and M. E. Nesheim (1995). "Purification and characterization of TAFI, a thrombin-activable fibrinolysis inhibitor." J Biol Chem **270**(24): 14477-14484.

Belvini, D., R. Salviato, P. Radossi, F. Pierobon, P. Mori, G. Castaldo, G. Tagariello and A. H. S. Group (2005). "Molecular genotyping of the Italian cohort of patients with hemophilia B." Haematologica **90**(5): 635-642.

Beresford, C. H. and M. C. Owen (1990). "Antithrombin III." Int J Biochem **22**(2): 121-128.

Bernardi, F., G. Marchetti, S. Guerra, A. Casonato, D. Gemmati, P. Patracchini, G. Ballerini and F. Conconi (1990). "A de novo and heterozygous gene deletion causing a variant of von Willebrand disease." Blood **75**(3): 677-683.

Bevers, E. M., P. Comfurius, J. L. van Rijn, H. C. Hemker and R. F. Zwaal (1982). "Generation of prothrombin-converting activity and the exposure of phosphatidylserine at the outer surface of platelets." Eur J Biochem **122**(2): 429-436.

Bevers, E. M., P. Comfurius and R. F. Zwaal (1983). "Changes in membrane phospholipid distribution during platelet activation." Biochim Biophys Acta **736**(1): 57-66.

Bidou, L., V. Allamand, J. P. Rousset and O. Namy (2012). "Sense from nonsense: therapies for premature stop codon diseases." Trends Mol Med **18**(11): 679-688.

Biggs, R., A. S. Douglas, R. G. Macfarlane, J. V. Dacie, W. R. Pitney, C. Merskey and J. R. O'Brien (1952). "Christmas Disease." Bmj **2**(4799): 1378-1382.

Bowen, D. J. (2002). "Haemophilia A and haemophilia B: molecular insights." Mol Pathol **55**(2): 127-144.

Brackmann, H. H. (1984). "Induced immunotolerance in factor VIII inhibitor patients." Prog Clin Biol Res **150**: 181-195.

Branchini, A., L. Rizzotto, G. Mariani, M. Napolitano, M. Lapecorella, M. Giansily-Blaizot, R. Mari, A. Canella, M. Pinotti and F. Bernardi (2012). "Natural and engineered carboxy-terminal variants: decreased secretion and gain-of-function result in asymptomatic coagulation factor VII deficiency." Haematologica **97**(5): 705-709.

Broze, G. J., Jr., T. J. Girard and W. F. Novotny (1990). "Regulation of coagulation by a multivalent Kunitz-type inhibitor." Biochemistry **29**(33): 7539-7546.

Carcao, M. D. and L. Aledort (2004). "Prophylactic factor replacement in hemophilia." Blood Rev **18**(2): 101-113.

Casari, C., P. J. Lenting, O. D. Christophe and C. V. Denis (2013). "Von Willebrand Factor Abnormalities Studied in the Mouse Model: What We Learned about VWF Functions." Mediterr J Hematol Infect Dis **5**(1): e2013047.

Casari, C., M. Pinotti, S. Lancellotti, E. Adinolfi, A. Casonato, R. De Cristofaro and F. Bernardi (2010). "The dominant-negative von Willebrand factor gene deletion p.P1127_C1948delinsR: molecular mechanism and modulation." Blood **116**(24): 5371-5376.

Chattoo, B. B., E. Palmer, B. Ono and F. Sherman (1979). "Patterns of Genetic and Phenotypic Suppression of lys2 Mutations in the Yeast SACCHAROMYCES CEREVISIAE." Genetics **93**(1): 67-79.

Christophe, O. D., P. J. Lenting, G. Cherel, M. Boon-Spijker, J. M. Lavergne, R. Boertjes, M. E. Briquel, A. de Goede-Bolder, J. Goudemand, S. Gaillard, R. d'Oiron, D. Meyer and K. Mertens (2001). "Functional mapping of anti-factor IX inhibitors developed in patients with severe hemophilia B." Blood **98**(5): 1416-1423.

Collen, D. (1999). "The plasminogen (fibrinolytic) system." Thromb Haemost **82**(2): 259-270.

Colman, R., J. Hirsh, V. J. Marder, A. W. Clowes and J. N. George (2001). Hemostasis and Thrombosis. Basic Principles and Clinical Practice, Fourth Edition.
Cooper, D. N. (1991). "The molecular genetics of familial venous thrombosis." Blood Rev **5**(1): 55-70.
Dahlback, B. (2000). "Blood coagulation." Lancet **355**(9215): 1627-1632.
Dahlback, B. (2004). "Progress in the understanding of the protein C anticoagulant pathway." Int J Hematol **79**(2): 109-116.
Dahlback, B. (2005). "Blood coagulation and its regulation by anticoagulant pathways: genetic pathogenesis of bleeding and thrombotic diseases." J Intern Med **257**(3): 209-223.
Del Conde, I., C. N. Shrimpton, P. Thiagarajan and J. A. Lopez (2005). "Tissue-factor-bearing microvesicles arise from lipid rafts and fuse with activated platelets to initiate coagulation." Blood **106**(5): 1604-1611.
Denis, C., N. Methia, P. S. Frenette, H. Rayburn, M. Ullman-Cullere, R. O. Hynes and D. D. Wagner (1998). "A mouse model of severe von Willebrand disease: defects in hemostasis and thrombosis." Proc Natl Acad Sci U S A **95**(16): 9524-9529.
Dever, T. E. and R. Green (2012). "The elongation, termination, and recycling phases of translation in eukaryotes." Cold Spring Harb Perspect Biol **4**(7): a013706.
Di Scipio, R. G., K. Kurachi and E. W. Davie (1978). "Activation of human factor IX (Christmas factor)." J Clin Invest **61**(6): 1528-1538.
Dietz, H. C., D. Valle, C. A. Francomano, R. J. Kendzior, Jr., R. E. Pyeritz and G. R. Cutting (1993). "The skipping of constitutive exons in vivo induced by nonsense mutations." Science **259**(5095): 680-683.
Dong, H. and C. G. Kurland (1995). "Ribosome mutants with altered accuracy translate with reduced processivity." J Mol Biol **248**(3): 551-561.
Drake, K. M., B. J. Dunmore, L. N. McNelly, N. W. Morrell and M. A. Aldred (2013). "Correction of Nonsense BMPR2 and SMAD9 Mutations by Ataluren in Pulmonary Arterial Hypertension." Am J Respir Cell Mol Biol **49**(3): 403-409.
Engin, F. and G. S. Hotamisligil (2010). "Restoring endoplasmic reticulum function by chemical chaperones: an emerging therapeutic approach for metabolic diseases." Diabetes Obes Metab **12 Suppl 2**: 108-115.
Floquet, C., I. Hatin, J. P. Rousset and L. Bidou (2012). "Statistical analysis of readthrough levels for nonsense mutations in mammalian cells reveals a major determinant of response to gentamicin." PLoS Genet **8**(3): e1002608.
Forge, A. and J. Schacht (2000). "Aminoglycoside antibiotics." Audiol Neurootol **5**(1): 3-22.
Freiburghaus, C., E. Berntorp, M. Ekman, M. Gunnarsson, B. M. Kjellberg and I. M. Nilsson (1999). "Tolerance induction using the Malmo treatment model 1982-1995." Haemophilia **5**(1): 32-39.
Fujikawa, K., H. Suzuki, B. McMullen and D. Chung (2001). "Purification of human von Willebrand factor-cleaving protease and its identification as a new member of the metalloproteinase family." Blood **98**(6): 1662-1666.
Furie, B. and B. C. Furie (1992). "Molecular and cellular biology of blood coagulation." N Engl J Med **326**(12): 800-806.
Garant, M. J., S. Kole, E. M. Maksimova and M. Bernier (1999). "Reversible change in thiol redox status of the insulin receptor alpha-subunit in intact cells." Biochemistry **38**(18): 5896-5904.
Giannelli, F. and P. M. Green (1996). "The molecular basis of haemophilia A and B." Baillieres Clin Haematol **9**(2): 211-228.
Gill, J. C., J. Endres-Brooks, P. J. Bauer, W. J. Marks, Jr. and R. R. Montgomery (1987). "The effect of ABO blood group on the diagnosis of von Willebrand disease." Blood **69**(6): 1691-1695.
Ginsburg, D. and J. E. Sadler (1993). "von Willebrand disease: a database of point mutations, insertions, and deletions. For the Consortium on von Willebrand Factor Mutations and Polymorphisms, and the Subcommittee on von Willebrand Factor of the Scientific and Standardization Committee of the International Society on Thrombosis and Haemostasis." Thromb Haemost **69**(2): 177-184.
Gonzalez-Hilarion, S., T. Beghyn, J. S. Jia, N. Debreuck, G. Berte, K. Mamchaoui, V. Mouly, D. C. Gruenert, B. Deprez and F. Lejeune (2012). "Rescue of nonsense mutations by amlexanox in human cells." Orphanet Journal of Rare Diseases **7**.

Greer, J. (1990). "Comparative modeling methods: application to the family of the mammalian serine proteases." Proteins **7**(4): 317-334.
Hoffman, M. (2003). "Remodeling the blood coagulation cascade." J Thromb Thrombolysis **16**(1-2): 17-20.
Ishigaki, Y., X. Li, G. Serin and L. E. Maquat (2001). "Evidence for a pioneer round of mRNA translation: mRNAs subject to nonsense-mediated decay in mammalian cells are bound by CBP80 and CBP20." Cell **106**(5): 607-617.
Jacobs, G. H., O. Rackham, P. A. Stockwell, W. Tate and C. M. Brown (2002). "Transterm: a database of mRNAs and translational control elements." Nucleic Acids Res **30**(1): 310-311.
Jaffe, E. A., L. W. Hoyer and R. L. Nachman (1974). "Synthesis of von Willebrand factor by cultured human endothelial cells." Proc Natl Acad Sci U S A **71**(5): 1906-1909.
Kandl, K. A., R. Munshi, P. A. Ortiz, G. R. Andersen, T. G. Kinzy and A. E. Adams (2002). "Identification of a role for actin in translational fidelity in yeast." Mol Genet Genomics **268**(1): 10-18.
Katsumi, A., T. Kojima, T. Senda, T. Yamazaki, H. Tsukamoto, I. Sugiura, S. Kobayashi, T. Miyata, H. Umeyama and H. Saito (1998). "The carboxyl-terminal region of protein C is essential for its secretion." Blood **91**(10): 3784-3791.
Katsumi, A., E. A. Tuley, I. Bodo and J. E. Sadler (2000). "Localization of disulfide bonds in the cystine knot domain of human von Willebrand factor." J Biol Chem **275**(33): 25585-25594.
Keeney, S. and A. M. Cumming (2001). "The molecular biology of von Willebrand disease." Clin Lab Haematol **23**(4): 209-230.
Ketterling, R. P., J. B. Drost, W. A. Scaringe, D. Z. Liao, J. Z. Liu, C. K. Kasper and S. S. Sommer (1999). "Reported in vivo splice-site mutations in the factor IX gene: severity of splicing defects and a hypothesis for predicting deleterious splice donor mutations." Hum Mutat **13**(3): 221-231.
Khajavi, M., K. Inoue and J. R. Lupski (2006). "Nonsense-mediated mRNA decay modulates clinical outcome of genetic disease." Eur J Hum Genet **14**(10): 1074-1081.
Kirchhofer, D., M. T. Lipari, P. Moran, C. Eigenbrot and R. F. Kelley (2000). "The tissue factor region that interacts with substrates factor IX and factor X." Biochemistry **39**(25): 7380-7387.
Kleinschnitz, C., G. Stoll, M. Bendszus, K. Schuh, H. U. Pauer, P. Burfeind, C. Renne, D. Gailani, B. Nieswandt and T. Renne (2006). "Targeting coagulation factor XII provides protection from pathological thrombosis in cerebral ischemia without interfering with hemostasis." Journal of Experimental Medicine **203**(3): 513-518.
Koeberl, D. D., C. D. Bottema, R. P. Ketterling, P. J. Bridge, D. P. Lillicrap and S. S. Sommer (1990). "Mutations causing hemophilia B: direct estimate of the underlying rates of spontaneous germ-line transitions, transversions, and deletions in a human gene." Am J Hum Genet **47**(2): 202-217.
Kurachi, S., D. P. Pantazatos and K. Kurachi (1997). "The carboxyl-terminal region of factor IX is essential for its secretion." Biochemistry **36**(14): 4337-4344.
Le Hir, H., E. Izaurralde, L. E. Maquat and M. J. Moore (2000). "The spliceosome deposits multiple proteins 20-24 nucleotides upstream of mRNA exon-exon junctions." EMBO J **19**(24): 6860-6869.
Lechner, D. and A. Weltermann (2008). "Circulating tissue factor-exposing microparticles." Thromb Res **122 Suppl 1**: S47-54.
Lejeune, F. and L. E. Maquat (2005). "Mechanistic links between nonsense-mediated mRNA decay and pre-mRNA splicing in mammalian cells." Curr Opin Cell Biol **17**(3): 309-315.
Li, L. P., T. A. Darden, S. J. Freedman, B. C. Furie, B. Furie, J. D. Baleja, H. Smith, R. G. Hiskey and L. G. Pedersen (1997). "Refinement of the NMR solution structure of the gamma-carboxyglutamic acid domain of coagulation factor IX using molecular dynamics simulation with initial Ca2+ positions determined by a genetic algorithm." Biochemistry **36**(8): 2132-2138.
Lillicrap, D. (2007). "Von Willebrand disease - phenotype versus genotype: deficiency versus disease." Thromb Res **120 Suppl 1**: S11-16.
Lorand, L. (2001). "Factor XIII: structure, activation, and interactions with fibrinogen and fibrin." Ann N Y Acad Sci **936**: 291-311.
Lozier, J. N., N. Tayebi and P. Zhang (2005). "Mapping of genes that control the antibody response to human factor IX in mice." Blood **105**(3): 1029-1035.
Luchtman-Jones, L. and G. J. Broze, Jr. (1995). "The current status of coagulation." Ann Med **27**(1): 47-52.

Malik, V., L. R. Rodino-Klapac, L. Viollet, C. Wall, W. King, R. Al-Dahhak, S. Lewis, C. J. Shilling, J. Kota, C. Serrano-Munuera, J. Hayes, J. D. Mahan, K. J. Campbell, B. Banwell, M. Dasouki, V. Watts, K. Sivakumar, R. Bien-Willner, K. M. Flanigan, Z. Sahenk, R. J. Barohn, C. M. Walker and J. R. Mendell (2010). "Gentamicin-induced readthrough of stop codons in Duchenne muscular dystrophy." Ann Neurol **67**(6): 771-780.
Mann, K. G., K. Brummel and S. Butenas (2003). "What is all that thrombin for?" Journal of Thrombosis and Haemostasis **1**(7): 1504-1514.
Mann, K. G., M. E. Nesheim, W. R. Church, P. Haley and S. Krishnaswamy (1990). "Surface-dependent reactions of the vitamin K-dependent enzyme complexes." Blood **76**(1): 1-16.
Manuvakhova, M., K. Keeling and D. M. Bedwell (2000). "Aminoglycoside antibiotics mediate context-dependent suppression of termination codons in a mammalian translation system." RNA **6**(7): 1044-1055.
Marchetti, G., P. Patracchini, S. Volinia, V. Aiello, M. Schiavoni, N. Ciavarella, E. Calzolari, C. Schwienbacher and F. Bernardi (1991). "Characterization of the pseudogenic and genic homologous regions of von Willebrand factor." Br J Haematol **78**(1): 71-79.
Michaux, G. and D. F. Cutler (2004). "How to roll an endothelial cigar: The biogenesis of Weibel-Palade bodies." Traffic **5**(2): 69-78.
Miller, G. J., D. J. Howarth, J. C. Attfield, C. J. Cooke, M. N. Nanjee, W. L. Olszewski, J. H. Morrissey and N. E. Miller (2000). "Haemostatic factors in human peripheral afferent lymph." Thromb Haemost **83**(3): 427-432.
Monkovic, D. and P. Tracy (1990). "Activation of human factor V by factor Xa and thrombin." Biochemistry: 1118-1128.
Monroe, D. M. and M. Hoffman (2006). "What does it take to make the perfect clot?" Arterioscler Thromb Vasc Biol **26**(1): 41-48.
Mort, M., D. Ivanov, D. N. Cooper and N. A. Chuzhanova (2008). "A meta-analysis of nonsense mutations causing human genetic disease." Hum Mutat **29**(8): 1037-1047.
Mosnier, L. O., T. Lisman, H. M. van den Berg, H. K. Nieuwenhuis, J. C. M. Meijers and B. N. Bouma (2001). "The defective down regulation of fibrinolysis in haemophilia A can be restored by increasing the TAFI plasma concentration." Thrombosis and Haemostasis **86**(4): 1035-1039.
Mullis, K. B. and F. A. Faloona (1987). "Specific synthesis of DNA in vitro via a polymerase-catalyzed chain reaction." Methods Enzymol **155**: 335-350.
Namy, O., I. Hatin and J. P. Rousset (2001). "Impact of the six nucleotides downstream of the stop codon on translation termination." Embo Reports **2**(9): 787-793.
Nathwani, A. C., E. G. Tuddenham, S. Rangarajan, C. Rosales, J. McIntosh, D. C. Linch, P. Chowdary, A. Riddell, A. J. Pie, C. Harrington, J. O'Beirne, K. Smith, J. Pasi, B. Glader, P. Rustagi, C. Y. Ng, M. A. Kay, J. Zhou, Y. Spence, C. L. Morton, J. Allay, J. Coleman, S. Sleep, J. M. Cunningham, D. Srivastava, E. Basner-Tschakarjan, F. Mingozzi, K. A. High, J. T. Gray, U. M. Reiss, A. W. Nienhuis and A. M. Davidoff (2011). "Adenovirus-associated virus vector-mediated gene transfer in hemophilia B." N Engl J Med **365**(25): 2357-2365.
Nesheim, M. (1998). "Fibrinolysis and the plasma carboxypeptidase." Curr Opin Hematol **5**(5): 309-313.
Neurath, H. (1984). "Evolution of proteolytic enzymes." Science **224**(4647): 350-357.
Nilsson, I. M., E. Berntorp and O. Zettervall (1986). "Induction of split tolerance and clinical cure in high-responding hemophiliacs with factor IX antibodies." Proc Natl Acad Sci U S A **83**(23): 9169-9173.
Ofosu, F. A. (2003). "Protease activated receptors 1 and 4 govern the responses of human platelets to thrombin." Transfus Apher Sci **28**(3): 265-268.
Osterud, B. and E. Bjorklid (2006). "Sources of tissue factor." Semin Thromb Hemost **32**(1): 11-23.
Pacho, F., G. Zambruno, V. Calabresi, D. Kiritsi and H. Schneider (2011). "Efficiency of translation termination in humans is highly dependent upon nucleotides in the neighbourhood of a (premature) termination codon." J Med Genet **48**(9): 640-644.
Peltz, S. W., M. Morsy, E. M. Welch and A. Jacobson (2013). "Ataluren as an agent for therapeutic nonsense suppression." Annu Rev Med **64**: 407-425.
Pimanda, J. and P. Hogg (2002). "Control of von Willebrand factor multimer size and implications for disease." Blood Reviews **16**(3): 185-192.

Pinotti, M., L. Rizzotto, P. Pinton, P. Ferraresi, A. Chuansumrit, P. Charoenkwan, G. Marchetti, R. Rizzuto, G. Mariani, F. Bernardi and V. I. I. D. S. G. International Factor (2006). "Intracellular readthrough of nonsense mutations by aminoglycosides in coagulation factor VII." J Thromb Haemost **4**(6): 1308-1314.
Pinotti, M., R. Toso, R. Redaelli, M. Berrettini, G. Marchetti and F. Bernardi (1998). "Molecular mechanisms of FVII deficiency: expression of mutations clustered in the IVS7 donor splice site of factor VII gene." Blood **92**(5): 1646-1651.
Pipe, S. W., K. A. High, K. Ohashi, A. U. Ural and D. Lillicrap (2008). "Progress in the molecular biology of inherited bleeding disorders." Haemophilia **14 Suppl 3**: 130-137.
Rallapalli, P. M., G. Kemball-Cook, E. G. Tuddenham, K. Gomez and S. J. Perkins (2013). "An interactive mutation database for human coagulation factor IX provides novel insights into the phenotypes and genetics of hemophilia B." J Thromb Haemost **11**(7): 1329-1340.
Reininger, A. J. (2008). "Function of von Willebrand factor in haemostasis and thrombosis." Haemophilia **14 Suppl 5**: 11-26.
Riddel, J. P., Jr., B. E. Aouizerat, C. Miaskowski and D. P. Lillicrap (2007). "Theories of blood coagulation." J Pediatr Oncol Nurs **24**(3): 123-131.
Rospert, S., M. Rakwalska and Y. Dubaquie (2005). "Polypeptide chain termination and stop codon readthrough on eukaryotic ribosomes." Rev Physiol Biochem Pharmacol **155**: 1-30.
Ruf, W., M. W. Kalnik, T. Lund-Hansen and T. S. Edgington (1991). "Characterization of factor VII association with tissue factor in solution. High and low affinity calcium binding sites in factor VII contribute to functionally distinct interactions." J Biol Chem **266**(24): 15719-15725.
Ruggeri, Z. M. (2007). "Von Willebrand factor: Looking back and looking forward." Thrombosis and Haemostasis.
Sadler, J. E. (2009). "von Willebrand factor assembly and secretion." J Thromb Haemost **7 Suppl 1**: 24-27.
Samor, B., J. C. Michalski, C. Mazurier, M. Goudemand, P. De Waard, J. F. Vliegenthart, G. Strecker and J. Montreuil (1989). "Primary structure of the major O-glycosidically linked carbohydrate unit of human von Willebrand factor." Glycoconj J **6**(3): 263-270.
Santagostino, E., P. M. Mannucci and A. Bianchi Bonomi (2000). "Guidelines on replacement therapy for haemophilia and inherited coagulation disorders in Italy." Haemophilia **6**(1): 1-10.
Sawamoto, Y., M. Shima, M. Yamamoto, S. Kamisue, H. Nakai, I. Tanaka, K. Hayashi, J. C. Giddings and A. Yoshioka (1996). "Measurement of anti-factor IX IgG subclasses in haemophilia B patients who developed inhibitors with episodes of allergic reactions to factor IX concentrates." Thromb Res **83**(4): 279-286.
Schneppenheim, R., J. Brassard, S. Krey, U. Budde, T. J. Kunicki, L. Holmberg, J. Ware and Z. M. Ruggeri (1996). "Defective dimerization of von Willebrand factor subunits due to a Cys- Arg mutation in type IID von Willebrand disease." Proc Natl Acad Sci U S A **93**(8): 3581-3586.
Schneppenheim, R. and U. Budde (2011). "von Willebrand factor: the complex molecular genetics of a multidomain and multifunctional protein." J Thromb Haemost **9 Suppl 1**: 209-215.
Schneppenheim, R., U. Budde, T. Obser, J. Brassard, K. Mainusch, Z. M. Ruggeri, S. Schneppenheim, R. Schwaab and J. Oldenburg (2001). "Expression and characterization of von Willebrand factor dimerization defects in different types of von Willebrand disease." Blood **97**(7): 2059-2066.
Schneppenheim, R., U. Budde and Z. M. Ruggeri (2001). "A molecular approach to the classification of von Willebrand disease." Best Pract Res Clin Haematol **14**(2): 281-298.
Springer, T. A. (2011). "Biology and physics of von Willebrand factor concatamers." J Thromb Haemost **9 Suppl 1**: 130-143.
Stansfield, I. and M. F. Tuite (1994). "Polypeptide chain termination in Saccharomyces cerevisiae." Curr Genet **25**(5): 385-395.
Sun, J., M. Chen, J. Xu and J. Luo (2005). "Relationships among stop codon usage bias, its context, isochores, and gene expression level in various eukaryotes." J Mol Evol **61**(4): 437-444.
Swan, S. K. (1997). "Aminoglycoside nephrotoxicity." Semin Nephrol **17**(1): 27-33.
Tanaka, R., D. Nakashima, A. Suzuki, Y. Miyawaki, Y. Fujimori, T. Yamada, A. Takagi, T. Murate, K. Yamamoto, A. Katsumi, T. Matsushita, T. Naoe and T. Kojima (2010). "Impaired secretion of carboxyl-

terminal truncated factor VII due to an F7 nonsense mutation associated with FVII deficiency." Thromb Res **125**(3): 262-266.
Taran, L. D. (1997). "Factor IX of the blood coagulation system: a review." Biochemistry (Mosc) **62**(7): 685-693.
Tavassoli, K., A. Eigel, B. Dworniczak, E. Valtseva and J. Horst (1998). "Identification of four novel mutations in the factor VIII gene: three missense mutations (E1875G, G2088S, I2185T) and a 2-bp deletion (1780delTC)." Hum Mutat **Suppl 1**: S260-262.
Tavassoli, K., A. Eigel, K. Wilke, H. Pollmann and J. Horst (1998). "Molecular diagnostics of 15 hemophilia A patients: characterization of eight novel mutations in the factor VIII gene, two of which result in exon skipping." Hum Mutat **12**(5): 301-303.
Thorland, E. C., J. B. Drost, J. M. Lusher, I. Warrier, A. Shapiro, M. A. Koerper, D. Dimichele, J. Westman, N. S. Key and S. S. Sommer (1999). "Anaphylactic response to factor IX replacement therapy in haemophilia B patients: complete gene deletions confer the highest risk." Haemophilia **5**(2): 101-105.
Tjernberg, P., H. L. Vos, G. Castaman, R. M. Bertima and J. C. J. Eikenboom (2004). "Dimerization and multimerization defects of von Willebrand factor due to mutated cysteine residues." Journal of Thrombosis and Haemostasis **2**(2): 257-265.
Valouev, I. A., V. V. Kushnirov and M. D. Ter-Avanesyan (2002). "Yeast polypeptide chain release factors eRF1 and eRF3 are involved in cytoskeleton organization and cell cycle regulation." Cell Motil Cytoskeleton **52**(3): 161-173.
Verweij, C. L. (1988). "Biosynthesis of human von Willebrand factor." Haemostasis **18**(4-6): 224-245.
Wang, J. W., D. J. Groeneveld, G. Cosemans, R. J. Dirven, K. M. Valentijn, J. Voorberg, P. H. Reitsma and J. Eikenboom (2012). "Biogenesis of Weibel-Palade bodies in von Willebrand's disease variants with impaired von Willebrand factor intrachain or interchain disulfide bond formation." Haematologica **97**(6): 859-866.
Wang, L., J. P. Louboutin, P. Bell, J. A. Greig, Y. Li, D. Wu and J. M. Wilson (2011). "Muscle-directed gene therapy for hemophilia B with more efficient and less immunogenic AAV vectors." Journal of Thrombosis and Haemostasis **9**(10): 2009-2019.
Weitz, J. I. (2003). "Heparan sulfate: antithrombotic or not?" J Clin Invest **111**(7): 952-954.
Willebrand, E. A. V. (1999 (1926)). "Hereditary pseudohaemophilia." Haemophilia **5**(3): 223-231.
Ye, J., N. L. Esmon, C. T. Esmon and A. E. Johnson (1991). "The active site of thrombin is altered upon binding to thrombomodulin. Two distinct structural changes are detected by fluorescence, but only one correlates with protein C activation." Journal of Biological Chemistry **266**(34): 23016-23021.
Yedjou, C. G., C. K. Tchounwou, S. Haile, F. Edwards and P. B. Tchounwou (2010). "N-acetyl-cysteine protects against DNA damage associated with lead toxicity in HepG2 cells." Ethn Dis **20**(1 Suppl 1): S1-101-103.
Zdziarska, J., A. Undas, J. Basa, T. Iwaniec, A. B. Skotnicki, P. de Moerloose and M. Neerman-Arbez (2009). "Severe bleeding and miscarriages in a hypofibrinogenemic woman heterozygous for the gamma Ala82Gly mutation." Blood Coagul Fibrinolysis **20**(5): 374-376.
Zhang, C., F. Liu, X. Liu and D. Chen (2010). "Protective effect of N-acetylcysteine against BDE-209-induced neurotoxicity in primary cultured neonatal rat hippocampal neurons in vitro." Int J Dev Neurosci **28**(6): 521-528.
Zhou, Y., Q. Jiang, S. Takahagi, C. Shao and J. Uitto (2013). "Premature Termination Codon Read-Through in the ABCC6 Gene: Potential Treatment for Pseudoxanthoma Elasticum." J Invest Dermatol.

Non-viral transfection systems for nucleic acids

long-chain cationic derivatives of PTA (1,3,5-triaza-7-phosphaadamantane) as new components of potential non-viral vectors

Cortesi R, Bergamini P, Ravani L, Drechsler M, Costenaro A, Pinotti M, Campioni M, Marvelli L, Esposito E.

Introduction

Gene transfection protocols typify important experimental therapeutics for tumor, infectious and genetic diseases (Deng et al., 2010; Edelstein et al., 2007, Brenner and Okur, 2009). The replacement of defect genes by introducing normal exogenous genes into target cells is an intriguing therapeutic system to restore the normal cell function (Patil et al., 2005). To replace or arrest the expression of specific genes, it is necessary that administered nucleic acid molecules maintain their stability within the extra- and intracellular environment for a sufficient period of time to exert a pharmacological effect (Patil et al., 2005, Pedroso de Lima et al., 2001; Merdan et al., 2002). In order to obtain this effect an efficient delivery system for nucleic acid molecules is required. There are two kinds of gene delivery vectors, viral and non-viral vectors. Viral vectors have shown high and stable gene expression *in vitro*. However, the immunogenicity and potential mutagenicity limit their applications *in vivo* (Chimurle et al., 1999; Manno et al., 2006). Therefore, more attention has been paid to non-viral vectors. Indeed, the use of non-viral vectors such as cationic systems (i.e. liposomes, nanoparticles, microparticles) (Patil et al., 2005) appears suitable since these carriers are known to be able to carry large inserts, to be the safer to use and the easier to produce in large scale with respect to viral vectors (Morille et al., 2008). However, these non-viral systems show low and transient expression levels owing to their inability to support the amplification, the cell-to-cell transmission (Ferrer-Miralles et al., 2008) and the toxicity at high doses (Somia et al., 2000). Among cationic non-viral systems, cationic solid lipid nanoparticles (SLN) have recently emerged as an alternative to liposomes due to their better stability profile and ease of industrial scalability (Tabatt et al., 2004).

Cationic systems bind DNA molecules by ionic interactions on their positively charged surface due to the presence of cationic detergents on carrier composition. Particularly, in the present paper, as cationic detergent two long-chain cationic phosphines (CP) have been considered.

CP are derivatives of PTA (1,3,5-triaza-7-phosphaadamantane), an hydrophilic phosphine firstly prepared in the early seventies (Daigle et al., 1974). CP have been designed as a new class of amino-phosphine bearing a large lipophilic portion beside the hydrophilic positively charged PTA cage and they have been obtained introducing long aliphatic chains on PTA nitrogen. CP structure, recalling cationic species with amphiphilic surfactant properties, makes them good candidates for the formation of positively charged SLN.

The purpose of this study was to investigate the potential of new positively charged SLN to convey nucleic acids. The cationic character of SLN was obtained by the addition of two long-chain CP, namely hexadecyl-PTA iodide (CP16) and octadecyl-PTA iodide (CP18). Particularly, this report describes: (a) the preparation and characterization of CP-SLN; (b) the ability of CP-SLN to bind DNA; (c) the effect of the obtained CP-SLN on cell proliferation of *in vitro* cultured human K562 erythroleukemic cells; (d) the effect on the stability of DNA molecules exposed to exo- and endo-nucleases after complexation to CP-SLN and (e) the ability of CP-SLN to transfect DNA into BHK-21 (Syrian hamster kidney fibroblast, PHLS) cultured cells.

Materials and Methods

Cationic derivatives of PTA (1,3,5-triaza-7-phosphaadamantane), namely CP16 and CP18, were synthesized by Dr. Paola Bergamini at the Department of Chemistry of our University as below reported. The reagents C16H33I and C18H37I were purchased and used without further purification. The phosphine PTA was prepared as described in the literature (Daigle, 1998).

Lutrol F 68, oxirane, methyl-, polymer with oxirane (75:30) (poloxamer 188) was obtained from BASF (Ludwigshafen, Germany). Miglyol 812, caprylic/capric triglyceride (tricaprin) was purchased from Eigenmann & Veronelli (Rho, Italy). Agarose and tristearin (stearic triglyceride) were purchased from Fluka (Buchs, Switzerland). The expression vectors for the red fluorescent protein (pHcRed1-N1) and the firefly luciferase (pGL3) were available in the laboratory. All other materials and solvents were from Sigma-Aldrich S.r.l. (Milan, Italy).

CP16 and CP18 have been prepared as iodides by treating in acetone PTA with $C_{16}H_{33}I$ and $C_{18}H_{37}I$, respectively. In the case of CP16, PTA (0.40 g, 2.58 mmol) was dissolved in 25 mL of degassed acetone and 1-iodohexadecane $C_{16}H_{33}I$ (1.62 ml, 5.14 mmol) was added to the solution, which was stirred at room temperature under argon for 20 hours. $(PTAC_{16}H_{33})I$, precipitated as a white solid, was filtered and washed with n-hexane (0.95 g, 1.87 mmol, 72%).

Concerning the synthesis of CP18, PTA (0.20 g, 1.29 mmol) and $C_{18}H_{37}I$ (0.98 g, 2.57 mmol) reacted in the same conditions as above to give $(PTAC_{18}H_{37})I$ as a white solid (0.57 g yield 83%).

Elemental analyses were carried out using a Carlo Erba instrument model EA1110. The ESI mass spectra were acquired with a Micromass LCQDuo Finningan. NMR spectra were recorded Varian Gemini 300 MHz spectrometer (^{1}H at 300 MHz, ^{13}C at 75.43 MHz, ^{31}P at 121.50 MHz). The ^{13}C and ^{31}P spectra were run with proton decoupling and ^{31}P spectra are reported in ppm relative to an external 85% H_3PO_4 standard, with positive shifts downfield. ^{13}C NMR spectra are reported in ppm relative to external tetramethylsilane (TMS), with positive shifts downfield.

CP-SLN were prepared by stirring, homogenization and ultrasonication (Esposito et al., 2008). Briefly, 1g of lipid was melted at 80°C. The lipid mixture was constituted of tristearine and CP in 200:1 by weight. The fused lipid phase was dispersed in 19 ml of an aqueous solution of poloxamer 188 (2.5 % w/w). The obtained emulsion was subjected to ultrasonication (Microson TM, Ultrasonic cell Disruptor) at 6.75 kHz for 15 min and then cooled down to room temperature by placing it in a water bath at 22°C. CP-SLN dispersions were stored at room temperature.

Characterization of CP-SLN: size, ζ potential and morphology

Submicron particle size analysis was performed using a Zetasizer 3000 PCS (Malvern Instr., Malvern, England) equipped with a 5 mW helium neon laser with a wavelength output of 633 nm. Glassware was cleaned of dust by washing with detergent and rinsing twice with water for injections. Measurements were made at 25°C at an angle of 90°. Samples were diluted with MilliQ water to an adequate scattering intensity prior the measurement. The results are presented as intensity weighted average (z-ave) value obtained from three measurements (10 runs each) with corresponding standard deviation. Each experimental value results from three independent experiments performed in triplicate.

The electrophoretic mobility of CP-SLN/pDNA complexes was measured at room temperature by mean of a Zetasizer 3000 PCS (Malvern Instr., Malvern, England) in 1 mM NaCl solution to avoid the fluctuation in the ζ potential due to variations in the conductivity

of purified water. Samples were injected in a glass capillary cell and analysed under a constant voltage after focusing with a 5 mW helium neon laser. The ζ potential, in mV, was automatically calculated from the electrophoretic mobility based on the Helmholtz–Smolukowski equation. Each sample was measured three times then mean value and standard deviation (SD) are presented.

Morphological characterization of CP-SLN was performed by Cryo-TEM. Samples were vitrified as described by Esposito et al. (2008). The vitrified specimen was transferred to a Zeiss EM922 transmission electron microscope for imaging using a cryoholder (CT3500, Gatan). The temperature of the sample was kept below -175 °C throughout the examination. Specimens were examined with doses of about 1000-2000 e/nm^2 at 200 kV. Images were recorded digitally by a CCD camera (Ultrascan 1000, Gatan) using a image processing system (GMS 1.4 software, Gatan). A drop of dispersion prepared for TEM measurements was placed on a bare copper grid and plunged frozen in liquid ethane at approximately 100 K. The sample was transferred into a cryo electron microscope (CEM902a, Zeiss, D-Oberkochen, Philips CM120, NL-Eindhoven) operated at 80 kV respectively 120 kV. Samples were viewed under low dose conditions at a constant temperature around 77–100 K. Images were acquired by a Dage SIT low intensity TV camera system and processed by a Kontron IBAS image processing system in the case of the Zeiss CEM902A and a Tietz Fastscan CCD camera system for the Philips CM120.

Analysis of the electrophoretic mobility of complexes between CP-SLN and DNA

CP-SLN were mixed with pHcRed1-N1 vector in different +/- molar ratios (i.e. from 0.5:1 to 32:1) and incubated at 37°C for 5 min, then each sample was subjected to electrophoresis. Electrophoresis was carried on in 0.8% agarose gel at constant voltage (100 mV) for 2 hours. The relative band migration was determined, after staining the gels with ethidium bromide.

DNA stability studies

The stability of CP-SLN/pDNA complexes towards fetal calf serum (FCS) contained nucleases was studied following the above protocol. 0.3 μg of pHcRed1-N1 vector were complexed to different amount of SLN resulting in final +/- molar charge ratios SLN/pDNA of 8:1 and 16:1, for CP16-SLN and CP18-SLN, respectively. The complexes were then incubated at 37°C in a thermostatic bath.

At different time intervals, between 0 and 240 min, samples were withdrawn and stored at -20°C until electrophoretic analysis was performed. Electrophoresis was performed on 0.8% (w/v) agarose gel containing 0.5 μg/ml ethidium bromide for 2 hours at 25 mV constant current. After electrophoresis, the bands corresponding to the pHcRed1-N1 vector were visualized by UV shadowing (Maniatis et al., 1982).

Effect of CP-SLN on cell proliferation

The effect of CP-SLN on cell proliferation was determined on cultured human leukemic K562 cells (Lozzio and Lozzio, 1975). Standard conditions for cell growth were α-medium (Gibco, Grand Island, NY), 50 mg/l streptomycin, 300 mg/l penicillin, supplemented with 10% fetal calf serum (Irvine Scientific, Santa Ana, CA) in 5% CO_2 at 90% humidity.

Human leukemic K562(S) cells were treated with different concentrations (10, 5, 2.5, 1.25 or 0.62 μg/ml) of cationic CP-SLN. After 5 days of culture, the cells were counted by a cell counter Fuchs (Tosenthal, Preciss, France) and the number of cells/ml was compared with the value obtained in untreated cell cultures in order to determine the percentage of surviving cells. As control the activity of SLN constituted of sole tristearine without CP,

named “blank SLN” were also assayed under the same conditions. Assays were carried out in triplicate and usually counts differed by <7%. Cells were counted with a Model ZF Coulter Counter (Coulter Electronics Inc., Hielah, FL) and the cell growth rate was computed. IC_{50} values, namely the compound concentration inhibiting the 50% of the cell growth, were calculated using the free ED50plus v1.0 software.

Transfection studies

BHK-2 cells were cultured as previously reported (Pinotti et al., 1998). For fluorescence microscopy, cells were cultured on 24-mm glass coverslips.

As control, BHK cells were transfected with 2 μg of plasmid DNA (pDNA) using the TransIT®-2020 (Mirus, Madison, Wisconsin, USA), in accordance to the manufacturer’s protocol.

CP-SLN/pDNA complexes were prepared by mixing the C16-SLN (8:1 +/- molar charge ratio) or C18-SLN (16:1 +/- molar charge ratio) with 2 μg of plasmid DNA for transfection experiments. The mixture was kept at room temperature (25 ± 0.5°C) for 20 min to allow the complexes to be formed. After the incubation, the SLN/pDNA complexes were used following the previously mentioned transfection protocol.

48 hours post-transfection cells were analyzed for red fluorescence (NIKON Eclipse 50i) or luciferase activity, as previously described (Bertolucci et al., 2008).

Results and Discussion

N-alkyl PTA derivatives CP16 and CP18 have been prepared in high yields by reacting 1,3,5-triaza-7-phosphaadamantane (PTA) with the appropriate alkyl iodide. Each product precipitated from solution as an air-stable solid that needed little purification (see Figure 1). The obtained products were firstly characterized by mass spectroscopy. Concerning CP16, Anal. Calcd for $C_{22}H_{45}IN_3P$ (509) C, 51.84; H, 8.91; N, 8.25. Found C, 51.84; H, 8.97; N 8.19. Electrospray MS (in H_2O): observed m/z 382, calcd. 382 for $C_{22}H_{45}N_3P$ $(M\text{-}I)^+$. In the case of CP18, Anal. Calcd. for $C_{24}H_{49}IN_3P$ (537): C, 53.60; H, 9.19; N, 7.82. Found C, 53.56; H, 9.35; N, 7.77. Electrospray MS (in H2O): observed m/z 410.3, calcd. 410 for $C_{24}H_{49}N_3P$ (M-I)+.

Secondly, CP16 and CP18 were characterized by ^{1}H, ^{13}C and ^{31}P NMR whose data are summarized in Table I. As clearly evident, ^{31}P NMR is diagnostic of the conversion of PTA into N-alkylated products, being the peak of PTA at - 100 ppm shifted downfield of about 20 ppm in $[(PTAC_nH_{2n+1})I]$ derivatives (δ - 84.27 and - 84.26 ppm for n =16, 18 respectively).

The octanol-water partition coefficient of the in $[(PTAC_nH_{2n+1})I]$ derivatives was obtained by a slow-stirring method providing accurate Log P results over a wide range of concentration values (Hajji et al., 2011). The obtained results are reported in Table II together with other physicochemical characteristics of CP16 and CP18.

The use of pure tristearin for producing CP-SLN allows the obtaining of stable and homogenous dispersions, free from aggregates (Esposito et al., 2008).

Table III summarizes the results concerning size, ζ potential and effect on K562 cell growth of the produced CP-SLN. From the analysis of these data it can be achieved that mean size is almost the same for both colloidal systems, being 216.8 ± 5.1 nm (P.I. 0.29) for CP16-SLN and 228.9 ± 6.3 nm (P.I. 0.22) for CP18-SLN. SLN dispersions maintained their dimensions almost unchanged for more than 6 months (data not shown).

Concerning ζ potential both systems show a slight cationic charge being +28.0 ± 0.63 and +26.9 ± 1.21, for CP16-SLN and CP18-SLN respectively.

Cryo-transmission electron microscopy (Cryo-TEM) analyses have been conducted in order to shed light on the structure of the dispersed particles in both CP-SLN dispersions. Figure 2 reports cryo-TEM images of CP containing colloidal dispersions.

The electron microscopic analysis demonstrates that CP16-SLN are mainly characterized by the presence of three-dimensional particles projected in a two dimensional way. In panel A elongated circular platelet-like crystalline particles and dark, “needle“ like structures edge-on viewed can be observed. The calculated thickness of nanoparticles was 10 nm.

On the other hand CP18-SLN (reported in panel B) showed a more inhomogeneous population of particles. Beside the "normal" SLN there were also many smaller and larger spherical particles characterized by a lamellar ultrastructure. In fact, together with the characteristics platelet-like structure of SLN, it is possible to note vesicular-like shapes with an internal multilamellar structure.

Moreover, it has to be underlined that due to the presence of phosphorus, the samples were very radiation sensitive on the surface therefore the images resulted a bit noisy.

To obtain information about the potential cytotoxic activity of CP-SLN, some *in vitro* assay were performed cultivating human erythroleukemic K562 cells in the presence of CP-SLN. Particularly, CP-SLN containing 0.5 or 2% of CP in their composition, corresponding to 0.6 to 10 μM of CP, were added to the cells. The results, reported in Figure 3 and Table II, indicate that both types of CP-SLN containing 2% of CP showed a rather pronounced cytotoxicity with an IC_{50} of 0.63 μM and IC_{50} of 0.61 μM for CP16-SLN and CP18-SLN, respectively (where IC_{50} is the compound concentration inhibiting the 50% of the cell growth). On the other hand when the content of CP was 0.5% of the total composition, the antiproliferative effect was obviously lower, being IC_{50}=7.83 μM for CP16-SLN and IC_{50}=6.86 μM for CP18-SLN.

It is well known that in general uncharged SLN do not exhibit any cytotoxic effects in vitro up to concentrations of 2.5% lipid (Schubert and Muller-Goymann, 2005), whilst lipid concentrations higher than 10% have been shown a viability of 80% in culture of human granulocytes (Muller et al., 1996). Moreover, the use of biocompatible fatty acids leads to no toxic effect from SLN degradation products. Hence, SLN cytotoxicity can be attributable to the presence of emulsifiers, surfactants, cationic lipiids and preservatives that are used in the production of these systems (Heydenreich et al., 2003; Tabatt et al., 2004). Cationic lipids are needed to prepare SLN used on gene therapy due to their surfactant activity and their positive charge. The surfactant activity is necessary to obtain the initial emulsion whilst the positive charge is needed to provide the superficial charge to SLN for their further interaction with negative charged DNA to form SLN-DNA complexes. However, cationic lipids can be toxic on repeated use (Han et al., 2000). One of the most commonly used cationic lipids in gene therapy is DOTAP. In particular, in the present study one-tailed cationic phosphines are used for the preparation on SLN. Many studies in literature reported that for these SLN formulations the presence of one-tailed cationic lipids is more critical with respect to cell toxicity than the usage of two tailed lipids (Tabatt et al., 2004; Olbrich et al., 2001), thus a higher toxicity is normally observed. Due to the risk of toxicity of cationic surfactant its concentration in the formulation has to be as lower as possible. Accordingly with the obtained results, the lower the concentration of CP used, the lower is expected to be the cytotoxic effect.

Binding migration studies of CP-SLN

In order to evaluate the strength of the interaction occurring between DNA and CP-SLN, CP-SLN were incubated with the pHcRed1-N1 plasmid DNA to different final charge +/- molar ratios SLN/DNA (see legend to Figure 4) and subjected to electrophoresis. The results

reported in Figure 4 indicate that DNA migration is retarded by the presence of CP-SLN, due to the formation of high-molecular-weight complexes with DNA molecules. These complexes were attributed to inter-nanoparticle bridges formed by DNA molecules (Sternberg et al., 1994). This hypothesis was supported by the presence of non-migrating bands in the agarose gels. From the analysis of Figure 4 it emerges that the strength of complex formation is higher in the case of CP16 with respect to CP18, being the charge +/- molar ratio between SLN and DNA 8:1 and 16:1, respectively.

Moreover we would like to mention that, as expected, when lower concentrations of cationic phosphines are used (i.e. 0.5% vs 2%), DNA migration is only slightly retarded by CP-SLN (data not shown).

Stability studies

An important advantage of non-viral systems in gene therapy is their capacity to protect DNA from components of the medium, and fundamentally from DNases digestion. The protective effect of SLN was studied on degradation of pHcRed1-N1 plasmid catalyzed by nucleases. It is to be underlined that we considered CP18-SLN as model CP-SLN and fetal calf serum (FCS) as source for nucleases. FCS was used since it is routinely employed in cell culture experiments. CP16-SLN/DNA and CP18-SLN/DNA complexes were incubated at 37°C from 0 to 120 min in the presence of 10% FCS, samples were then loaded on agarose gel and subjected to electrophoresis. As control, the same amount of pHcRed1-N1 plasmid was incubated in the absence of CP-SLN. The result of this experiment indicates that the complete degradation of free pHcRed1-N1 plasmid occurs within 90 min (see Fig. 5A), whilst the complexation of DNA to CP-SLN protects pHcRed1-N1 plasmid from degradation (Fig. 5B-C).

As above reported, the formation of CP-SLN/ pHcRed1-N1 complex leads to high-molecular-weight aggregates that give rise to a non-migrating band on agarose gel. However, we cannot formally exclude that DNA complexed to CP-SLN would be still integer after exposure to FCS nucleases. In order to answer this question, we performed a further experiment. Both CP16-SLN/pHcRed1-N1 and CP18-SLN/pHcRed1-N1 complexes were exposed to FCS nucleases, then phenol extraction of DNA was performed and the extracted DNA was analyzed by gel-electrophoresis. As reported in Fig. 6, the extracted DNA shows a single band with a molecular weight superimposable to that of undigested DNA. This result confirms the maintenance of DNA integrity in the presence of CP-SLN, whilst in their absence the DNA completely degrades within 60 min.

Gene transfection experiments

Once the formulations possessed the technologically suitable characteristics for the desired application, the next step was to test their transfection activity "*in vitro*". For transfection assays we worked with those +/- molar ratios that bound all DNA, provided high positive surface charge and protected DNA from enzyme degradation.

The ability of CP-SLN to transfect DNA was tested on BHK cells by exploiting the expression i) of the red fluorescent protein (RFP) through fluorescence microscopy (Fig. 7A-C) and ii) of the firefly luciferase through luciferase activity assays (Fig. 7D), which allows a better quantitative evaluation. Particularly the expression levels of RFP and firefly luciferase was evaluated after incubating BHK cells with the corresponding vectors complexed either to C16-SLN or C18-SLN, or TransIT® as control. As clearly reported in Figure 7, notwithstanding the ability of CP-SLN to efficiently bind DNA, their transfection efficiency appeared very limited as compared to the commercial product TransIT®. While the red fluorescence in cell

transfected with the TransIT® reagent and pHcRed1-N1 was very intense (Fig. 7C), that in cells transfected with C16-SLN and C18-SLN was barely appreciable (Fig. 7A-B).

Moreover, the luciferase activity levels measured upon transfection of cells with the pGL3 vector and the C16-SLN or C18-SLN was 3.9% and 5.5% of that detected with the TransIT® reagent (Fig. 7D). These low transfection efficiencies might be attributable either to the cytotoxic of the CP-SLN or to their ability to deliver the DNA into cells.

In fact, many findings on this topic indicated that the low transfection activity could be attributed to the excessive condensation at high +/− molar charge ratio, which make difficult the dissociation of DNA from cationic SLN (Faneca et al., 2002; del Pozo-Rodríguez et al., 2007). Indeed, DNA condensation is a crucial factor that determines the transfection capacity of SLN, because it influences the superficial charge of the complexes and thus cell entry, DNA delivery from nanoparticles, gene protection from DNAses and hence DNA topology. An optimal DNA condensation must be achieved when designing non-viral vectors. Complexes must have enough DNA condensation capacity to create equilibrium between those factors to obtain good transfection levels.

Conclusions

Taking into account these results, we demonstrated that both hexadecyl-PTA iodide (CP16) and octadecyl-PTA iodide (CP18) cationic phosphines can be exploited to produce CP-SLN. The obtained CP-SLN are characterized by a net positive charge on the surface and a reproducible size. Moreover, these nanosystems can bind nucleic acid molecules allowing the formation of stable complexes that are able to protect DNA from the activity of exo- and endo-nucleases present in serum. Lastly, *in vitro* experiments demonstrated that CP-SLN exhibit a quite pronounced antiproliferative effect on cultured human K562 erythroleukemic cells and a limited effect as transfecting adjuvant. The “in vitro” transfection levels provided by the formulations developed could be mainly conditioned by their DNA condensation capacity. There must be equilibrium between the gene protection degree, the binding forces of DNA to SLN and the DNA topology. This equilibrium is determined by cationic lipid/DNA ratio and it must be optimized with every new formulation.

Notwithstanding the scarce ability of CP-SLN to transfect RFP into mammalian cells, our results indicated the capacity of CP-SLN to protect DNA from degradation and encourage further studies aimed at proposing this approach as an innovative potential approach to deliver nucleic acid to cells in living organisms.

Acknowledgements

Authors thank Fondazione Cassa di Risparmio di Cento for financial support. The authors are grateful to Dr. Federica Dimitri for technical issues.

Table I. NMR data for CP16 and CP18

	^{1}H δ (ppm), *J* (Hz)	$^{13}C\{^{1}H\}$ δ (ppm), *J* (Hz)	$^{31}P\{^{1}H\}$ δ (ppm), *J* (Hz)
CP16	0.85, bt, 3H, CH_3 1.23, s, 26H, C*CH*$_2$C 1.62, m, 2H, *CH*$_2$CH$_2$N$^+$ 2.80, m, 2H, CH$_2$*CH*$_2$N 3.90, m, 4H, PCH$_2$N 4.35, bs, 2H, PCH$_2$N$^+$, 4.35, d, $^2J_{HH}$ 14, 1H, NCH$_2$N, 4.55, d, $^2J_{HH}$ 14, 1H, NCH$_2$N 4.80, d, $^2J_{HH}$ 11, 2H, NCH$_2$N$^+$ 4.92, d, $^2J_{HH}$ 11, 2H, NCH$_2$N$^+$	13.9, s, CH_3 18.9, s, CH_2 22.1, 26.1, 28.4, 28.7, 28.8, s, CH_2 29.0, bs, 7CH_2 31.3, s, CH_2 45.4, d, $^1J_{PC}$ 20.6, PCH$_2$N 51.7, d, $^1J_{PC}$ 31.2, PCH$_2$N$^+$ 61.4, s, RCH$_2$N$^+$ 69.3, s, NCH$_2$N 78.6, s, NCH$_2$N$^+$	- 84.27, s
CP18	0.92, t, 3H, CH_3 1.24, s, 30H, C*CH*$_2$C 1.62, m, 2H, *CH*$_2$CH$_2$N$^+$ 2.80, m, 2H, CH$_2$*CH*$_2$N 3.90, m, 4H, PCH$_2$N 4.33, d, 2H, PCH$_2$N$^+$, 4.35, d, 1H, NCH$_2$N, 4.53, d, $^2J_{HH}$ 14, 1H, NCH$_2$N 4.77, d, $^2J_{HH}$ 11, 2H, NCH$_2$N$^+$ 4.95, d, $^2J_{HH}$ 11, 2H, NCH$_2$N$^+$	13.9, s, CH_3 18.9, s, CH_2 22.1, 26.1, 28.4, 28.7, 28.8, s, CH_2 29.0, bs, 9 CH_2 31.3, s, CH_2 45.4, d, $^1J_{PC}$ 20.6, PCH$_2$N 51.7, d, $^1J_{PC}$ 32.2, PCH$_2$N$^+$ 61.4, s, RCH$_2$N$^+$ 69.3, s, NCH$_2$N 78.6, s, NCH$_2$N$^+$	- 84.26, s

The spectra were recorded at 25°C in d_6-dmso, at 300 MHz (^{1}H), 100.58 MHz ($^{13}C\{^1H\}$) and 121.50 MHz ($^{31}P\{^1H\}$) respectively

Table II. Some physicochemical characteristics of long-chain cationic phosphines.

Cationic phosphine	**Molecular Weight**	**λ_{max} * (nm)**	**logP°**
CP16	509	219 octanol 227 water	0.53
CP18	537	219 octanol 227 water	0.70

*λ_{max}: lambda max. It is the wavelength yielding the highest absorbance value

°logP: the logarithm of the partition coefficient (P) of a compound, being P the ratio of the concentration of the compound in octanol to the concentration of the same compound in water

Table III. Average diameter, ζ potential and effect on human erythroleukemic K562 cell growth of the produced carrier systems

carrier system	Mean diameter (nm)	Polydispersity	ζ potential (mV)	CP 0.5% IC_{50} (μM)	CP 2% IC_{50} (μM)
CP16-SLN	216.8 ± 5.1	0.29 ± 0.07	+28.0 ± 0.63	7.83 ± 0.12	0.63 ± 0.04
CP18-SLN	228.9 ± 6.3	0.22 ±0.04	+26.9 ± 1.21	6.86 ± 0.09	0.61 ± 0.07

Data represent the mean of three independent experiments ± SD

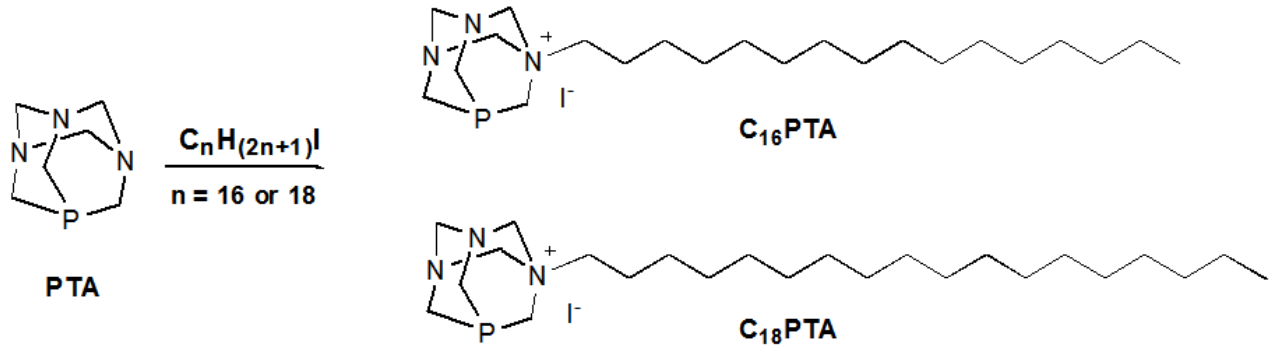

Figure 1. Synthetic scheme and chemical structure of the cationic phosphines hexadecyl-PTA iodide (CP16) and octadecyl-PTA iodide (CP18).

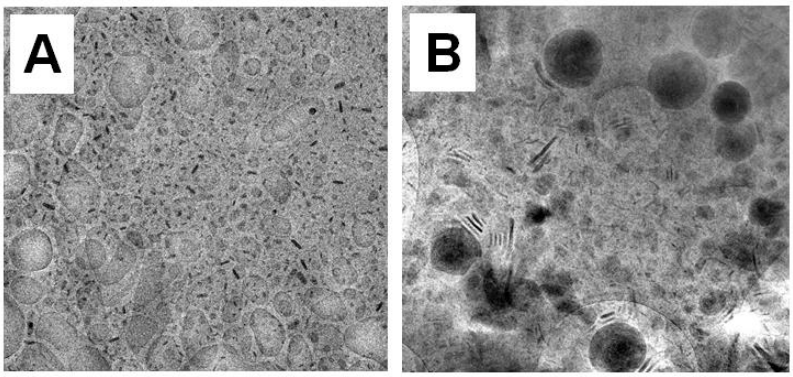

Figure 2. Cryo-TEM photographs of CP-SLN studied in the present paper. Panel A: CP16-SLN; Panel B: CP18-SLN. Bar represents 0.2 μm.

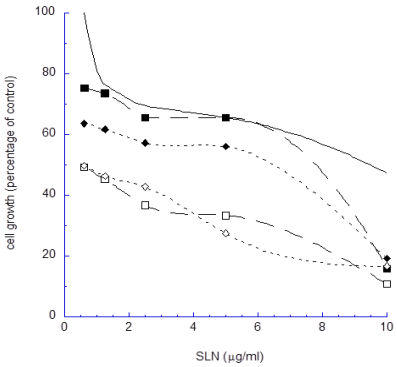

Figure 3. *In vitro* antiproliferative effect of different cationic SLN containing CP16 (squares) or CP18 (diamonds) and blank SLN (line) on human erythroleukemic K562 cells. The

concentration of CP was 0.5% (black symbols) or 2% (white symbols). Determinations were performed after 5 days of cell culture. Data represent the % of cell number/ml compared to untreated control K562 cells. The reported results are the average of 3 independent experiments, SD≤7%.

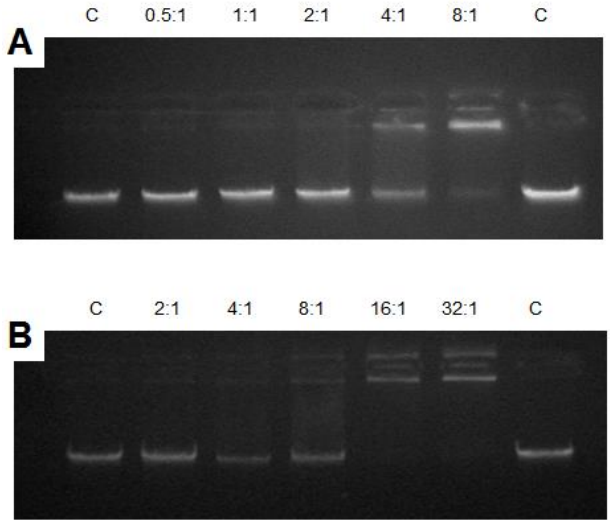

Figure 4. Effect of cationic complexation on electrophoretic migration of pHcRed1-N1 plasmid. For each type of CP-SLN the used +/- molar charge ratio between CP-SLN and DNA was indicated. c= free DNA. Panel A: CP16-SLN. Panel B: CP18-SLN.

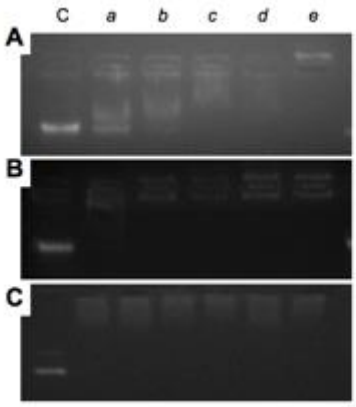

Figure 5. Agarose gel electrophoresis patterns of pHcRed1-N1 plasmid (0.3 μg) incubated in the presence of 10% FCS at 37°C for different length of time, namely 0 (lane a), 30 (lane b), 60 (lane c), 90 (lane d), and 120 (lane e) minutes, untreated DNA (C). Panel A: uncomplexed DNA. Panel B: CP16-SLN at a final +/- molar charge ratio of 8:1. Panel C: CP18-SLN at a final +/- molar charge ratio 16:1.

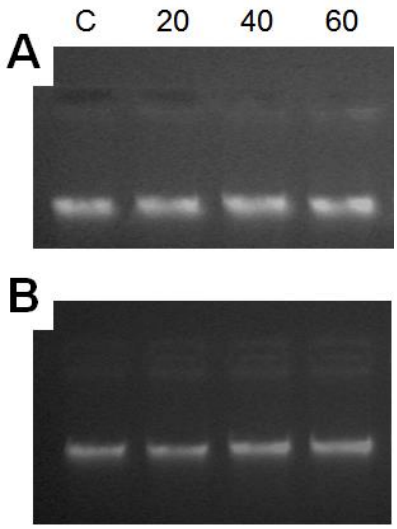

Figure 6. Electrophoretic analysis of pHcRed1-N1 plasmid DNA phenol extracted from CP-SLN. pHcRed1-N1 plasmid (0.3 μg) was ~~previously~~ incubated at 37°C in the presence of CP-SLN for 20, 40 and 60 min, then DNA was extracted with a standard protocol and analyzed by agarose gel electrophoresis. Panel A: CP16-SLN. Panel B: CP18-SLN.

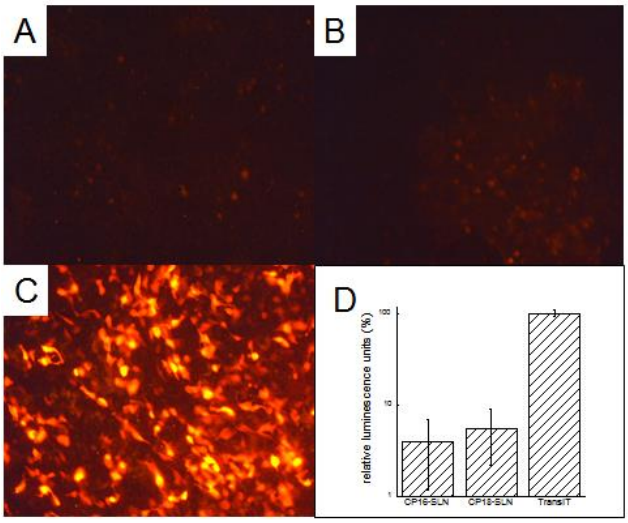

Figure 7. Transfection efficiency of CP-SLN in BHK-21 cells.

A-C) Representative examples of fluorescence microscopy images of cells transfected with the pHcRed1-N1 and the CP16-SLN (A), CP18-SLN (B) or TransIT® (C).

D) Luciferase activity levels in cells transfected with the pGL3 and TransIT®, CP16-SLN or CP18-SLN. The histograms report the mean ± standard deviation from three independent experiments.

References

Bertolucci, C., Cavallari, N., Colognesi, I., Aguzzi, J., Chen, Z., Caruso, P., Foá, A., Tosini G., Bernardi, F., Pinotti, M. 2008. Evidence for an overlapping role of CLOCK and NPAS2 transcription factors in liver circadian oscillators. Mol Cell Biol. 28(9), 3070-3075.

Brenner, M.K., Okur, F.V. 2009. Overview of gene therapy clinical progress including cancer treatment with gene-modified T cells. Hematology Am. Soc. Hematol. Educ. Program, 675–681.

Chirmule, N., Propert, K.J., Magosin, S.A., Qian, Y., Qian, R., Wilson, J.M. 1999. Immune responses to adenovirus and adeno-associated virus in humans. Gene Ther. 6, 1574–1583.

Daigle, D.J., Pepperman Jr., A.B., Vail, S.L. 1974. Synthesis of a monphosphorus analog of hexamethylenetetramine J. Heterocycl. Chem. 11, 407-408.

Daigle, D.J. 1998. 1,3,5-Triaza-7-phosphatricyclo[3.3.1.13,7]decane and derivatives. Inorg. Synth. 32, 40-45.

del Pozo-Rodríguez, A., Delgado, D., Solinís, M.A., Gascón, A.R., Pedraz, J.L. 2007. Solid lipid nanoparticles: Formulation factors affecting cell transfection capacity. Int. J. Pharm., 339, 261-268

Deng, W., Bivalacqua, T.J., Champion, H.C., Hellstrom, W.J., Murthy, S.N., Kadowitz, P.J. 2010. Gene therapy techniques for the delivery of endothelial nitric oxide synthase to the lung for pulmonary hypertension. Methods Mol. Biol. 610 (3), 309–321.

Edelstein, M.L., Abedi, M.R., Wixon, J. 2007. Gene therapy clinical trials worldwide to 2007: an update. J. Gene Med. 9, 833–842

Esposito, E., Fantin, M., Marti, M., Drechsler, M., Paccamiccio, L., Mariani, P., Sivieri, E., Lain, F., Menegatti, E., Morari, M., Cortesi, R. 2008. Solid Lipid Nanoparticles as delivery systems for bromocriptine. Pharm. Res. 25, 1521-1530.

Faneca, H., Simoes, S., de Lima, M.C.P. 2002. Evaluation of lipid-based reagents to mediate intracellular gene delivery. Biochim. Biophys. Acta, 1567, p 23-33.

Ferrer-Miralles, N., Vasquez, E., Villaverde, A. 2008. Membrane-active peptides for nonviral gene therapy: making the safest easier. Trends Biotechnol. 26, 267–275.

Hajji, L., Saraiba-Bello, C., Romerosa, A., Segovia-Torrente, G., Serrano-Ruiz, M., Bergamini, P., Canella, A. 2011. Water-soluble cp ruthenium complex containing 1,3,5-triaza-7-phosphaadamantane and 8-thiotheophylline derivatives: synthesis, characterization, and antiproliferative activity. Inorg. Chem. 50 (3), 873–882.

Han, S., Mahato, R.I., Sung, Y.K., Kim, S.W. 2000. Development of biomaterials for gene therapy. Molec. Ther. 2, 302-317

Heydenreich, A.V., Westmeier, R., Pedersen, N., Poulsen, H.S., Kristensen, H.G. 2003. Preparation and purification of cationic solid lipid nanospheres - effects on particle size, physical stability and cell toxicity. Int J Pharm. 254, 83-87.

Lozzio, C.B., Lozzio, B.B. 1975. Human chronic myelogeneous leukemia cell line with positive Philadelphia chromosome. Blood 45, 321-334.

Maniatis, T., Fritsch, E.F., Sambrook, J. 1982. Molecular cloning: a laboratory manual Cold Spring Harbor Laboratory, ed. Cold Spring Harbor, New York.

Manno, C.S., Arruda, V.R., Pierce, G.F., Glader, B., Ragni, M., Rasko, J., Ozelo, M.C., Hoots, K., Blatt, P., et al. 2006. Successful transduction of liver in hemophilia by AAV-factor IX and limitations imposed by the host immune response. Nat. Med. 12, 342–347.

Merdan, T., Kopecek, J., Kissel, T. 2002. Prospects for cationic polymers in gene and oligonucleotide therapy against cancer. Adv Drug Deliv Rev. 54, 715-758

Morille, M., Passirani, C., Vonarbourg, A., Clavreul, A., Benoit, J.P. 2008. Progress in developing cationic vectors for nonviral systemic gene therapy against cancer. Biomaterials 29, 3477–3496.

Muller, R.H., Maaßen, S., Weyhers, H., Specht, F., Lucks, J.S. 1996. Cytotoxicity of magnetite-loaded polylactide, polylactide/glycolide particles and solid lipid nanoparticles. Int. J. Pharm. 138, 85-94.

Olbrich, C., Bakowsky, U., Lehr, C.M., Müller, R.H., Kneuer, C. 2001. Cationic solid-lipid nanoparticles can efficiently bind and transfect plasmid DNA. J. Control. Rel. 77, 345-355.

Patil, S.D., Rhodes, D.G., Burgess, D.J. 2005. DNA-based therapeutics and DNA delivery systems: a comprehensive review. AAPS J. 7, pp. E61–E77

Pedroso de Lima, M.C., Simoes, S., Pires, P., Faneca, H., Duzgunes, N. 2001. Cationic lipid-DNA complexes in gene delivery: from biophysics to biological applications. Adv Drug Deliv Rev. 47(2-3), 277-294.

Pinotti, M., Toso, R., Redaelli, R., Berrettini, M., Marchetti, G., Bernardi, F. 1998. Molecular mechanisms of FVII deficiency: expression of mutations clustered in the IVS7 donor splice site of factor VII gene. Blood. 92, 1646-1651.

Schubert, M.A., Muller-Goymann, C.C. 2005. Characterization of surface-modified solid lipid nanoparticles (SLN): influence of lecithin and nonionic emulsifier. Eur. J. Pharm. Biopharm. 61, 77–86.

Somia, N., Verma, I.M. 2000. Gene therapy: trials and tribulations, Nat. Rev. Genet. 1, 91–99.

Sternberg, B., Sorgi, F.L., and Huang, L. 1994. New structures in complex formation between DNA and cationic liposomes visualized by freeze-fracture electron microscopy. FEBS Letters 356, 361-366.

Tabatt, K., Sameti, M., Olbrich, C., Muller, R.H., Lehr, C.M. 2004. Effect of cationic lipid and matrix lipid composition on solid lipid nanoparticles-mediated gene transfer. Eur. J. Pharm. Biopharm. 57, 155–162.

Cationic lipid nanosystems as carriers for nucleic acids

Rita Cortesi, Matteo Campioni, Laura Ravani, Markus Drechsler, Mirko Pinotti Elisabetta Esposito.

Introduction

Over the last decade, gene transfer has received enormous attention as therapeutic strategy for a large number of pathologies including genetic, neoplastic and infectious diseases [1-5]. In the substitutive gene therapy, a normal copy of the affected gene, or better its coding sequence, is delivered into target cells to restore normal gene expression and thus the physiological function. Other therapeutic strategies are based on delivery of oligonucleotides [6] or of vectors driving the expression of regulatory/antisense RNAs [7-8]. In all cases, a major issue is the design of an efficient system for their delivery into target cells and assuring their stability for a sufficient period of time to exert a pharmacological effect [9-11].

Various approaches, including the use of viral vectors, have been proposed [9,12-13], each possessing advantages and drawbacks. However, the use of lipid dispersions as gene delivery systems has attracted wide attention of worldwide formulators due to their potential applications [14-15].

Amid lipid dispersions, solid lipid nanoparticles (SLN) represent a new generation of delivery systems. These sub-micron colloidal carriers are composed of physiological lipid, dispersed in water or in aqueous surfactant solution. Nanodisperse phase has a solid matrix of crystalline solid lipids, able to protect encapsulated molecules from degradation and to modulate their release [14,16-17]. It is well known that mixture of surfactants and lipids are able to form a variety of assemblies determined by packing parameter or spontaneous curvature (i.e. micelles, liquid crystalline phase) [18]. Moreover, the emulsification in water of surfactant-like lipid leads to the formation of aqueous nanostructured dispersions of complex lyotropic liquid crystalline phase that can be characterized by lamellar, hexagonal or cubic structure [18]. The predominance of one species over the other depends on temperature and water content of the system [19].

Monoolein aqueous dispersions (MAD) typify a newer attractive delivery system. In particular MAD stabilized by the addition of a block copolymer like poloxamer 407, are mainly constituted of dispersed nanoparticles, such as cubosomes and hexosomes often in coexistence with vesicles [19-20]. Cubosomes are nanostructured particles of cubic liquid crystalline phases dispersed in water characterized by an inner structure with a cubic crystallographic symmetry [21]. On the other hand, hexasomes are particles of hexagonal shape with an inner structure with hexagonal symmetry and/or curved concentric striations [22]. The methods of MAD production [23-25] and the inner structure of dispersed nanoparticles [26-29] have been widely investigated [23-29].

It should be pointed out that cationic nanosystems are able to bind DNA molecules on their surface by ionic interactions. The surface of these preformed cationic nanoparticles is indeed positively charged due to the presence of cationic molecule within the nanosystem composition. In this way, negatively charged nucleic acid is complexed to the surface of preformed cationic nanocarriers, namely MAD and SLN. In the present paper, as cationic molecule we explored two different cationic surfactants, namely diisobutylphenoxyethyl-dimethylbenzyl ammonium chloride (DEBDA) and PEG-15 Cocopolyamine (PCPA). The purpose was to investigate the potential of new positively charged lipid nanocarriers (i.e. MAD and SLN) to convey nucleic acids. In particular, the specific aims were (a) the preparation and characterization of positively charged nanocarriers, namely MAD and SLN by using DEBDA or PCPA; (b) to test their ability to complex DNA; (c) to assess their effects

on cell proliferation of *in vitro* cultured human hepatocellular carcinoma HepG2 cells and finally (d) to evaluate the ability of these cationic nanosystems to transfect DNA into HepG2 cells.

Materials and methods

The glyceryl monooleate RYLO MG 19 (MO) was a gift from Danisco Cultor (Grindsted, Denmark). Poloxamer 407 (Pluronic F127) (PEO98-POP67-PEO98) and poloxamer 188 (Lutrol F 68), oxirane, methyl-, polymer with oxirane (75:30) were obtained from BASF (Ludwigshafen, Germany).

Compritol 888 ATO, a mixture of approximately 15% mono-, 50% di- and 35% triglycerides of behenic acid (tribehenin), was provided by Gattefossé (Saint Priest-France).

Salmon sperm DNA (SS-DNA) was obtained from Sigma-Aldrich (Milano, Italy). The pGL3-control vector, having the firefly luciferase coding region under the control of the SV40 promoter, was obtained by PROMEGA (Madison, WI, USA). The pCMV5-FIX and pPKCβ-GFP are eukaryotic expression vectors in which the coding sequence for coagulation factor IX (FIX) or for the chimearic protein kinase PKCß - green fluorescent protein (GFP), respectively, are cloned under the control of the CMV promoter [30, 31]. Hyamine 1622 (diisobutylphenoxyethyl-dimethylbenzyl ammonium chloride, DEDBA), Polyquart H81 (PEG-15 Cocopolyamine, PCPA) and Tristearin (stearic triglyceride) were purchased from Fluka (Buchs, Switzerland). All chemicals were used as received.

MAD preparation

Production of dispersions was based on the emulsification of MO (4.5% w/w) and Poloxamer 407 (0.5% w/w) in water (90%, w/w), as described by Esposito et al. [32]. In the present study, after emulsification, the dispersion was subjected to homogenization (15,000 rev min-1, Ultra Turrax, Janke & Kunkel, Ika-Werke, Sardo, Italy) at 60°C for 1 min, then cooled and maintained at room temperature in glass vials.

The dispersion was then filtered through Whatman™ mixed esters cellulose membrane (0.6 μm pore size) (Sigma-Aldrich, Milano, Italy) in order to separate big MO/poloxamer aggregates. Dispersion characterization of the MO dispersions as well as in vitro experiments were performed after filtration, without taking into account the fraction of larger particles whose dimensions have been measured by laser diffraction (Horiba, LA-920, Horiba Ltd., Tokyo, Japan).

SLN preparation

SLN were prepared by stirring, followed by ultrasonication [33]. Briefly, 1g of lipid consisting in tristearin or tribehenin in mixture with the cationic surfactant DEBDA or PCPA at the indicated concentrations, was melted at 75°C. The fused lipid phase was dispersed in 19 ml of an aqueous poloxamer 188 solution (2.5 % w/w). The obtained emulsion was subjected to ultrasonication (Microson TM, Ultrasonic cell Disruptor) at 6.75 kHz for 15 min and then cooled down to room temperature by placing it in a water bath at 22 °C. SLN dispersions were stored at room temperature.

Characterization of lipid dispersions

Submicron particle size analysis was performed using a Zetasizer 3000 PCS (Malvern Instr., Malvern, England) equipped with a 5 mW helium neon laser with a wavelength output of 633 nm. Measurements were made at 25 °C at an angle of 90°. Data were interpreted using the “method of cumulants” [32-33]. Samples were diluted with MilliQ water to an adequate scattering intensity prior the measurement. The results are presented as intensity weighted average (z-ave) value obtained from three measurements (10 runs each) with corresponding

standard deviation. Each experimental value results from three independent experiments performed in triplicate.

The electrophoretic mobility of cSLN/DNA complexes was measured at room temperature by mean of a Zetasizer 3000 PCS (Malvern Instr., Malvern, England) in 1 mM NaCl solution to avoid the fluctuation in the ζ potential due to variations in the conductivity of purified water. Samples were injected in a glass capillary cell and analysed under a constant voltage after focusing with a 5 mW helium neon laser. The ζ potential, in mV, was automatically calculated from the electrophoretic mobility based on the Helmholtz–Smolukowski equation. Each sample was measured three times then mean value and standard deviation (SD) are presented.

Morphological characterization of cationic SLN was performed by Cryo-TEM. Samples were vitrified as described by Esposito et al. [33]. The vitrified specimen was transferred to a Zeiss EM922 transmission electron microscope for imaging using a cryoholder (CT3500, Gatan). The temperature of the sample was kept below -175 °C throughout the examination. Specimens were examined with doses of about 1000-2000 e/nm^2 at 200 kV. Images were recorded digitally by a CCD camera (Ultrascan 1000, Gatan) using a image processing system (GMS 1.4 software, Gatan). A drop of dispersion prepared for TEM measurements was placed on a bare copper grid and plunged frozen in liquid ethane at approximately 100 °K. The sample was transferred into a cryo electron microscope (CEM902a, Zeiss, D-Oberkochen, Philips CM120, NL-Eindhoven) operated at 80 kV respectively 120 kV. Samples were viewed under low dose conditions at a constant temperature around 77–100 °K. Images were acquired by a Dage SIT low intensity TV camera system and processed by a Kontron IBAS image processing system in the case of the Zeiss CEM902A and a Tietz Fastscan CCD camera system for the Philips CM120.

Electrophoretic mobility of complexes between nanocarriers and nucleic acids

MAD or SLN containing increasing concentration of cationic detergent (namely 1% or 1.5% w/w) were mixed with SS-DNA or pCMV5-FIX vector in different +/- molar ratios (i.e. from 0.125:1 to 16:1) and incubated at 37°C for 5 min, then each sample was subjected to electrophoresis. Electrophoresis was carried on in 0.8% agarose gel at constant voltage (100 mV) for 2 hours in the absence or in the presence of increasing concentrations of cationic surfactant. The relative band migration was determined, after staining the gels with ethidium bromide.

Effect of cationic nanocarriers on cell proliferation

The effect of cationic nanocarriers on cell proliferation was determined in cultured human liver hepatocellular carcinoma HepG2 cells [34]. Standard conditions for cell growth were D-MEM/F-12 (1:1) (1X), liquid - with L-Glutamine (Invitrogen), medium supplemented with 10% foetal calf serum (Irvine Scientific, Santa Ana, CA) and Pen-Strep 1x (Omega Scientific Inc., Tarzana, CA) in 5% CO_2 at 90% humidity.

Cell viability was determined by MTT test [35]. HepG2 cells were seeded one day before the starting of the treatment into 96 wells with 100 μl of complete media. The next day cells were washed 2 times with PBS 1X and then medium was replaced with Opti-MEM containing different concentration of cationic nanocarriers in terms of cationic detergent, from 0 to 50 μM.

After 24h, 20 μl of MTT solution 5mg/ml were added to each well; then cells were incubated for 3.5h at 37°C in culture hood. After incubation cell medium was removed and 150 μl of MTT solvent were added to each well, subsequently wells were covered with a tinfoil and agitated on orbital shaker for 15 minutes. Afterwards absorbance was read at 590 nm.

IC_{50} values, namely the compound concentration inhibiting the 50% of the cell growth, were calculated using the free ED50plus v1.0 software.

Transfection studies

2 μg of plasmid DNA, either pPKCβ-GFP or pGL3, were transfected into HepG2 cells using Lipofectamine™ (Invitrogen) according to the manufacturer's protocol [36].

Nanocarrier/pDNA complexes were prepared by mixing preformed SLN and MAD (see Table I and II) with 2 μg of plasmid DNA, either pPKCβ-GFP or pGL3, at the minimum +/- molar charge ratio able to give a complex for transfection experiments. The mixture was kept at room temperature (25 ± 0.5°C) for 20 min to allow the complexes to be formed. 48 hours post-transfection cells were analysed for green fluorescence (NIKON Eclipse 50i) or luciferase activity, as previously described [36-37].

Statistical analyses

Comparison between groups were performed with Student's test and a P value <0.05 was considered significant.

Results and Discussion

Production and characterization of lipid dispersions

SLN composed either by tristearin (TS) or tribehenin (TB) were produced following the sonication method as described by Esposito et al. [33]. In these conditions stable and homogenous dispersions at least completely free from aggregates were obtained. However, as previously found, the highest loss of disperse phase was on the vessel (around 4% w/w with respect to the weight of lipid phase before dispersion) while larger particles represented less than 1% with respect to the total weight of disperse phase.

Table I summarizes the results concerning size, ζ potential and macroscopic aspect of the produced SLN dispersions. From the analysis of these data it can be achieved that, in general, the mean size of TS-based SLN is almost the same for both types of cationic surfactant, being comprised between 221.9 ± 2.2 nm (P.I. 0.21) for TS-PCPA 1,5% and 225.7 ± 22.1 nm (P.I. 0.39) for TS-DEBDA 1%. On the other hand the Z-average of TB-based SLN dispersions depends on the type of cationic molecule used, being comprised between 104.1 ± 1.7 nm (P.I. 0.56) and 225.7 ± 22.1 nm (P.I. 0.58) for DEBDA and between 246.7 ± 10.7 nm (P.I. 0.38) and 272.4 ± 9.3 nm (P.I. 0.38) for PCPA.

Concerning ζ potential all the systems show a slight cationic charge.

MADs were produced by the emulsification-hot homogenization method described by Esposito et al. [32]. All preparations showed a homogeneous opalescent aspect with no aggregates. The recovered weight of MAD was around 87% (w/w) with respect to the total weight of water/MO/poloxamer/cationic surfactant before production, indicating an extent of water loss (calculated by difference) around 13% by weight.

Table II reports the results concerning size, ζ potential and macroscopic aspect of the produced MADs. From the analysis of the reported results, it is evident that MAD-containing DEBDA are smaller in size as compared to MAD-containing PCPA, being the mean size around 210 nm for the first ones and 270 the other ones. Polydispersity indexes were comprised between 0.36 ± 0.11 and 0.64 ± 0.05, indicating a large dimensional distribution [32-33].

In addition, MAD-containing DEBDA are characterized by a more transparent aspect with respect to MAD-containing PCPA.

Concerning ζ potential, MADs show evident cationic charge, suggesting for these systems good efficiency to complex DNA by ionic interaction. In particular MAD-containing DEBDA are characterized by a two-fold ζ potential with respect PCPA-containing formulations.

Morphological analysis

Cryo-transmission electron microscopy (Cryo-TEM) analyses have been conducted in order to shed light on the structure of the dispersed particles in SLN and MAD dispersions.

Figure 1 reports cryo-TEM images of SLN dispersions, namely TS-DEBDA 1% SLN, TB-DEBDA 1% SLN, TS-PCPA 1.5% SLN and TB-PCPA 1.5% SLN.

All panels show deformed hexagonal, elongated and circular platelet-like particles, most likely viewed from the top. In addition, "needle"-like structures probably due to the presence of lipid crystals and hemi-elliptical particles, characterized by inner striations, can be also observed. The calculated thickness of nanoparticles was 10 nm.

Figure 2 reports cryo-TEM images of MAD. It has to be underlined that depending on the detergent's type used, two different kinds of colloidal systems are obtained. In fact, DEBDA-containing formulations give rise to the formation of multivesicular systems; while in the case of PCPA-containing formulations cubic particles with homogeneous and ordered inner structure coexisting with vesicular structures attached on their surface are observed. These last structures are characteristics of dispersions produced using monoolein and poloxamer 407 as previously reported [37].

The formation of vesicles instead of nanoparticles could be possibly ascribed to the molecular structure of the detergent used and to its interaction with monooleine. For instance, other authors have found that monooleine in dilute micellar bile salt solutions give rise to the formation of vesicles and different liquid crystalline phases [38].

The different type of nanosystem in suspension (vesicles vs nanoparticles) justifies the obtaining of a more transparent aspect of MAD-containing DEBDA with respect to MAD-containing PCPA, as above reported.

Cytotoxicity studies

To obtain information about the potential cytotoxic activity of the produced nanosystems, in vitro MTT assays were performed on HepG2 cells. Particularly, cells were treated with SLN and MAD at the same concentrations (ranging from 1 to 50 μM) in terms of cationic detergent molarity. Table III summarizes the IC_{50} values (i.e. the compound concentration inhibiting the 50% of the cell growth) found for each nanocarrier. The obtained results indicate that in general MAD formulations are less cytotoxic than SLN. Moreover, PCPA-containing MAD showed a moderate cytotoxicity (IC_{50} >50μM) as compared to DEBDA-containing MAD (IC_{50} around 15 μM). On the other hand, in the case of SLN, at the same surfactants concentration, TB-SLN are slightly less cytotoxic than TS-SLN, being the IC_{50} 2.42 μM vs 1.33 μM for DEBDA-SLN and 4.64 μM vs 1.10 μM for PCPA-SLN.

It is well known that in general uncharged SLN do not exhibit any cytotoxic effects in vitro up to lipid concentrations of 2.5% [39], whilst lipid concentrations higher than 10% have been shown a viability of 80% in culture of human granulocytes [40]. Moreover, the use of biocompatible fatty acids leads to no toxic effect from SLN degradation products. Hence, SLN cytotoxicity can be mainly attributable to the presence of emulsifiers, cationic surfactants and preservatives used in the production of these nanocarriers [41-42]. Cationic surfactants

are essential to prepare nanoparticles for gene therapy due to their activity and ability in conferring a positive charge on particle's surface. In addition, the surfactant activity is necessary to obtain the initial emulsion whilst the positive charge is needed to SLN for the interaction with negative charged DNA to form SLN-DNA complexes. Due to the risk of toxicity of cationic surfactant its concentration in the formulation has to be as lower as possible. Accordingly with the obtained results, the lower the concentration, the lower the cytotoxic effect is expected to be.

Binding migration studies

In order to evaluate the strength of the interaction occurring between DNA and each nanocarrier and also whether different cationic detergents could cause variation in binding capability, the following experiment was performed. Nanocarriers containing cationic detergent (see Fig. 3 and 4) were incubated with of SS-DNA or an expression plasmid for coagulation factor IX (pCMV5-FIX) used as model for linear or circular nucleic acids, respectively. Particularly, the concentration of nanocarriers was adjusted to obtain +/- molar charge ratios ranging from 0.12:1 up to 16:1 between cationic detergent and DNA. Samples were then electrophoresed to determine the electrophoretic migration of the nanocarrier/DNA complex. The results reported in Figure 3 indicate that SS-DNA migration is completely retarded by DEBDA-SLN at 2:1 +/- molar charge ratios due to the formation of high-molecular-weight complexes with DNA molecules, independently of the type of lipid constituting the SLN (Fig. 3A and 3B). The high-molecular-weight complexes were attributed to inter-nanoparticle bridges formed by DNA molecules [43] and this hypothesis was supported by the presence of non-migrating bands in agarose gels. On the other hand, the strength of the interaction occurring between DNA and both types of PCPA-SLN result less efficient with respect to DEBDA-SLN since the complexes were obtained at 16:1 +/- molar charge ratios between nanocarrier and DNA (Figure 3C and 3D).

The same trend is also evident in the case of MAD. In fact, as shown in Figure 3 SS-DNA migration is more efficiently retarded by the presence of DEBDA (Fig. 3E and 3F) with respect to PCPA (Figure 3G and 3H) being the +/- molar charge ratios needed to the formation of high-molecular-weight complexes in of 0.5:1 the first case versus 8:1 in the second case.

From the analysis of Figure 4, when pCMV5-FIX was used, it emerges again that the strength of complex formation is higher in the case of DEBDA-containing formulations with respect to PCPA-containing ones. In fact, the +/- molar charge ratios are 2:1 and 1:1 for DEBDA-SLN and DEBDA-MAD (Figure 4A, 4B, 4E, 4F) versus 8:1 and 4:1 for PCPA-SLN and PCPA-MAD (Figure 4C, 4D, 4G, 4H).

Thus, it can be concluded that independently of the DNA molecular weight, both for SLN or MAD, the strength of complex formation is higher in the presence of DEBDA instead of PCPA.

Transfection experiments

It is well known that cationic lipid-based gene delivery systems including liposomes, emulsions and lipid nanoparticles, are largely explored as non-viral systems. Gene transfections using cationic liposomes and cationic lipid emulsions have been widely reported [43-46]. However, there are only few reports on lipid nanoparticles for gene delivery [42, 47-48] and no paper concerning MAD. Thus, in our study the transfection activity of some of the produced cationic lipidic nanosystems, namely TS-PCPA 1.5% SLN, TB-PCPA 1.5% SLN, MAD-DEBDA, MAD-PCPA 1% and MAD-PCPA 1.5%, was tested on HepG2 cells by exploiting plasmids driving the expression of two widely-used reporter genes, the green fluorescent protein (GFP) and the firefly luciferase. The intracellular expression of the green fluorescent protein (GFP) permits the direct visualization of transfected cells by

fluorescence microscopy whereas the measurement of the firefly luciferase activity by a very sensitive functional assay allows a precise evaluation of the overall transfection efficiency. Particularly the expression level of GFP and firefly luciferase was evaluated after incubating HepG2 cells with the corresponding vectors complexed either to SLN or MAD, or Lipofectamine™ as control. As clearly reported in Figure 5, notwithstanding the ability of both SLN and MAD to efficiently bind DNA, their transfection efficiency appeared limited as compared to the commercial product Lipofectamine™. The luciferase activity levels measured upon transfection of cells with the pGL3 vector and the TS-PCPA 1.5% SLN, TB-PCPA 1.5% SLN, MAD-DEBDA, MAD-PCPA 1%, MAD-PCPA 1.5% was respectively 41.9 ± 4.3%, 1.5 ± 0.4%, 0.18 ± 0.06%, 0.22 ± 0.08% and 0.21 ± 0.03% of that detected with the Lipofectamine™ reagent (Fig. 5G). In addition it has to be underlined that the strength of the complex seems not important for the transfection efficiency since TS-PCPA (together with TB-PCPA) showed the higher +/- molar charge ratio to complex DNA (i.e. 16:1 for SS-DNA) as compared to other systems but give rise to the higher luciferase activity level (41.9%).

In general, the low transfection efficiencies might be attributable either to the cytotoxicity of cationic lipidic nanosystems or, more probably, to their ability to deliver the DNA into cells. The cationic nanosystems here described showed only moderate transfection efficiencies. On the other hand, the transfection activities here reported are accompanied by moderate degree of cytotoxicity. A number of possibilities exist to optimize the activity of the system, including choice of lipid matrix, size and modifier. Moreover, transfection enhancers can be encapsulated within cationic nanosystems [47]. For instance, it was demonstrated that the PEG conjugation can minimize SLN aggregation in buffers especially in the transfection medium and improve the transfection efficiency [48].

Indeed, great attention has been applied on the development of several strategies aimed to improve the transfection efficiency of the cationic SLN, including the use of endosomolytic agents as clorochine [42], or of synthetic cationic lipids used normally in the preparation of liposomes, such as DOTAP (N-(1-(2,3-dioleoyloxy) propyl)-N,N,N-trimethylammoniumchloride) [49] and the application of cell penetrating peptides [50]. Additionally, SLN made of tricaprin, DOPE (dioleoylphosphatidyl ethanolamine) and tween 80 were found able to transfect human non-small cell lung cancer cells [51] and the capacity of SLN–DNA vectors to induce the expression of a foreign protein after intravenous administration has been demonstrated [52].

To avoid interactions with plasma components, erythrocytes and the reticuloendothelial system thus improving systemic circulation, the masking of the surface charge of DNA complexes has to be accomplished. In this view, polyplexes based on polyethylenimine (PEI), shielded with polyethylene glycol and linked to the receptor binding ligands transferrin or epidermal growth factors have been proposed [53].

The improvement in the transfection can be also obtained by the presence of dextran on the nanoparticle surface [54]. The surface features of the vector may induce a lower opsonization and a slower uptake by the RES. Moreover, the high DNA condensation of protamine that contributes to the nuclease resistance may result in an extended stay of plasmid in the organism [55].

By means of electrostatic interactions, the cationic nanosystems condense nucleic acids on their surface. This is beneficial for transfection because condensation facilitates the mobility of nucleic acids, protects them from environmental enzymes and the cationic character of the vectors allows the interaction with negatively charged cell surface. The ability of nanosystems to condense the DNA depends not only on the value of their charge but also on the surface composition of the carrier. However, there must be equilibrium between the

binding forces of the nucleic acids and nanosystem to achieve protection without hampering the subsequent release in the site of action [56]. Release of DNA from the complexes may be one of the most crucial steps determining the optimal ratio for cationic lipid system-mediated transfection [57]. When the complexes display a too much high ζ-potential, a low capacity to release the DNA may be observed [58].

Moreover, the positive charge of the non-viral systems is necessary for the interaction with the negative charged cell surface and the cell entry facilitating the invagination of the cell plasma membrane [59]. Finally, good transfection efficiency may be due to the nuclear transfer of complexes that promotes penetration of DNA into the nucleus and transcription of exogenous DNA [55,60].

In addition, the small particle size of the complexes would facilitate the cellular uptake and enhance transfection efficiency [61].

Taking into account these considerations, further studies will be aimed at designing new nanoparticle compositions, at testing different components such as PEG or dextran, at trying to obtain cationic lipid nanosystems smaller in size as compared to that presented in this paper and at taking care of the balance ratio between the nanoparticles and the nucleic acids. In addition, other cell lines will be tested to evaluate the transfection efficiency and studies of cell localization will be performed in order to evaluate the capacity of the obtained non-viral nanosystem complexes to be internalized in the cells and to clarify how the different composition affects the cell entry capacity of the complexes.

Conclusions

Taken together these results demonstrated that both the cationic surfactant DEBDA and PCPA can be exploited to produce cationic nanosystems for DNA carrier. In particular, the obtained nanosystems are characterized by a positive charge on the surface and a reproducible size. The morphological structure of MAD is influenced by the type of cationic surfactant used resulting in the formation of vesicles in the case of DEBDA and of well-shaped particles coexisting with vesicles attached on their surface in the case of PCPA. Moreover, these nanosystems can bind nucleic acid molecules allowing the formation of stable complexes with DNA. Lastly, *in vitro* experiments demonstrated that both SLN and MAD exhibit a quite pronounced anti-proliferative and toxic effect on cultured human HepG2 cells and a limited effect as transfecting adjuvant.

The development of safe and efficient non-viral systems for gene delivery is a major challenge in the field of gene therapy. SLN and MAD are obtained using physiologically well-tolerated ingredients already approved for pharmaceutical applications in humans [62] and show low toxicity when injected intravenously [63]. The use of G.R.A.S. materials (i.e. triglycerides, partial glycerides, fatty acids, steroids) [64] leads to an advantageous toxicity profile [47] when compared with many highly efficient cationic polymers vectors [65-66].

The increasing attention toward the potentialities of such vectors is highlighted in the recent reviews and papers [36,67-70]. Additionally cationic lipid nanosystems have advantages under the technological point of view, including good storage stability, the possibility of steam sterilization and lyophilization [14,71].

The obtained data suggest that the cationic lipid nanosystems here described may be safe and may efficiently delivery complexed DNA, supporting their potential use for in vivo applications as non-viral transfection agents. We believe that the real potential of these vectors should be found in these aspects. Of course, many aspects need to be investigated and the data here obtained encourage further study aimed at improving these new

formulations as *in vitro* transfection reagents with potential application to *in vivo* delivery of nucleic acids.

Acknowledgements

Authors thank the University of Ferrara for financial support. The authors are grateful to dr. Stefania Bertolini for technical issues.

TABLE 1.

Characteristics of the produced SLN dispersions before and after the binding of nucleic acid

SLN	**Z average (nm) ± s.d.**	**polydispersity index**	**zeta potential (mV) ± s.d.**	**aspect**
before binding				
TS-DEBDA 1%	225.7 ± 22.1	0.39 ± 0.02	+ 17.2 ± 1.9	Milky
TS-PCPA 1%	222.5 ± 6.7	0.19 ± 0.03	+ 10.7 ± 6.4	Milky
TS-PCPA 1,5%	221.9 ± 2.2	0.21 ± 0.02	+ 10.0 ± 3.1	Milky
TB-DEBDA 1%	157.4 ± 12.5	0.58 ± 0.04	+ 9.2 ± 1.3	Opalescent
TB-DEBDA 1,5%	104.1 ± 1.7	0.56 ± 0.02	+ 23.4 ± 0.4	Opalescent
TB-PCPA 1%	272.4 ± 9.3	0.38 ± 0.04	+ 11.8 ± 2.1	Milky
TB-PCPA 1,5%	246.7 ± 10.7	0.38 ± 0.07	+ 15.6 ± 1.1	Milky
after binding SS-DNA				
TS-DEBDA 1%	282.7 ± 8.1	0.31 ± 0.04	+ 1.2 ± 0.2	Milky
TS-PCPA 1%	276.5 ± 7.7	0.22 ± 0.05	+ 0.7 ± 0.1	Milky
TS-PCPA 1,5%	284.2 ± 2.2	0.28 ± 0.02	+ 0.8 ± 0.1	Milky
TB-DEBDA 1%	227.2 ± 8.5	0.56 ± 0.06	- 0.2 ± 0.1	Opalescent
TB-DEBDA 1,5%	192.1 ± 3.7	0.33 ± 0.04	- 3.4 ± 0.4	Opalescent
TB-PCPA 1%	302.4 ± 12.3	0.58 ± 0.06	+ 1.8 ± 0.3	Milky
TB-PCPA 1,5%	297.7 ± 11.2	0.37 ± 0.11	- 0.6 ± 0.1	Milky
after binding pCMV5-FIX				
TS-DEBDA 1%	295.2 ± 12.0	0.42 ± 0.05	- 1.7 ± 0.6	Milky
TS-PCPA 1%	282.5 ± 8.7	0.29 ± 0.04	- 0.8 ± 0.4	Milky
TS-PCPA 1,5%	291.9 ± 9.2	0.26 ± 0.03	+ 1.0 ± 0.2	Milky
TB-DEBDA 1%	207.4 ± 12.8	0.33 ± 0.03	- 0.6 ± 0.3	Opalescent

TB-DEBDA 1,5%	199.1 ± 9.7	0.36 ± 0.03	- 2.4 ± 0.2	Opalescent
TB-PCPA 1%	307.2 ± 9.8	0.56 ± 0.07	+ 0.9 ± 0.1	Milky
TB-PCPA 1,5%	306.7 ± 10.4	0.48 ± 0.08	- 1.5 ± 0.3	Milky

Data are the mean of 6 independent analyses ± SD.

$p < 0.05$ always

TABLE 2.

Characteristics of MAD before and after complexation with nucleic acid

MAD	Z average (nm) ± s.d.	polydispersity index	zeta potential (mV) ± s.d.	aspect
before binding				
DEBDA 1%	235.0 ± 7.9	0.36 ± 0.11	+ 51.3 ± 2.12	Opalescent
DEBDA 1,5%	204.4 ± 9.7	0.55 ± 0.04	+ 45.2 ± 0.42	Opalescent
PCPA 1%	270.4 ± 5.8	0.41 ± 0.08	+ 22.1 ± 0.21	Milky
PCPA 1,5%	273.2 ± 4.4	0.64 ± 0.05	+ 26.2 ± 0.49	Milky
after binding SS-DNA				
DEBDA 1%	295.9 ± 6.3	0.33 ± 0.14	- 1.3 ± 0.14	Opalescent
DEBDA 1,5%	284.4 ± 8.8	0.45 ± 0.09	+ 4.2 ± 0.12	Opalescent
PCPA 1%	309.4 ± 5.2	0.48 ± 0.18	+ 2.1 ± 0.02	Milky
PCPA 1,5%	323.3 ± 8.3	0.42 ± 0.11	+ 2.2 ± 0.23	Milky
after binding pCMV5-FIX				
DEBDA 1%	301.0 ± 8.9	0.23 ± 0.08	+ 2.4 ± 0.15	Opalescent
DEBDA 1,5%	296.4 ± 7.7	0.41 ± 0.06	- 2.2 ± 0.04	Opalescent
PCPA 1%	310.2 ± 6.8	0.51 ± 0.07	+ 3.2 ± 0.01	Milky
PCPA 1,5%	331.2 ± 5.4	0.61 ± 0.15	- 1.2 ± 0.04	Milky

Data are the mean of 6 independent analyses ± SD.

$p < 0.05$ always

TABLE 3

Effect of SLN- and MAD-containing cationic detergent on cell growth of hepatocarcinoma HepG2 cells

Cationic compound (% w/w)	**SLN IC_{50} (μM)[a]**	**MAD IC_{50} (μM)[a]**
DEBDA 1%	1.33 (TS)	14.58
DEBDA 1,5%	2.42 (TB)	16.39
PCPA 1%	n.d.	> 50
PCPA 1,5%	1.10 (TS)	> 50
PCPA 1,5%	4.64 (TB)	> 50

[a]IC_{50}: Inhibitory concentration 50%: cationic detergent concentration (μM) required to cause the 50% inhibition of in vitro cell growth.

n.d.= not determined

Data represent the average of 3 independent experiments.

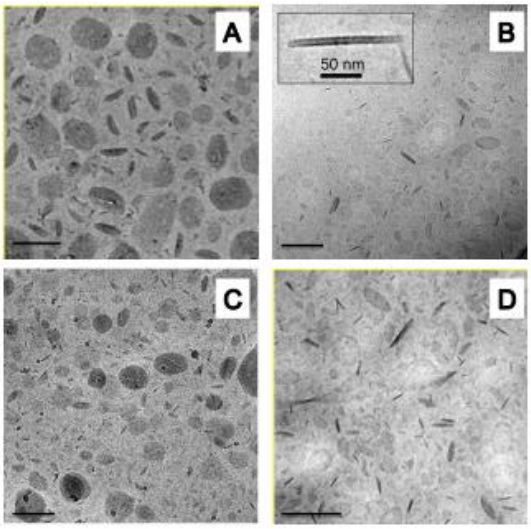

FIGURE 1. Cryo-transmission electron microscopy images (Cryo-TEM) of cationic SLN dispersions. (A) TS-DEBDA 1% SLN. (B) TB-DEBDA 1% SLN. The inset shows one particle side viewed. (C) TS-PCPA 1.5% SLN. (D) TB-PCPA 1.5% SLN. Bar represents 0.2 μm.

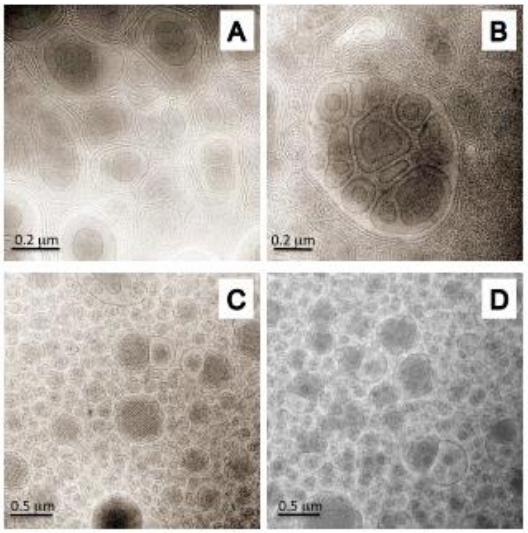

FIGURE 2. Cryo-TEM images of cationic MAD. (A) MAD-DEBDA 1%. (B) MAD-DEBDA 1.5%. (C) MAD-PCPA 1%. (D) MAD-PCPA 1.5%.

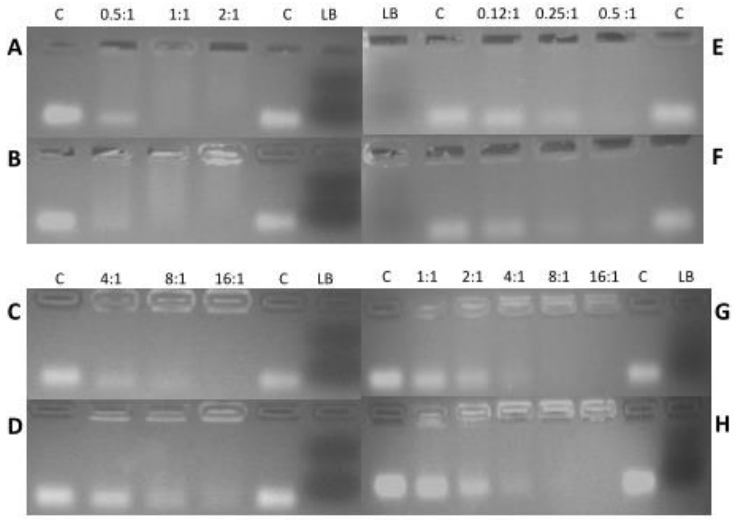

FIGURE 3. Effect of cationic complexation on the electrophoretic migration of salmon sperm (SS-DNA). The indicated +/- molar charge ratio between cationic nanosystem and SS-DNA ranges from 0.12:1 to 16:1. C= free SS. LB= loading buffer.

(A) TS-DEBDA 1% SLN. (B) TB-DEBDA 1.5% SLN. (C) TB-PCPA 1.5% SLN. (D) TS-PCPA 1.5% SLN. (E) MAD-DEBDA 1%. (F) MAD-DEBDA 1.5%. (G) MAD-PCPA 1%. (H) MAD-PCPA 1.5%.

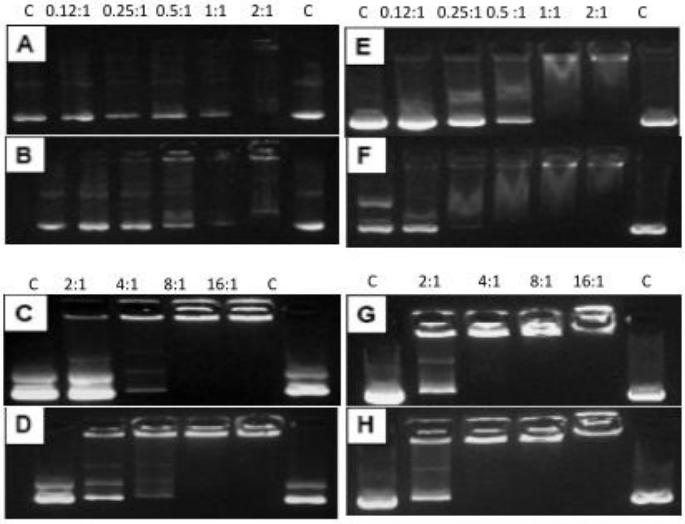

FIGURE 4. Effect of cationic complexation on the electrophoretic migration of the plasmid for coagulation factor IX (pCMV5-FIX). The indicated +/- molar charge ratio between cationic nanosystem and DNA ranges from 0.12:1 to 16:1. C= free DNA. (A) TS-DEBDA 1% SLN. (B) TB-DEBDA 1.5% SLN. (C) TB-PCPA 1.5% SLN. (D) TS-PCPA 1.5% SLN. (E) MAD-DEBDA 1%. (F) MAD-DEBDA 1.5%. (G) MAD-PCPA 1%. (H) MAD-PCPA 1.5%.

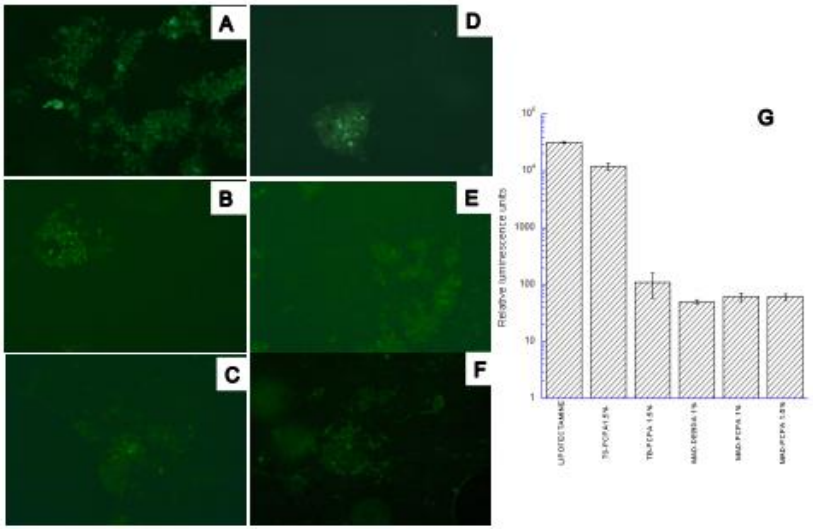

FIGURE 5. Transfection efficiency in HepG2 cells.

(A-F) Representative examples of fluorescence microscopy images of cells transfected by mean of Lipofectamine™ (A), TS- PCPA 1.5% SLN (B), TB-PCPA 1.5% SLN (C), MAD-DEBDA (D), MAD-PCPA 1% (E), MAD-PCPA 1.5% (F).

(G) Luciferase activity levels in cells transfected by mean of Lipofectamine™, TS- PCPA 1.5% SLN, TB-PCP 1.5% SLN, MAD-DEBDA, MAD-PCPA 1% and MAD-PCPA 1.5%. The histograms report the mean ± standard deviation obtained from three independent experiments.

References

1. Deng, W. *et al.* (2010) Gene therapy techniques for the delivery of endothelial nitric oxide synthase to the lung for pulmonary hypertension. *Methods Mol. Biol*. 610, 309–321
2. Edelstein, M.L. *et al.* (2007) Gene therapy clinical trials worldwide to 2007: an update. *J. Gene Med.* 9, 833–842
3. Brenner, M.K. and Okur, F,V. (2009) Overview of gene therapy clinical progress including cancer treatment with gene-modified T cells. *Hematology Am. Soc. Hematol. Educ. Program* 675–681
4. Assi, H. *et al.* (2012) Gene therapy for brain tumors: basic developments and clinical implementation. *Neurosci. Lett.* 527, 71-77.
5. Keeler, A.M. Flotte, T.R. *et al.* (2012) Cell and gene therapy for genetic diseases: inherited disorders affecting the lung and those mimicking sudden infant death syndrome. *Hum. Gene Ther*. 23, 548-556
6. Spitali, P. and Aartsma-Rus, A. *et al.* (2012) Splice modulating therapies for human disease. *Cell* 148, 1085-1088
7. Pinotti, M. *et al.* (2011) RNA-based therapeutic approaches for coagulation factor deficiencies. *J. Thromb. Haemost*. 9, 2143-2152.
8. Martone, J. *et al.* (2012) U1 snRNA as an effective vector for stable expression of antisense molecules and for the inhibition of the splicing reaction. *Methods Mol. Biol.* 867, 239-257.
9. Patil, S.D. *et al.* (2005) DNA-based therapeutics and DNA delivery systems: a comprehensive review. *AAPS J.* 7, E61–E77
10. Merdan, T. *et al.* (2002) Prospects for cationic polymers in gene and oligonucleotide therapy against cancer. *Adv. Drug Deliv. Rev.* 54, 715-758
11. Pedroso de Lima, M.C. *et al.* (2001) Cationic lipid-DNA complexes in gene delivery: from biophysics to biological applications. *Adv. Drug Deliv. Rev.* 47, 277-294
12. Chirmule, N. *et al.* (1999) Immune responses to adenovirus and adeno-associated virus in humans. *Gene Ther.* 6, 1574-1583
13. Manno, C.S. *et al.* (2006) Successful transduction of liver in hemophilia by AAV-factor IX and limitations imposed by the host immune response. *Nat. Med.* 12, 342–347
14. Muller, R.H. *et al.* (2000) Solid lipid nanoparticles (SLN) for controlled delivery-a review of the state of the art. *Eur. J. Pharm. Biopharm*. 50:161-177
15. Westesen, K. and Siekmann, B. (1996) Biodegradable colloidal drug carrier systems based on solid lipids. In: Benita S. Microencapsulation. New York: Marcel Dekker, 213–258
16. Westesen, K. *et al.* (1997) Physicochemical characterization of lipid nanoparticles and evaluation of their drug loading capacity and sustained release potential. *J. Control. Rel.* 48, 223-230
17. Yaghmur, A. and Glatter, O. (2009) Characterization and potential applications of nanostructured aqueous dispersions. *Adv. Coll. Interf. Sci.* 148, 333-342
18. Siekmann, B *et al.* (2002) Preparation and structural investigations of colloidal dispersions prepared from cubic monoglyceride/water phases. *Int. J. Pharm.* 244, 33-43
19. de Campo, L. *et al.* (2004) Reversible Phase Transitions in Emulsified Nanostructured Lipid Systems. *Langmuir* 20, 5254-5261
20. Gustafsson, J. *et al.* (1997) Submicron particles of reversed lipid phases in water stabilized by a nonionic amphiphilic polymer. *Langmuir* 13, 6964-6971

21. Larsson, K. (2000) Aqueous dispersions of cubic lipid/water phases. *Curr. Opin. Colloid Interface Sci.* 5, 64-69
22. Boyd, B.J. *et al.* (2006) Hexosomes formed from glycerate surfactants-Formulation as a colloidal carrier for irinotecan. *Int. J. Pharm.* 318, 154-162
23. Esposito, E. *et al.* (2003) Lipid based supramolecular systems for topical application: a preformulatory study. *AAPS PharmSci.* 4:article 30
24. Kim, J.S. *et al.* (2000) Drug formulations that form a dispersed cubic phase when mixed with water. *Proc. Int. Symp. Control. Rel. Bioact. Mater.* 27, 1118-1119
25. Spicer, P.T. and Hayden, K.L. (2001) Novel process for producing cubic liquid crystalline nanoparticles (cubosomes). *Langmuir* 17, 5748-5756
26. Worle, G. *et al.* (2007) Influence of composition and preparation parameters on the properties of aqueous monoolein dispersions. *Int. J. Pharm.* 329, 150-157
27. Nakano, M. *et al.* (2001) Small angle X-ray scattering and 13C NMR investigation on the internal structure of cubosome. *Langmuir* 17, 3917-3922
28. Almgrem, M. *et al.* (2000) Cryo transmission electron microscopy of liposomes and related structures. *Colloids Surf. A* 174, 3-21
29. Sagalowicz, L. *et al.* (2006) Investigating reversed liquid crystalline mesophases. *Curr. Opin. Colloid Interface Sci.* 11, 224-229
30. Fernandez Alanis, E. *et al.* (2012) An exon-specific U1 small nuclear RNA (snRNA) strategy to correct splicing defects. *Hum. Mol. Genet*. 21, 2389-2398
31. Rizzotto, L. *et al.* (2006) Intracellular evaluation of ER targeting elucidates a mild form of inherited coagulation deficiency. *Mol. Med.* 12, 137-142
32. Esposito, E. *et al.* (2005) Cubosome dispersions as delivery systems for percutaneous administration of indomethacin. *Pharm. Res.* 22, 2163-73
33. Esposito, E. *et al.* (2008) Solid lipid nanoparticles as delivery systems for bromocriptine. *Pharm. Res.* 25, 1521-1530
34. Hiramatsu, N. *et al.* (1997) HCV cDNA transfection to HepG2 cells. *J. Viral Hepat.* 4, 61-67
35. van de Loosdrecht A.A. *et al.* (1994) A tetrazolium-based colorimetric MTT assay to quantitate human monocyte mediated cytotoxicity against leukemic cells from cell lines and patients with acute myeloid leukemia. *Immunol. Methods* 174, 311-320
36. Cortesi, R. *et al.* (2012) Long-chain cationic derivatives of PTA (1,3,5-triaza-7-phosphaadamantane) as new components of potential non-viral vectors. *Int. J. Pharm.* 431,176-182
37. Worle, G. *et al.* (2006) Transformation of vesicular into cubic nanoparticles by autoclaving of aqueous monoolein/poloxamer dispersions. *Eur. J. Pharm. Sci*. 27, 44-53
38. Lindstrom, M. *et al.* (1981) Aqueous lipid phases of relevance to intestinal fat digestion and absorption. *Lipids* 16, 749-754
39. Schubert, M.A. and Muller-Goymann, C.C. (2005) Characterization of surface-modified solid lipid nanoparticles (SLN): influence of lecithin and nonionic emulsifier. *Eur. J. Pharm. Biopharm.* 61, 77-86
40. Muller, R.H. *et al.* (1996) Cytotoxicity of magnetite-loaded polylactide, polylactide/glycolide particles and solid lipid nanoparticles. *Int. J. Pharm.* 138, 85-94
41. Heydenreich, A.V. *et al.* (2003) Preparation and purification of cationic solid lipid nanospheres - effects on particle size, physical stability and cell toxicity. *Int. J. Pharm.* 254, 83-87

42. Tabatt, K. *et al.* (2004) Effect of cationic lipid and matrix lipid composition on solid lipid nanoparticles-mediated gene transfer. *Eur. J. Pharm. Biopharm.* 57:155-162
43. Sternberg, B. *et al.* (1994) New structures in complex formation between DNA and cationic liposomes visualized by freeze-fracture electron microscopy. *FEBS Letters* 356, 361-366
44. Faneca, H. *et al.* (2002) Evaluation of lipid-based reagents to mediate intracellular gene delivery. *Biochim. Biophys. Acta* 1567, 23-33
45. Liu, F. *et al.* (1996). New cationic lipid formulations for gene transfer. *Pharm. Res.* 13, 1856-1860
46. Kim, T.W. *et al.* (2002) The role of non-ionic surfactants on cationic lipid mediated gene transfer. *J. Control. Rel.* 82, 455-465
47. Olbrich, C. *et al.* (2001) Cationic solidlipid nanoparticles can efficiently bind and transfect plasmid DNA. *J. Control. Rel.* 77, 345-355
48. Chen J. *et al.* (2007) Preparation, characterization and transfection efficiency of cationic PEGylated PLA nanoparticles as gene delivery systems. *J. Biotechnol.* 130, 107-113
49. del Pozo-Rodríguez, A. *et al.* (2007) Solid lipid nanoparticles: Formulation factors affecting cell transfection capacity. *Int. J. Pharm.* 339, 261-268
50. del Pozo-Rodríguez A. *et al*. (2009) Proline-rich peptide improves cell transfection of solid lipid nanoparticle-based non-viral vectors. *J. Control. Rel.* 133, 52-59.
51. Choi S.H. *et al.* (2008) Novel cationic solid lipid nanoparticles enhanced p53 gene transfer to lung cancer cells. *Eur. J. Pharm. Biopharm*. 68, 545-554.
52. del Pozo-Rodríguez A. *et al.* (2010) Solid lipid nanoparticles as potential tools for gene therapy: in vivo protein expression after intravenous administration. *Int. J. Pharm.* 385, 157-162.
53. Ogris, M., Wagner, E. (2002) Tumor-targeted gene transfer with DNA polyplexes. *Somat Cell Mol Genet.* 27, 85-95.
54. Delgado, D. *et al.* (2012) Dextran-Protamine-Solid Lipid Nanoparticles as a non-viral vector for gene therapy: in vitro characterization and in vivo transfection after intravenous administration to mice. *Int. J. Pharm.* 425, 35-43.
55. Masuda, T. *et al.* (2005) Evaluation of nuclear transfer and transcription of plasmid DNA condensed with protamine by microinjection: the use of a nuclear transfer score. *FEBS Letters* 579, 2143-2148.
56. del Pozo-Rodríguez A. *et al.* (2011) Lipid nanoparticles as vehicles for macromolecules: nucleic acids and peptides. *Recent Patents on Drug Delivery & Formulation* 5, 214-226.
57. Sakurai, F. *et al.* (2000) Effect of NA/Liposome mixing ratio on the physicochemical characteristics, cellular uptake and intracellular trafficking of plasmid DNA/cationic liposome complexes and subsequent gene expression. *J. Control. Rel.* 66, 255-269.
58. Moore, N.M. *et al.* (2009) Characterization of a multifunctional PEG-based gene delivery system containing nuclear localization signals and endosomal escape peptide. *Acta Biomater.* 5, 854-864
59. Rejman, J. *et al.* (2005) Role of clathrin- and caveolae mediated endocytosis in gene transfer mediated by lipo- and polyplexes. *Mol. Ther.* 12, 468-474.
60. Noguchi, A. *et al.* (2002) Cationic cholesterol promotes gene transfection using the nuclear localization signal in Protamine. *Pharm. Res.* 19, 933-938.
61. Lv, H. *et al.* (2006) Toxicity of cationic lipids and cationic polymers in gene delivery. *J. Control. Rel.* 114, 100–109.

62. Wissing *et al.* (2004) Solid lipid nano-particles for parenteral drug delivery. Adv Drug Del Rev 56:1257-1272,
63. Yang *et al.* (1999) Body distribution in mice of intravenously injected camptothecin solid lipid nanoparticles and targeting effect on brain.J. Control. Rel. 59, 299–307,
64. Mehnert and Mader (2001) Solid lipid nanoparticles. Production, characterization and applications. Adv. Drug Deliv. Rev. 47, 165-196,
65. Jeong and Park (2002) Poly(L-lysine)-g-poly(D,L-lactic-co-glycolic acid) micelles for low cytotoxic biodegradable gene delivery carriers. J. Control. Rel. 82, 159-166.
66. Chollet et al. (2002) Side-effects of a systemic injection of linear polyethylenimine-DNA complexes. J. Gene Med. 4, 84-91
67. Kaur et al. (2008) Potential of solid lipid nanoparticles in brain targeting J. Control. Rel. 127, 97–109
68. Joshi and Müller (2009) Lipid nanoparticles for parenteral delivery of actives. Eur. J. Pharm. Biopharm. 71, 161–172
69. Tseng et al. (2009) Lipid-based systemic delivery of siRNA. Adv. Drug Del. Rev. 61, 721–731
70. Vighi et al. (2010) pDNA condensation capacity and in vitro gene delivery properties of cationic solid lipid nanoparticles. Int. J. Pharm. 389, 254-261
71. Vighi et al. (2007) Re-dispersible cationic solid lipid nanoparticles (SLNs) freeze-dried without cryoprotectors: characterization and ability to bind pEGFP-plasmid.Eur. J. Pharm. Biopharm. 67, 320-328.

Acknowledgments

I am grateful to Prof. Francesco Bernardi and Prof. Mirko Pinotti for supporting me and my work in laboratory from my bachelor degree to my PhD project and to giving me the opportunity to archive this great experience in their laboratory.

I want also to thank Prof. Cécile Denis who hosted and guided me in his laboratory during my period in Paris and of course to Caterina Casari that helped me in that formative experience.

Moreover I want to thank Prof. Rita Cortesi for these three years of fruitful collaboration with hers laboratory.

Last but not least I also thank all my colleagues for their support and the lots of advices that they give to me, but especially for their patience.

Thank you very much to all